Investigating the control of striatal dopamine neurotransmission by axonal calcium channels and by striatal neuromodulators: Insights for Parkinson's disease

DPhil in Physiology, Anatomy and Genetics

Katherine Brimblecombe

September (Trinity term) 2013

Pembroke College, Oxford

Investigating the control of striatal dopamine neurotransmission by axonal Ca^{2+} channels and by striatal neuromodulators: Insights for Parkinson's disease

DPhil in Physiology, Anatomy and Genetics. Trinity term 2013

Katherine Brimblecombe, Pembroke College

Abstract

Dopamine (DA) is a key striatal neuromodulator which is central to processes including action selection and reward-related learning. DA dysfunction is associated with a number of psychomotor disorders, most notably of which is Parkinson's disease (PD). This thesis uses fast-scan cyclic voltammetry in acute mouse striatal slices to detect DA release at carbon fibre microelectrodes with subsecond temporal resolution, to investigate factors affecting the presynaptic control of DA release.

In this thesis, I have investigated the roles of voltage dependent calcium channels (VDCCs) and the neuromodulator, substance P (SP), in the presynaptic control of DA, in the presence of nicotinic acetylcholine receptor (nAChR) blockade. This is because ACh has profound modulatory and driving effects on DA release, via activation of nAChRs on DA terminals.

In CPu, blockers for N-, P/Q-, T- or L-type VDCCs (ω-Conotoxin GVIA, ω-Agatoxin IVA, NNC 55-0396, isradipine) reduced DA release to varying degrees (N>P/Q>T>L). Furthermore, L-type function was eliminated by α-synuclein knockout. In NAc, only N and P/Q-blockers modified DA release (N>P/Q) and more weakly than in CPu. Frequency-specific effects of some VGCCs were reproduced by changes to extracellular Ca^{2+} or release probability, consistent with Ca^{2+} entry governing the relationship between DA release probability and its short-term plasticity. Finally I have shown that SP can directly modulate striatal DA release in a manner that depends on striosome-matrix location. To date there is much conflict in the literature on the role of SP in a number of striatal processes, this finding may help to resolve these conflicts and shed light on the little understood role of the striosome-matrix division of the striatum.

Table of Contents

Funded by
PARKINSON'S UK
CHANGE ATTITUDES.
FIND A CURE.
JOIN US.

Acknowledgements

I would like to take this opportunity to formally thank Dr Stephanie Cragg for her limitless support, patience and enthusiasm, which have made being part of her lab a thoroughly enjoyable and rewarding experience. Conversely, I lament my secondary school teacher, Mr Shelley, who failed to teach me how to use hyphens properly, which has plagued my writing of this thesis!

I would also like to thank the other members of the Cragg lab both past and present, particularly to Dr Sarah Threlfell and Dr Katie Jennings who have constantly supported me throughout my DPhil with encouragement and good humour. Sarah can testify that this thesis was literally labour inducing, because when she started to read through Chapter 5 of this thesis, her beautiful baby boy James decided he was ready to join the world! I am hugely grateful to Dr Nicola Platt for sharing tissue from surgically injected mice for optogenetic experiments. Many thanks also to other members of the Cragg lab, Dr Richard Exley, Dr Tatiana Lalic, Dawid Potgieter and Polina Kosillo for sharing their resources, experience and insights, and not least their cake over the past three years.

I am grateful to the BMS staff who have helped with breeding and animal maintenance and members of the Wade-Martins group for supplying *SNCA* OVX and *Snca-/-* mice, especially Steffie Janezic for her help in genotyping the mice.

I would also like to thank Parkinson's UK for their generous funding.

I am so incredibly grateful for my wonderful family and friends for their support over the past three years. I particularly want to thank Adam, whose constant love, support and faith in me has kept me sane over the last few months.

Finally I want to apologise to Simon (which is the name I gave to this thesis), I uttered many cruel and hurtful words towards you, for which there is no excuse. I hope you enjoy your time in the Bod.

Abbreviations

6-OHDA	6-hydroxydopamine
AAV5	adeno-associated virus, serotype 5
AC	adenylate cyclase
ACh	acetylcholine
AChE	acetylcholinesterase
aCSF	artificial cerebrospinal fluid
ADHD	attention deficit hyperactivity disorder
AP	anterior-posterior
ATP	adenosine triphosphate
$[Ca^{2+}]_o$	extracellular calcium concentration
cAMP	cyclic adenosine monophosphate
CFMs	carbon fibre microelectrodes
ChAT	choline acetyltransferase
ChIs	cholinergic interneurons
ChR2	channelrhodopsin 2
CPu	caudate-putamen
$D_{1\text{-}5}Rs$	dopamine (1-5) receptors
D_2L/D_2S	long/short splice variants of dopamine 2 receptor
D-AP5	D-(2*R*)-amino-5-phosphonopentanoate
DA	dopamine
$[DA]_o$	extracellular evoked dopamine concentration
DAT	dopamine uptake transporter
DHβE	dihydro-β-erythroidine
dlCPu	dorsolateral caudate-putamen
DMSO	dimethyl sulphoxide
DOR	δ-opioid receptor
DV	dorsal-ventral
eYFP	enhanced yellow fluorescent protein
FCV	fast-scan cyclic voltammetry
Gβγ	βγ subunit of G-proteins

GIRK2	G protein-activated inward rectifying potassium channel 2
GPe	globus pallidus external segment
GPi	globus pallidus internal segment
GYKI25466 hydrochloride	4-(8-methyl-9*H*-1,3-dioxolo[4,5-*h*][2,3]benzodiazepin-5-yl)-benzenamine
H_2O_2	hydrogen peroxide
HD	Huntington's disease
LED	light emitting diode
$M_{1\text{-}5}Rs$	muscarinic (1-5) receptors
mAChRs	muscarinic acetylcholine receptors
MCPG	(S)-α-methyl-4-carboxyphenylglycine
ML	medial-lateral
MOR	μ-opioid receptor
(d/i)MSNs	(direct /indirect pathway) medium spiny neurons
NAc	nucleus accumbens
NAcC	nucleus accumbens core
nAChRs	nicotinic acetylcholine receptors
NNC 55-0396	1*S*,2*S*)-2-[2-[[3-(1*H*-Benzimidazol-2-yl)propyl]methylamino]ethyl]-6-fluoro-1,2,3,4-tetrahydro-1-(1-methylethyl)-2-naphthalenyl cyclopropanecarboxylate dihydrochloride
NO	nitric oxide
NOS	nitric oxide synthase
PBS	phosphate buffered saline
PBS-TX	phosphate buffered saline containing 0.5% Triton X-100
PET	positron emission tomography
PD	Parkinson's disease
P_r	initial release probability
SEM	standard error of the mean
SOP	slow oscillatory potential
SNARE	soluble NSF attachment protein receptor
SNc	substantia nigra pars compacta
Snca-/-	human and mouse α-synuclein null mouse line
SNCA OVX	human α-synuclein over-expression mouse model
SNr	substantia nigra pars reticulata
SP	substance P

STN	subthalamic nucleus
TANs	tonically active neurons
TH	tyrosine hydroxylase
VDCC	voltage-gated calcium channel
VGSC	voltage-gated sodium channel
VTA	ventral tegmental area
WT	wild-type

1. Introduction

Striatal dopamine (DA) transmission is central to processes including reward-related learning and motor control, and DA dysfunction is associated with many psychomotor disorders including Parkinson's disease (PD). In this thesis I explore the control of striatal DA release by voltage-dependent calcium channels (VDCCs) in both wild-type mice and a mouse model of PD. I also investigate the modulatory effects of substance P (SP) on DA release, and explore how these modulatory effects vary between striosome and matrix territories of the striatum. Throughout this thesis I will highlight the powerful modulatory action of acetyl choline (ACh) on DA release, and much of the data which tests how presynaptic DA is controlled in this thesis, is collected in the absence cholinergic effects.

In this chapter I will introduce topics that are relevant to this thesis as a whole. Firstly this chapter will discuss the role of DA in the basal ganglia and outline the function of the basal ganglia as a whole. Secondly it will discuss the control of presynaptic release, firstly focusing on the role of VDCCs in neurotransmission and secondly the effect of neuromodulators on DA release, particularly ACh. The final section of this introduction will discuss the role of DA dysfunction in PD.

1.1. The striatum and the basal ganglia

1.1.1 Overview

The basal ganglia is formed of a group of interconnected subcortical nuclei which are known to function in a number of important behaviours including action selection, reinforcement learning and decision making (Graybiel et al., 1994; Balleine et al., 2007; Crittenden and Graybiel, 2011). The nuclei that form the basal ganglia are the striatum, globus pallidus external (GPe) and internal (GPi) segments, subthalamic nucleus (STN) and substantia nigra (SN). The SN is divided into the pars compacta (SNc) and pars reticulata (SNr) (Bolam et al., 2000). These nuclei form the dorsal aspect of the basal ganglia, which are generally associated with motor and associative functions. Limbic functions are generally associated with the ventral aspect of the basal ganglia, which

consists of the nucleus accumbens (NAc), ventral pallidum and the medial aspects of the STN and SN (Smith and Kieval, 2000; Voorn et al., 2004; Tepper et al., 2007).

1.1.2 Midbrain DA neurons

The striatum is the input nucleus of the basal ganglia, and is innervated by two populations of dopaminergic midbrain neurons, SNc and VTA neurons which target CPu and NAc regions of the striatum respectively. DA neurons have huge axonal arbors, where the axonal field of a single neuron can occupy over 5% of striatal volume (Matsuda et al., 2009). There are approximately 30,000 midbrain dopaminergic neurons in mice, of which between 40-50% reside in SNc, whereas in humans of the 400,000 midbrain DA neurons over 70% are SNc (Nelson et al., 1996; Björklund and Dunnett, 2007). Midbrain DA neurons can be classified according to their anatomical location, functional roles and expression of certain biochemical markers. VTA DA neurons are located more medially compared to SNc DA neurons, and the VTA DA neurons are commonly associated with limbic functions. SNc DA neurons innervate more dorsolateral aspects of the striatum, and are associated with motor functions (Gerfen et al., 1987b; Voorn et al., 2004). Midbrain DA neurons can also be distinguished based on their expression of certain biochemical markers including the G-protein regulated inward-rectifier potassium channel 2 (GIRK2) and the calcium binding protein calbindin. VTA and dorsal tier SNc DA neurons express calbindin but not GIRK2, whereas ventral tier SNc neurons express GIRK2 but not calbindin. The ventral tier SNc DA neurons that express GIRK2 are the most sensitive to degeneration in PD (Björklund and Dunnett, 2007; Roeper, 2013).

Midbrain DA neurons can be identified by a number of biophysical characteristics: They have broad action potentials (>2 ms) with a prominent shoulder in the falling phase, due to the activation of Ca^{2+} channels. Two phases of the action potential can be visualised during extracellular recordings, an initial segment spike and a somatodendritic spike (Bean, 2007). *In vitro*, midbrain DA neurons exhibit autonomous pacemaker activity (1-8 Hz), which is driven by

sub-threshold oscillations, called slow oscillatory potentials (SOP). The SOP of SNc neurons are generated by L-type calcium channels, whereas in VTA neurons they are generated by Na^+ channels (Bean, 2007; Chan et al., 2007; Puopolo et al., 2007). *In vivo*, DA neurons still exhibit low frequency firing, but it is more irregular due to inputs acting upon the DA neurons; the neurons also display burst firing, of 2-5 pulses of 10-40 Hz (although firing of up to 100Hz has been reported) (Grace and Bunney, 1984a, 1984b; Hyland et al., 2002). Burst firing is thought to be generated by NMDA activation by glutamatergic afferents (Charlety et al., 1991; Overton and Clark, 1992). The inputs to midbrain DA neurons, which modulate their firing, are still incompletely defined. However with the advent of new genetic technologies that enable the retrograde labelling of neurons which synapse onto midbrain DA neurons, a more complete picture is emerging: Midbrain DA neurons receive excitatory input from cortex, hypothalamus, superior colliculus, lateral tegmental nucleus and pedunculopontine tegmental nucleus; inhibitory inputs from a number of basal ganglia nuclei including striatum and SNr; and modulatory inputs from the raphe nucleus and locus coeruleus (Somogyi et al., 1981; Hervé et al., 1987; Comoli et al., 2003; Watabe-Uchida et al., 2012).

Much of our understanding of the roles of DA neurons in behaviour has been guided by diseases caused by aberrant DA neuron activity and transmission, the archetypal example of this is PD. The loss of striatal DA due to death of midbrain DA neurons clearly illustrates the importance of DA in the execution of motor function and action selection. Aberrant DA transmission also occurs in personality disorders including schizophrenia, impulse control disorders and addiction, which illustrate the role DA plays in associations and reinforcement learning (Schultz, 2007a); additionally, exogenous driving of DA neurons to burst fire can result in behavioural conditioning (Tsai et al., 2009; Adamantidis et al., 2011).

DA neuron firing is thought to facilitate reinforcement learning by encoding “reward prediction error” of an outcome under specific circumstances: DA neurons switch from low

frequency “tonic” firing to high frequency burst firing when an individual experiences an unexpected reward; conversely if an expected reward is not presented, DA neuron activity depresses. The response of DA neurons to a reward is scaled to the size of the reward (Mirenowicz and Schultz, 1996; Morris et al., 2004; Schultz, 2007b). If a reward becomes associated with a neutral cue e.g. light flash or auditory tone, the phasic DA activity becomes progressively time-locked to the cue and reciprocally fades from the presentation of the reward (Schultz et al., 1997).

There is much evidence supporting the hypothesis that DA encodes reward prediction error, however there are still a number of factors which are unexplained. The response of DA neurons to aversive stimuli, is an area of controversy: In accordance with DA neurons encoding reward prediction error, aversive stimuli have been shown to inhibit DA neuron firing (Mirenowicz and Schultz, 1996; Ungless et al., 2004), however some studies have identified a small population of DA neurons that are activated following aversive stimuli (Mirenowicz and Schultz, 1996; Brown et al., 2009; Matsumoto and Hikosaka, 2009). The activation of DA neurons in response to aversive stimuli may indicate that the role of DA neurons is to encode salience rather than reflect a positive outcome (Redgrave et al., 2008). It could be surmised that there is a discrete population of DA neurons that are activated in response to aversive stimuli, which would allow rewarding, neutral and aversive stimuli to be encoded by summating the responses of distinct populations of neurons.

In addition to DA transmission playing a central role in reinforcement learning by signalling rewarding and salient information, DA transmission is also central to processes such as action selection and motor control. The importance of DA in motor control is made apparent in disorders such as PD, where striatal DA is depleted and results in a loss of motor control. Although it is clear that DA transmission is central in processes such as action selection and motor control, how DA neurons fire to encode this information is unclear. One of the problems in

identifying how DA neurons fire during initiations of movements is that DA neurons are activated by salient sensory information, which is both temporally and functionally linked to movements. Furthermore, many of the *in vivo* recordings of rodent DA neurons were performed in anaesthetised animals, which obviously are immobile but still show bursting of DA neurons, indicating that bursting of DA neurons occurs in the absence of motor activity (Jeong et al., 2012). In experiments where monkeys would reach into a box where a food reward was either present or absent, it was found that DA neuron bursting was in relation to rewarding sensory information of the food and not from the initiation of the arm movement (Romo and Schultz, 1990; Overton and Clark, 1997). It therefore seems that DA helps to encode the behavioural significance of sensory information that supports the integrative computations in the striatum that select a specific movement rather than DA neurons driving actions themselves.

1.1.3 The role of striatal DA

The role of DA in various behavioural paradigms is often investigated by measuring the activity of DA neurons under various conditions. DA neurons have been shown to alter their firing patterns in response to a number of conditions including rewarding and aversive stimuli, and various pharmacological interventions. Changes in DA neuron firing are often assumed to be reflected by a change in axonal DA release, meaning that the effect of DA on its downstream targets can be altered by changes in DA neuron firing. In other words, it is assumed that the information encoded by the firing patterns of DA neurons is faithfully transmitted to its downstream targets. In the following chapters of this thesis I will focus on how DA release is controlled in the striatum, and draw attention to emerging evidence that illustrates why it should not be assumed that DA release is wholly determined by DA neuron activity.

DA exerts its downstream effects by acting upon metabotropic G-protein coupled receptors (GPCRs). Five DA receptors have been identified ($D_{1\text{-}5}$Rs), which can be sub-grouped into D_1R-like and D_2R-like which includes $D_{1,5}$-Rs and $D_{2\text{-}4}$Rs respectively (Niznik and Van Tol,

1992). In the striatum D_1-and D2-receptors are the most abundantly expressed receptor type (Levey et al., 1993). D_1-like receptors are $G_{\alpha s}$ coupled, which activates adenylate cyclase (AC), leading to increased cyclic adenosine monophosphate (cAMP) production. D_2-like receptors are coupled to $G_{\alpha i}$, which inhibits AC and therefore decreases cAMP production. Activation of D_2-like receptors can affect downstream targets by Gβγ-modulation. D_1-like receptors are transcribed from a single exon, so that there are no splice variants; whereas D_2R exist in two isoforms, short (D_2S) and long (D_2L), where D_2L has an extra 29 amino acids in the third intracellular loop, which affects their coupling to downstream pathways (Sidhu and Niznik, 2000). D_2S and D_2L are mostly pre- and postsynaptically located respectively, the isoforms also have slightly different pharmacological and physiological signalling properties (Richfield et al., 1989; Beaulieu and Gainetdinov, 2011). DA receptors can exist in both a high and low affinity state, where the low affinity state is thought to reflect receptors that are uncoupled from their G proteins (Skinbjerg et al., 2012). In the striatum D_1–like receptors are thought to occur primarily in the low affinity state, compared to D_2-like receptors that are mostly found in the high affinity state (Richfield et al., 1989)

DA can have highly variable effects on its downstream targets by virtue of the different coupling of the DA receptors. Striatal projection neurons, knows as the medium spiny neurons (MSNs) can be divided into two groups by their expression of either D_1R or D_2R, therefore DA has contrasting effects on D_1R-expressing and D_2R-expressing MSNs. Activation of D_1R by DA increases the excitability of MSNs, whereas D_2R activation reduces the excitability of MSNs (Planert et al., 2013). Although there is some evidence for co-expression of D_1 and D_2R, the functional significance of these neurons is unclear (Valjent et al., 2009). Activation of D_1R on MSNs results in increased AC activity that increases glutamate-receptor expression and L-type VDCC conductivity; and decreases the conductance of voltage-dependent Na^+ channels (VDSC). Therefore the net effect of D_1R activation is an increase in excitability of D_1-R-expressing MSNs when depolarised but a decrease in their excitability when hyperpolarised, which serves to

increase the signal to noise ratio of the inputs received by D_1R-expressing MSNs (Yan et al., 1997; Vilchis et al., 1999; Surmeier et al., 2007). In contrast, activation of D_2R makes on MSNs makes them less excitable. In addition to D_2R having inverse effects to D_1R by virtue of their inhibiting action on AC, D_2R can also have downstream effects via Gβγ mechanisms: Gβγ activation can modulate Ca^{2+} availability of the cell by activating phospholipase C (PLC), which increases cytoplasmic Ca^{2+}; or can decrease cytoplasmic Ca^{2+} by inhibition of L-type VDCC conductivity. Gβγ activation of GIRKs shifts the resting membrane potential by ~-8 mv reducing the excitability of cells (Lüscher and Slesinger, 2010; Beaulieu and Gainetdinov, 2011; Chun et al., 2013).

In addition to being present on MSNs, there are several other striatal targets for DA including glutamatergic afferents, GABAergic interneurons and ChIs. Analogously to the effect of DA-receptor activation on MSNs, D_1R and D_2R activation increases and decreases excitability of cells respectively, by modulating cAMP levels and Ca^{2+}, K^+, Na^+ channel conductance (Le Moine et al., 1990, 1991; Bracci et al., 2002; Wang and Pickel, 2002; Centonze et al., 2003; Bamford et al., 2004). Glutamatergic inputs are negatively regulated by DA acting on D_2Rs (Bamford et al., 2004), whereas fast-spiking interneurons in the striatum are activated by DA (Bracci et al., 2002). ChIs express both D_1-like and D_2-like receptors, which regulate distinct aspects of ChI physiology (Le Moine et al., 1991; Centonze et al., 2003). D_1R activation depolarises ChIs by inhibiting K^+ conductance, whereas D_2R activation decreases ChI firing and reduces ACh release, via inhibition of N-type VDCCs (DeBoer and Abercrombie, 1996; Yan et al., 1997; Centonze et al., 2003). D_5Rs are also expressed in the striatum at low levels by both D_1R- and D_2R-expressing MSNs and at higher levels by ChIs, somatostatin positive, parvalbumin positive and calretinin positive interneurons (Rivera et al., 2002). The effect of D_5R activation are harder to predict than D_1R and D_2R, as D_5Rs are capable of coupling to both $G_{\alpha s}$and $G_{q/11}$, which activates AC and PLC respectively (Sidhu and Niznik, 2000). It is not fully understood which conditions promote D_5R coupling to either of the G proteins but it may be due to lipid composition of the membrane, calmodulin,

DARRP32 expression or heterodimerisation with other GPCRs (Tate and Grisshammer, 1996; Franco et al., 2010).

One of the major targets for DA is on the DA terminals themselves, which express the short isoform of D_2Rs. Activation of D_2R on DA terminals decreases DA release and synthesis via modulation of ion channel conductance, and changes in quantal size, and over longer time courses, by phosphorylation of TH (Cardozo and Bean, 1995; Cragg et al., 1997; Sulzer and Pothos, 2000; Lindgren et al., 2001). In addition to DA neurons releasing DA from their axons, these neurons also release DA from the somatodendritic portion of the cells. Therefore DA acting on D_2R can also modulate the firing of DA neurons. D_2R activation on the soma of DA neurons hyperpolarise the neurons and a decrease in firing (Centonze et al., 2003)

1.1.4 Basal ganglia organisation and the striatum

Models of the basal ganglia have been expanded from a simple circuit connecting nuclei to a complex and computationally powerful machine, which subdivides these original nuclei, based their function, anatomical location, biochemical markers and synaptic contacts. The function of the basal ganglia is to integrate information received by the striatum to allow the execution of appropriate behaviours. The basal ganglia achieves action selection, by inhibition of undesired actions. Selected behaviours are allowed by disinhibition of specific pathways, whilst the default inhibition of non-selective pathways remains (Gerfen, 1992; Bolam et al., 2000; Gerfen and Surmeier, 2010).

The striatum is the input nucleus of the basal ganglia and is composed of the caudate and putamen (CPu) and NAc, which are functionally divided by their roles in motor control and limbic behaviours, respectively. CPu and NAc are also divided anatomically, where CPu forms the dorsal striatum and is innervated by SNc dopaminergic neurons and NAc is ventral and more rostral and is innervated by VTA dopaminergic neurons (Gerfen et al., 1985; Smith and Kieval, 2000; Voorn et

al., 2004). Despite the anatomical and functional separation of the dorsal and ventral striatum, there are no defined boundaries between the two regions, rather the functional aspects of the striatum lie along gradients formed along dorsal-ventral, medial-lateral and rostral-caudal anatomical axes (Voorn et al., 2004). In addition to dopaminergic innervation to the striatum, there are also glutamatergic afferents from the cortex and thalamus (Smith and Bolam, 1990; Flaherty and Graybiel, 1994; Smith et al., 1994; Doig et al., 2010) and In addition to cortical and thalamic inputs, the striatum receives, serotonergic afferents from the dorsal raphe, and glutamatergic afferents from the amygdala and hippocampus (Gerfen et al., 1985; Smith and Kieval, 2000; Di Matteo et al., 2008; Pennartz et al., 2011). These inputs form synapses with the neurons in the striatum. Approximately 90% of striatal neurons are the GABAergic MSNs and the remaining neurons are striatal interneurons (Bolam et al., 2000; Kreitzer, 2009). Although the interneurons only provide 10% of the neuronal population they are important for modulating how MSNs signal information out of the striatum. There are four clearly defined types of interneurons: large aspiny ChIs; fast-spiking parvalbumin-positive GABAergic interneurons; calretinin-positive GABAergic interneurons; and somatostatin, neuropeptide Y and nitric oxide synthase (NOS)-positive GABAergic interneurons (Kreitzer, 2009). These interneurons modulate the flow of information out of the striatum carried by the striatal efferents, the medium spiny projection neurons (MSNs) (Bolam et al., 2000).

Information is transmitted from the striatum by GABAergic MSNs, through to the output nuclei of the basal ganglia, GPi and SNr, which send inhibitory projections to the thalamus (Smith and Bolam, 1990). The MSNs can be divided into two populations: DA receptor type 1 (D1)-expressing and DA receptor type 2 (D2)-expressing MSNs. D1- and D2-expressing MSNs form the direct and indirect pathways respectively, in an approximately 1:1 ratio (Smith and Bolam, 1990; Gerfen, 1992). The direct pathway is formed by MSNs (dMSNs) projecting from the striatum to the GPi and SNr. Indirect pathway MSNs (iMSNs) innervate GPe that in turn innervates STN, which sends excitatory glutamatergic projections to the output nuclei (GPi and SNr) (**Figure 1.1**).

In essence, activation of the direct pathway inhibits the inhibitory action of the basal ganglia (disinhibition), resulting in excitation of the thalamus; whereas activation of the indirect pathway stimulates the inhibitory action of the basal ganglia of the thalamus, therefore the direct and indirect pathways are often referred to as “go” and “no-go” pathways respectively (Gerfen and Surmeier, 2010).

The basal ganglia, are by default inhibitory, with tonic suppression of unwanted actions. It is thought that in order to facilitate a specific action, the default suppression of the basal ganglia output is lifted. Passage through the direct pathway, via dMSNs allows the disinhibition of a selected pathway (Gerfen, 1992; Yung et al., 1996; Gerfen and Surmeier, 2010). However, how an input to the striatum is steered correctly along either direct or indirect pathway to select or inhibit an input respectively, in a plastic manner is incompletely understood.

1.1.5 Striosome and matrix organisation of the striatum

The striatum is required to act as a “switchboard operator”, differentiating inputs and then relaying the information to appropriate MSNs, therefore the striatum must be heterogeneous to enable inputs and outputs to be categorised. The striatum is known to be a highly heterogeneous structure with respect to anatomical locations, where dorsolateral, medial and ventral regions are associated with motor, associative and limbic actions respectively (Smith and Kieval, 2000; Voorn et al., 2004). In addition to the striatum being subdivided anatomically and functionally, the striatum can also be distinguished according to variable “patchy” expression of certain biochemical markers, which correspond to striosome and matrix regions. Striosomes are characterised by high levels of μ-opioid receptor (MOR), D1-receptor (D1R), substance P (SP), calretinin and Nr4a1 expression, whereas the matrix is enriched with calbindin and ACh esterase (AChE) (Besson et al., 1988; Sakamoto et al., 1992; Crittenden and Graybiel, 2011; Davis and Puhl, 2011).

Striosome-matrix division of the striatum has been known about for over 30 years, yet its physiological role is not fully understood, however they are known to differ in terms of their development, circuitry and sensitivity to certain diseases (Pert et al., 1976; Graybiel and Ragsdale, 1978; Gerfen, 1984; Crittenden and Graybiel, 2011). During early development, tyrosine hydroxylase (TH) expression is heterogeneous, resulting TH-rich patches, known as DA islands (Graybiel et al., 1981; Graybiel, 1984). TH expression becomes uniform in mice at ~P20, and the regions which were previously "DA islands" develop into the striosomes of the adult brain (Graybiel, 1984; Roffler-Tarlov and Graybiel, 1987). During late embryonic and early postnatal development, striatal DA islands are also AChE rich regions, however in the adult brain it is the matrix that is enriched with AChE (Graybiel et al., 1981; Malach and Graybiel, 1986). Understanding why striosomes go from being AChE-rich to AChE-poor in development may provide insights into the function of striosomes. It is unclear whether being AChE-poor indicates a high or low level of ACh signalling in the striosomes, as having low levels of AChE, could allow ACh to be present at high enough concentrations to have modulatory effects on striosomal targets; alternatively low AChE levels could indicate low levels of ACh, meaning AChE is unnecessary. It would be interesting to investigate if altering ACh levels or ChI distribution in the striatum affects the formation of the striosome-matrix axis, as is seen when DA levels and innervation is altered. When DA release is increased with systemically delivered amphetamine or reserpine, it results in patchy DA expression in the striatum, and increases in striosomal markers including SP and dynorphin and conversely decreasing DA levels with 6-OHDA lesions preferentially reduces DA in the striosomes and results in increased levels of matrix markers including enkephalin (Fukui et al., 1986; Bannon et al., 1987; Gerfen et al., 1987a, 1991; Gerfen, 1992).

The differing effects of increasing or decreasing DA levels with amphetamine or 6-OHDA treatment respectively, on striosome and matrix regions could be due to intrinsic differences in the DA neurons that innervate striosome and matrix regions. Early studies found that DA neurons

that innervate the matrix express calbindin, are less sensitive to dopaminergic toxins, and correspond to dorsal tier DA neurons (Gerfen et al., 1987b, 1991). However with the advent of advanced single neuron tracer studies and the use of specific genetically encoded fluorescent markers, the innervation of striatal compartments has been shown to not be so clear cut. In a pioneering study by Matsuda et al (2009), it was found that the majority of DA neuron fibres non-selectively innervate striosome or matrix compartments; however some fibres did preferentially innervate striosome or matrix regions. In agreement with previous studies, striosomes and matrix regions tended to be innervated more favourably by ventral and dorsal tier midbrain neurons respectively. Furthermore, despite many of the neurons showing no preference for striosome or matrix innervation, it was noted that axonal bushes of a single neuron would preferentially innervate either striatal territory (Matsuda et al., 2009). This may indicate that the vast axonal arbors of DA neurons are not homogeneous, and different territories of a single neuron may function independently from one-another, possibly in a striosome-matrix dependent manner.

Innervation from the cortex also differs between striosome and matrix compartments, where limbic innervate striosomes, and motor and associative cortices innervate matrix regions (Gerfen, 1984, 1989; Donoghue and Herkenham, 1986). As D1R, SP and dynorphin are all striosomally enriched and markers of dMSNs it would be logical to predict that striosome-matrix axis and direct-indirect pathways are two sides of the same coin. However, becuase there are approximately equal numbers of dMSNs and iMSNs, and yet striosomes only form ~15% of the striatum, the equivalence of dMSNs and striosomal MSNs is unsurprisingly not supported by experimental data (Davis and Puhl, 2011). The majority of both dMSNs and iMSNs project from matrix regions, and both types of MSNs do project from striosomes, yet dMSNs are more prevalent in striosomes (Johnston et al., 1990; Fujiyama et al., 2011). However only striosomal MSNs directly innervate the DA neurons of the SNc and VTA (Gerfen, 1984; Watabe-Uchida et al., 2012). The collaterals and dendrites of striosome and matrix MSNs tend to remain in their

respective territories, and MSNs on the boundaries seem to be split into two populations, one which is influenced by neurons of adjacent territories and ones which are unaffected (Gerfen, 1985; Bolam et al., 1988; van Dongen et al., 2008).

The striatum is required to sort and integrate the information it receives, to allow appropriate behavioural responses to be selected. The compartmentalisation of the striatum into striosome and matrix territories could function to allow input and output pathways to be appropriately segregated, however how the division between striosome and matrix regions corresponds to selection of behaviours via the direct and indirect pathways, remains unresolved. In chapter 5 I investigate how the control of DA release varies between striosome and matrix regions.

1.2 Control of DA release

1.2.1 Presynaptic neurotransmitter release

SNc DA neurons from symmetric synapses, which mainly contact the necks of dendritic spines of MSNs (Bolam et al., 2000). However many of the DA receptors and DA transporters (DAT) in the striatum are extrasynaptic, indicating that DA exerts its effects via volume transmission as well as at classical synapses (Yung et al., 1995; Pickel et al., 1996; Nirenberg et al., 1997; Cragg and Rice, 2004). Despite DA exerting some of its effects extrasynaptically, the gross mechanisms controlling its release are thought to be equivalent to classical central synapses, namely that it is action potential dependent, and DA is stored in small synaptic vesicles in striatal DA terminals and shows Ca^{2+} dependent quantal release (Sulzer and Pothos, 2000; Rice et al., 2011; Trueta and De-Miguel, 2012).

Synaptic vesicle exocytosis utilises the same cellular machinery that facilitates other exocytotic and membrane fusion events. The phospholipid membrane is a thermodynamically stable structure; therefore disrupting the membrane requires a significant input of energy to overcome the energetic barrier. The energy required for exocytosis is generated by the ATP-

dependent dissociation of soluble NSF attachment receptor proteins (SNARE) complexes into the constitutive reactive monomers; membrane fusion is then coupled to the energetically favourable process of SNARE assembly (Südhof and Rizo, 2011). SNARE proteins can be subdivided according to which membranes they are located in (v-SNAREs and t-SNAREs are located in vesicular and target membranes respectively); and their structural features (Q-SNAREs and R-SNAREs, contribute glutamine and arginine residues to the zero ionic layer of the SNARE complex). Synaptobrevin is both the v-SNARE and R-SNARE and contributes one α-helix to the SNARE complex. Syntaxin and SNAP-25 are located in the plasma membrane, are Q-SNAREs and contribute one and two α-helices to the core SNARE complex respectively. When the three SNARE proteins initially interact, the vesicular and target membranes are brought into proximity with one-another, forming the trans-SNARE complex; then following membrane fusion, the cis-SNARE complex is formed (Südhof and Rothman, 2009). The mechanism by which the trans-SNARE complex transitions to the cis-SNARE complex is not fully understood. Ca^{2+} is known to trigger the completion of the fusion event, which is thought to be mediated by the putative Ca^{2+} sensor synaptotagmin and the clamping protein complexin (**Figure 1.2**). *In vitro* the SNARE proteins are sufficient to drive membrane fusion events, however *in vivo* many additional proteins are required. Such proteins include Sec-1/Munc-18-like proteins (SM proteins). In contrast to SNARE proteins, SM proteins are cytosolic and interact with the SNARE complex facilitating and regulating exocytosis. The manner and role of SM-SNARE interactions are not fully understood, but it is thought that SM proteins wrap around SNARE complexes to spatially orientate them, and may promote phospholipid mixing during cis-complex formation (Giraudo et al., 2006; Südhof and Rothman, 2009; Südhof and Rizo, 2011).

1.2.2 The role of voltage-dependent Ca^{2+} channels (VDCCs) in neurotransmission

Ca^{2+} is required for synaptic exocytosis, and is supplied in an action potential dependent manner via the VDCCs, which are highly selective for Ca^{2+}, positioned at synaptic membranes and their opening is triggered by membrane depolarisations (Katz and Miledi, 1968; Catterall, 2000;

Chapman, 2002). The VDCCs consist of an α-subunit, which is the pore forming subunit, and β-, γ- and δ2- accessory subunits, which are thought to modulate membrane trafficking and turnover, Gβγ interactions and kinetic properties of the channels. There are 10 genes which encode α-subunits of VDCCs, and all of the genes have multiple splice variants. The α-subunits are grouped according to genetic homology, pharmacological and physical properties (Table 1) (Catterall, 2000; Lipscombe et al., 2004; Catterall et al., 2005; Dolphin, 2006).

Table 1

Protein name	Type	Blocked by	Typical location	Reference
Cav1.1	L	dihydropyridine	Skeletal muscle	(Lipscombe et al., 2004; Dolphin, 2006; Catterall, 2011)
Cav1.2			Cardiac/neuronal/endocrine	
Cav1.3			Endocrine/neuronal /cardiac	
Cav1.4			retina	
Cav2.1	N	ω-conotoxin GVIA	Neuronal	(Catterall et al., 2005)
Cav2.2	P and Q are splice variants of the same gene	ω-agatoxin IVA (P at low concentrations)	Neuronal	(Bourinet et al., 1999; Catterall et al., 2005)
Cav2.3	R	Selectively but incompletely by SNX 482 and non-selectively by milimolar concentrations Ni^{2+}	Neuronal	(Catterall, 2011; Myoga and Regehr, 2011)

Cav3.1	T	Non-selectively by sub-milimolar concentrations of Ni^{2+} Selectively by mibefradil and its derivatives (including NNC 55-0936)	Neuronal	(Martin et al., 2000; Catterall et al., 2005; Li et al., 2005; Dolphin, 2006)
Cav3.2			Neuronal	
Cav3.3			Neuronal	

N- and P/Q-type VDCCs are classically thought to control synaptic exocytosis, as they both have synprint sequences in their large intracellular loops connecting domains II and III, which allows them to directly interact with SNARE proteins (Sheng et al., 1994; Rettig et al., 1996). Blockade or genetic deletions of N- and P/Q-type channels are well documented to disrupt synaptic transmission in a number of neuron types in many regions of the brain (Turner et al., 1992; Mintz and Bean, 1993; Jan et al., 2005). In addition to the well classified roles of N- and P/Q-type channels in controlling presynaptic exocytosis, the other channel types have also found to have presynaptic roles, and despite only N- and P/Q-type channels expressing synprint domains, L-, R- and T-type channels have been shown to directly interact with the presynaptic exocytotic machinery (Wiser et al., 1999; Ramakrishnan et al., 2009; Watanabe et al., 2010; Weiss et al., 2012). R-type channels are often presynaptically located, and control exocytosis in hippocampal neurons, however R-type channels do not cluster at the presynaptic zone compared to other Cav2 subtypes (Kamp et al., 2005). The L-type channels, Cav1.3 and 1.4 control release in inner hair cells (IHC) and retinal bipolar cells respectively, and T-type channels have been found to couple to nicotinic receptors to increase glutamate release in the striatum (Wu et al., 1998; Brandt et al., 2003, 2005; Zanazzi and Matthews, 2009; Myoga and Regehr, 2011; Tang et al., 2011).

In addition to facilitating synaptic release, VDCCs serve a number of other functions in neurons: L-type VDCCs modulate transcription and support SOP in SNc DA neurons as well as coupling to intracellular Ca^{2+} stores; R and T-type channels are crucial in establishing action potentials at the axon initiation segment; and T-type channels can couple to other ion channels including small conductance K^+ (SK) channels (Nakai, 1998; Wolfart and Roeper, 2002; Lipscombe et al., 2004; Guzman et al., 2009; Bender et al., 2012) .

Specific pharmacological blockers of VDCC have been hugely important in improving our understanding of their roles in various aspects of neurotransmission. The identification of multiple classes of VDCCs was in part, due to the discovery of dihydropyridine sensitive and resistant Ca^{2+} currents. Since then, N- and P/Q-type channels have been found to be selectively and specifically inhibited by ω-conotoxin IVA and ω-agatoxin IVA respectively (Catterall et al., 2005; Dolphin, 2006). The development of specific pharmacological blockers for R- and T-type channels was slightly more problematic; initially both channels were blocked found to be with micromolar concentrations of Ni^{2+} (Zamponi et al., 1996). However, more recent pharmacological studies have shown that the spider toxin SNX 482 incompletely but selectively blocks R-type channels , and that mibefradil blocks T-type channel at ~13 time greater affinity than L-type channels (Martin et al., 2000; Myoga and Regehr, 2011). Since the initial discovery of mibefradil, analogues have been developed to increase its selectivity of T-type channels over L-types and to distinguish between Cav3.1 and 3.2 sub-type of T-type channel (Li et al., 2005). Distinguishing between channel subtypes of the same class is also problematic for dihydropyridine sensitive L-type channels; Cav1.1 and 1.2 are inhibited by lower concentrations of dihydropyridines than Cav1.3 and 1.4, but there are no pharmacological agents for any one particular sub-type (Lipscombe et al., 2004). However a line of transgenic mice are available, whose Cav1.2 gene has been mutated so that the channels are no longer sensitive to dihydropyridines, allowing the functional significance of Cav1.2 and Cav1.3 to be dissected, as

these channel types often have overlapping expression patterns in the brain (Moosmang et al., 2005).

All 10 VDCC α1 subunits have been cloned and expressed to determine many of their pharmacological properties, leading to the preliminary determination that N,P/Q, L and R-types could be classed as high voltage-activating (HVA), and T-type channels are low voltage-activating (LVA) (Dolphin, 2006). Channel types could also be separated by their electrophysiological properties: T-and N-type channels rapidly and intermediately inactivate over time respectively, compared to L-type channels which were found to be non-inactivating to voltage but did show calcium-dependent inactivation (Catterall et al., 2005). The single channels conductance of VDCCs also varies, where L-type has the greatest and T-type has the least (Fox et al., 1987). Despite the established hierarchy of single channel conductance of VDCCs, with L>N>T-type, recent studies using more physiological experimental preparations have found that *in vivo* N-type channels are likely to carry the greatest charge (Weber et al., 2010).

The VDCCs have been defined in terms of their pharmacological and physiological properties, which has been helpful in determining their functions *in vivo*. However it is important to be aware that the conditions of certain assays, including charge carrier, extracellular ion concentrations and the presence of accessory subunits can affect the apparent properties of channels, as was illustrated with hierarchy of VDCC conductance. Expression systems including Xenopus oocytes and HEK-293 cells are often used to investigate the properties of VDCCs, and found that expression of the β-subunit is required for successful expression of α1-subunits (Brice et al., 1997). Interestingly T-type channels can be functional without any accessory subunits; however their expression can be altered by both β- and $\alpha_2\delta$-subunits. In addition to β-subunits modulating α_1-subunit expression and trafficking to the membrane, the $\alpha_2\delta$-subunit is also involved in trafficking α_1-subunits to the membrane and can modulate pharmacological properties, inactivation kinetics and the voltage dependence of both activation and inactivation

of the α_1-subunit (Snutch et al., 2005; Saheki and Bargmann, 2009). Because the VDCC auxiliary subunits can affect many of a channel's properties, the properties of VDCCs are likely to be variable between different tissue types, and may be highly plastic over time, especially during developmental stages (Arikkath and Campbell, 2003; King and Meriney, 2005; Dolphin, 2006; Snutch et al., 2013). When the properties of VDCC are investigated in expression systems, Ba^{2+} is often used as the charge carrier, which could result in measured properties of the channels being different to those that occur in vivo due to inactivation conduction properties being different for different ions. Additionally high concentrations of Ca^{2+} and Ba^{2+}, can create surface charge screening, so that channels activate at more depolarised potentials than would occur *in vivo* (Lipscombe et al., 2004; Catterall et al., 2005).

In the case of L-type channels, understanding their characterisation has been hampered by the assumption that channel properties are similar between subtypes, which turns out to be false: Cav1.3 and 1.4 are relatively insensitive to dihydropyridines; however a high sensitivity to dihydropyridines is often a criterion for identifying L-type roles, so that their action in physiological processes may have been overlooked. L-types are also assumed to have slow inactivation kinetics and require strong membrane depolarisation, however Cav1.3 channels activate at much more hyperpolarised potentials than that of Cav1.2, so much so, that their properties may be considered closer to the LVA than other L-type channels (Lipscombe et al., 2004; Helton et al., 2005).

Studies have previously investigated the roles of VDCCs in the control of DA release in CPu, and have found that N- and P/Q-type channels play major roles (Bergquist et al., 1998; Phillips and Stamford, 2000b; Chen et al., 2006). However many questions still remain, including how the contribution of the channels vary with stimulation paradigms; between dorsal and ventral striatal regions and, most crucially, if the role of VDCCs is affected by the presence of ACh,

which is known to powerfully modulate DA release. In chapter 3 I have aimed to address these points.

1.2.3 Somatodendritic DA release

Midbrain DA neurons have very few collateral axons, rather they release DA from their somata and dendrites that binds to D2 receptors present on the DA cells, which are autoreceptors (Björklund and Lindvall, 1975; Geffen et al., 1976; Beckstead et al., 2004; Björklund and Dunnett, 2007; Rice et al., 2011). Despite Geffen et al (1976) initially proposing that dendritic release is vesicular and action potential dependent, as it is in DA axons, later studies suggested that somatodendritic DA release occurs by reversal of DAT, rather than by classical exocytotic mechanisms (Falkenburger et al., 2001). However other studies have found that neither pharmacological blockade or genetic deletion of DAT inhibits somatodendritic DA release (Cragg et al., 1997; John and Jones, 2006), which implies that the reversal of DAT as the primary mechanism of somatodendritic DA release is improbable.

Evoked extracellular DA concentration ($[DA]_O$) detected using techniques such as FCV is considerably lower in midbrain compared to striatal regions, and also varies between midbrain regions, where evoked DA release is higher in VTA than SNc (Cragg et al., 1997; Chen and Rice, 2001; Chen et al., 2006; Ford et al., 2010). An additional difference between DA release in midbrain regions is the existence of both axonal and somatodendritic release in VTA compared to only somatodendritic release in SNc (Rice et al., 2011). The Ca^{2+} dependence of somatodendritic DA release is still a point of controversy. Somatodendritic release has been shown to occur in zero extracellular calcium (Chen and Rice, 2001), and only be partially inhibited by a cocktail of VDCC blockers that is sufficient to prevent release in the striatum (Chen et al., 2006), however there have also been reports that somatodendritic DA release is highly sensitive to both extracellular Ca^{2+} concentrations and inhibition of VDCCs (Ford et al., 2007; Kim et al., 2008), therefore further investigations are required to explain these conflicting reports.

Somatodendritic DA release has been shown to be dependent on the exocytotic SNARE proteins, however the proteins that form the SNARE complex may differ to those that operate in axonal release (Fortin et al., 2006; Witkovsky et al., 2009). In summary somatodendritic DA release is known to occur and thought to have important physiological roles; however there is still much to be understood about the mechanisms controlling somatodendritic DA release.

1.2.4 Modulators of DA release

The firing frequencies and firing patterns of DA neurons clearly have important roles in both healthy and disease states of the brain, however striatal DA release is dependent on factors besides neuron firing patterns. It is therefore important to investigate how these additional factors can modulate DA release. One of the most powerful modulators of striatal DA release is ACh (Zhou et al., 2001; Rice and Cragg, 2004; Cragg, 2006). In the striatum ACh is released from large aspiny, tonically active ChIs, which constitute approximately 1% of all striatal neurons (Kawaguchi et al., 1995; Rymar et al., 2004). Despite the ChIs being so few in number, it has been shown that there is high density of cholinergic markers including choline acetyltransfersase (ChAT) and AChE in the striatum; furthermore, ChIs have an enormous influence throughout the striatum by virtue of their extended dendritic trees and dense axonal arbors, and the large number of vesicle containing varicosities (Hoover et al., 1978; Graveland and DiFiglia, 1985; Kawaguchi, 1993; Descarries and Mechawar, 2000). Similar to striatal DA release, striatal ACh signals by both point-to-point transmission and via volume transmission (Izzo and Bolam, 1988; Descarries and Mechawar, 2000).

There are two families of ACh receptor, muscarinic ACh receptors (mAChR) and nicotinic ACh receptors (nAChR). There are five classes of metabotropic mAChRs, $M_{1\text{-}5}$, which can be divided into two groups, M_1-like ($M_{1,3,5}$) and M_2-like ($M_{2,4}$) receptors. The mAChR are often postsynaptic, but when located presynaptically on ChI axons tend to act as autoreceptors. M_1-like receptors couple to $G_{q/11}$, and have excitatory effects by inhibiting K^+ currents, whereas M_2-like

receptors couple to $G_{i/o}$ and are inhibitory due to βγ inhibition of VDCC and activation of inwardly rectifying K^+ channels (Brown, 2010; Leach et al., 2012). mAChR are expressed throughout the striatum, with M_1R and M_4R having the highest tissue expression (Hersch et al., 1994). mAChRs have broad and complex cellular effects following their activation due to the different classes of mAChRs having opposing actions on neuronal excitability depending on which G proteins they couple to, and many cell types express multiple classes of mAChRs (Brown, 2010; Leach et al., 2012). However the focus of this thesis work is to explore the modulatory effects of ACh on DA release which is directly mediated via nAChRs.

nAChRs are ligand-gated cation channels and belong to the cys-loop receptor family of ion channels, and therefore have high structural homology to $GABA_A$ receptors, glycine receptors and 5-HT_3-receptors. Cys-loop receptors are pentameric structures, where each subunit contributes to the large extracellular ligand-binding domain, the membrane spanning pore and a smaller intracellular C-terminus domain. The extracellular ligand-binding domain is formed of mostly β-sheet, and there are two ligand-binding sites at the interface between two of the subunits. Each subunit has four membrane-spanning α-helices, of which one contributes to the lining of the pore, while the other three act to shield the pore from the lipid membrane (Unwin, 2003). In comparison to nAChRs at the neuromuscular junction (NMJ), nAChR in the central nervous system (CNS) are often presynaptically located, where they function to modulate the release of many neurotransmitters, by virtue of their permeability to K^+, Na^+ and Ca^{2+}. The functional diversity of neuronal nAChRs is achieved by the large number of possible combinations of the nine α-subunits and three β-subunits. Varying the subunit composition of nAChR affects both pharmacological and physiological properties including sensitivity to ACh, desensitisation rates and Ca^{2+} permeability (Exley and Cragg, 2008; Bertrand et al., 2009).

Striatal DA terminals express nAChRs, mediating the modulatory action of ACh released from ChIs on DA release. Activation of nAChRs on DA terminals can be seen to have two

modulatory effects on DA release, the first is a gating effect, which affects how DA is released to different patterns of neuronal activity; the second is a driving effect on DA release. When nAChRs on DA terminals are activated, single pulse (1p) DA release is "clamped" so that release probability (Pr) is very high, meaning that there is very little facilitation of DA release with subsequent pulses. However, when nAChRs are blocked or desensitised this clamp is relieved, so that 1p DA release is depressed, and phasic patterns of activity evoke more DA than occurs with 1p (**Figure 1.3**) (Zhou et al., 2001; Rice and Cragg, 2004; Exley and Cragg, 2008). ACh is therefore capable of gating how DA release occurs in response to different patterns of activity, so that when nAChRs are activate, DA release is unresponsive to changes in DA neuron firing. In addition to the gating properties of ACh on DA release, it has recently been found that synchronised activation of a small population of ChIs, can activate nAChRs on DA terminals and drive DA release independently from activity in DA neurons both *in vitro* and *in vivo* (**Figure 1.4**) (Cachope et al., 2012; Threlfell et al., 2012). In order to fully understand how striatal DA release is controlled, it is therefore important to be aware of both the modulatory and driving actions of ACh on DA release.

Like DA neurons, ChIs exhibit a range of firing patterns, including low frequency tonic, irregular and burst firing both *in vivo* and *in vitro*. The low frequency tonic activity of ChIs is considered so characteristic of these neurons, that *in vivo* tonically active neurons (TANS) are often assumed to be ChIs (Wilson et al., 1990; Aosaki et al., 1995; Bennett and Wilson, 1999; Goldberg and Reynolds, 2011). Similarly to DA neurons, TANs change their firing patterns in response to salient and reward-related events. However in contrast to DA neurons, TANs show a pause in burst firing of 100-300 ms in response to a reward. The pause in burst firing is often flanked by a preceding burst of activity and then a rebound burst after the pause. When the response of DA neurons and TANs to a reward are considered together, the burst in DA neuron activity in response to reward corresponds to pauses in TAN activity (Aosaki et al., 1994; Morris et al., 2004).

Both ACh and DA have powerful modulatory effects on the flow of information through the striatum and therefore the transmission of information to other basal ganglia nuclei via MSNs (Bracci et al., 2002; Surmeier et al., 2011a; Tang et al., 2011). When considering the roles of these neuromodulators, it is crucially important to be aware of their complex and interconnected nature, where ACh can both increase and decrease DA, and DA can have both excitatory and inhibitory effects on the ChIs, and therefore ACh release (Consolo et al., 1992; DeBoer and Abercrombie, 1996; Pisani et al., 2000; Rice and Cragg, 2004; Zhang and Sulzer, 2004).

In addition to ACh, there are other modulatory molecules in the striatum including small molecules (ATP, NO, H_2O_2), peptides (SP and cholecystokinin (CCK)) and monoamines (histamine and serotonin (5-HT))(Starr, 1982; Guevara Guzman et al., 1993; Avshalumov and Rice, 2003; Kombian et al., 2003; Blomeley and Bracci, 2009; Hartung et al., 2011; Tautenhahn et al., 2012; Alfaro-Rodriguez et al., 2013). Many of these neuromodulators have been shown to modulate DA release, however for some of the neuromodulators it is not fully characterised if their effects on DA are direct or via the cholinergic system. In chapter 5 I discuss my investigation of the modulatory effects of SP on DA release in the absence of the potentially confounding effects of ACh. Understanding how these neuromodulators affect one another will greatly enhance our understanding of striatal function, and the highly integrated nature of these systems should be borne in mind when considering the properties and functions of each individual transmitter.

1.3 Pathophysiology

As discussed above, DA is essential for the control of a wide range of behaviours including locomotion and reinforcement learning. Due to the broad physiological function of DA in the brain, aberrant DA neurotransmission is associated with a number of psychomotor disorders including Parkinson's disease (PD), addiction, schizophrenia and attention deficit and hyperactivity disorder (ADHD) (Graybiel, 2008; Crittenden and Graybiel, 2011; Dean, 2012; Surmeier and Sulzer, 2013). The studies described in chapter 3 investigated the role of VDCCs in

controlling DA release between striatal regions, which are differently affected in PD. I further explore the possible relationship between Ca^{2+} and DA release in disease, using a mouse model of PD in chapter 4.

1.3.1 Parkinson's disease (PD)

PD is the second most common neurodegenerative diseases after Alzheimer's disease (AD), which is estimated to affect around 1% of people over the age of 65 (Tanner and Goldman, 1996). PD is characterised by a triad of motor symptoms, namely resting tremor, bradykinesia and rigidity, in addition to a number of non-motor symptoms including constipation, loss of smell and sleep disturbances (Samii et al., 2004; Park and Stacy, 2009). In an aging population, the health and economic burden of PD is only going to increase, meaning that understanding the aetiology and progression of PD is timely and necessary to facilitate discovery of potential drug and treatment options.

PD is most commonly an idiopathic disorder, although rare inherited forms of the disease do exist (Singleton et al., 2003; Chartier-Harlin et al., 2004; Samii et al., 2004). The motor symptoms of PD are thought to be primarily due to the progressive and dramatic loss of striatal DA, due to the death of SNc DA neurons, which innervate the dorsolateral aspect of striatum (Hornykiewicz, 1998). A hallmark of both inherited and idiopathic forms of PD is the differential sensitivities of distinct populations of DA neurons to degeneration in PD; the calbindin-negative, ventral tier of SNc DA neurons are especially sensitive to death in PD, whilst calbindin-positive SNc dorsal tier and VTA DA neurons are relatively spared (Gerfen et al., 1985; Iacopino et al., 1992; Hornykiewicz, 1998; Surmeier and Sulzer, 2013). Understanding physiological differences between SNc and VTA neurons may provide insights to why SNc DA neurons degenerate and how to slow or even reverse damage to them.

When investigating why dopaminergic neurons are especially sensitive in PD, it has been proposed that DA itself is a source of oxidative stress, and predisposes these neurons to die in PD

(Miyazaki and Asanuma, 2008). If DA is the reason why midbrain DA neurons are so sensitive in PD, it raises the question of why are VTA dopamine neurons relatively resistant in PD. However this may be due to PD resistant areas express dopaminergic markers at lower levels: The NAc has lower TH and DAT expression levels, releases less DA and has lower DA content compared to CPu, despite VTA having a greater number of DA neurons but innervating a smaller volume (Nelson et al., 1996; Cragg et al., 1997; Björklund and Dunnett, 2007; Threlfell and Cragg, 2011). It may be true that the energetic burden caused by DA axons is less in VTA dopaminergic neurons because the "density" of DA is less, making them less sensitive in PD. In accordance with this hypothesis SNc DA neurons, consistently show high levels of vulnerability during normal aging and other neurodegenerative diseases (Surmeier, 2007).

Although it may be true that DA is a source of oxidative stress for neurons that may contribute to cell death in PD, the SNc DA neurons also have particular anatomical properties that place huge energetic demands on the neuron and likely to make them particularly sensitive to cellular stress: SNc DA neurons have long unmyelinated axons, which form extensive arbors, estimated as being ten times larger and more complex than other, less susceptible neurons (Braak et al., 2004; Arbuthnott and Wickens, 2007; Matsuda et al., 2009; Bolam and Pissadaki, 2012). Normal physiological processes including maintenance of resting membrane potential, propagation of action potentials, and synaptic transmission places an enormous energetic demand on SNc DA neurons, due to their vast and complex axonal architecture (Arbuthnott and Wickens, 2007; Bolam and Pissadaki, 2012; Harris et al., 2012).

Considering the vast differences in sensitivity to degeneration in PD, between SNc and VTA neurons, they have surprisingly similar transcriptomes that vary by less than 1% (Grimm et al., 2004; Greene et al., 2005). Despite this, some differences have been identified including the expression of calbindin-D28K in DA neurons resistant to cell death in PD which has led to the proposition that calbindin-D28K is neuroprotective (Yamada et al., 1990; Lavoie and Parent, 1991;

Iacopino et al., 1992). Contradictory to this hypothesis, it has been shown that calbindin-D28K null mice are no more sensitive to dopaminergic toxins than their littermate controls, despite not showing compensatory up regulation other calcium binding proteins, however it has been found that overexpression of calbindin-D28K promotes neurite growth and protects against toxins (Airaksinen et al., 1997; Yuan et al., 2013). In summary, calbindin-D28K may have some neuroprotective qualities, however calbindin-D28K does not account for all of the resistance VTA DA neurons show to PD induced cell death.

Many parkinsonian animal models are created by inducing oxidative stress exclusively in DA neurons e.g. 6-OHDA and MPTP, and that a common source of oxidative stress is excessive Ca^{2+} load (Blandini and Armentero, 2012). Excess Ca^{2+} can induce oxidative stress for a number of reasons; firstly Ca^{2+} is a ubiquitous intracellular signalling molecule, which is capable of activating multiple cellular cascades including the apoptotic pathway. Secondly because Ca^{2+} is a divalent cation, it is necessary for its concentration to be kept low to maintain resting membrane potential, and finally Ca^{2+} homeostasis is strictly monitored because removing intracellular Ca^{2+} is energetically expensive. The mitochondria act as cellular sinks for Ca^{2+}, however this dissipates some of the electrostatic potential of mitochondria, requiring more H^{+} to be transferred out of mitochondria to generate ATP. Therefore it is imperative for Ca^{2+} homoeostasis to be maintained in an as energy efficient process as possible (Ermak and Davies, 2002; Nedergaard et al., 2010; Surmeier et al., 2011b).

SNc and VTA DA neurons differentially rely on Ca^{2+} to establish slow oscillatory potentials (SOP) which support their autonomous pacemaker firing: In adolescence (in mice) both SNc and VTA DA neurons generate their SOP by Na^{+} currents, however in adulthood SNc neurons switch to using Ca^{2+} currents via Cav1.3 channels, whilst VTA neurons continue to utilise Na^{+} (Chan et al., 2007). Additional experiments discovered that by inhibiting Cav1.3 channels, adult SNc neurons could revert to using Na^{+} to generate SOP, and it was found that inhibiting Cav1.3 channels

decreased oxidative state of SNc neurons, via a mechanism that involves the mitochondrial protein DJ1 (Guzman et al., 2009; Surmeier et al., 2011b). The finding that Cav1.3 induced oxidative stress in SNc DA neurons involves DJ1 was particularly illuminating as mutations in DJ1 cause a rare inherited form of PD, possibly illustrating a common mechanism for inherited and idiopathic forms of PD (Bekris et al., 2010).

A common feature of PD is the accumulation of protein aggregates called Lewy bodies, of which the main component is α-synuclein (Marques and Outeiro, 2012). Mutations and increases in copy number of the α-synuclein gene (*SNCA*), can cause rare familial forms of PD, and *SNCA* is often identified as a common risk factor in genome wide association studies (GWAS) (Singleton et al., 2003; Chartier-Harlin et al., 2004; Simón-Sánchez et al., 2009; Bekris et al., 2010; Marques and Outeiro, 2012). The function of α-synuclein is still not fully understood, but it appears to bind to vesicles and is usually presynaptically located (Clayton and George, 1998; Kahle et al., 2000), however α-synuclein has been shown to modulate transcription (Baptista et al., 2003; Goers et al., 2003; Yu et al., 2007). Additionally, α-synuclein can modify both DA content and DA release in the striatum in a dose and age dependent manner, which shows that α-synuclein does have a functional role in striatal release, despite a mechanism not being known (Senior et al., 2008; Anwar et al., 2011; Janezic et al., 2013). Mutations in α-synuclein are likely to be one of many risk factors that interact to induce cell death in SNc DA neurons, as α-synuclein is a ubiquitously expressed protein and functions in multiple neuron types (Sulzer, 2007; Mosharov et al., 2009; Surmeier and Sulzer, 2013).

The loss of striatal DA is thought to cause the motor symptoms of PD because of over activation of the indirect pathway, leading to excessive inhibition of motor pathways (Wiecki and Frank, 2010). It has also been found that striatal DA depletion leads to increased synchrony in the basal ganglia circuitry especially in beta oscillating neurons, which has been associated with the motor symptoms of PD (Brown, 2003; Moran et al., 2011).

1.4 Summary

Striatal DA is central to a number of processes including motor control and reward-related behaviours, and dysfunction in striatal DA signalling is associated with a number of psychomotor disorders including PD and addiction. Changes in DA neuron firing are known to occur during reward-related behaviours, and it is assumed that increase in DA neuron firing correspond to increases in striatal DA release. However striatal DA release is known to be dynamically controlled at the terminals by a number of neuromodulators, most notably ACh. Therefore to fully understand the function and dysfunction of DA neuron activity, it is crucially important to understand how presynaptic DA release is controlled. In this thesis work I have used fast-scan cyclic voltammetry (FCV) in acute murine slices to investigate the presynaptic control of DA release. The methods used in this thesis work will be discussed in chapter 2. Chapter 3 explores the role of VDCCs in the control of DA release in two striatal regions, in the absence of the potentially confounding effects of ACh. Chapter 4 investigates if α-synuclein affects which VDCCs control DA release in the PD-sensitive region of the striatum. And finally, chapter 5 aims to resolve the current conflicting evidence surrounding the modulatory effects of SP on DA release by investigating the modulatory effects of SP along the striosome-matrix axis of the striatum.

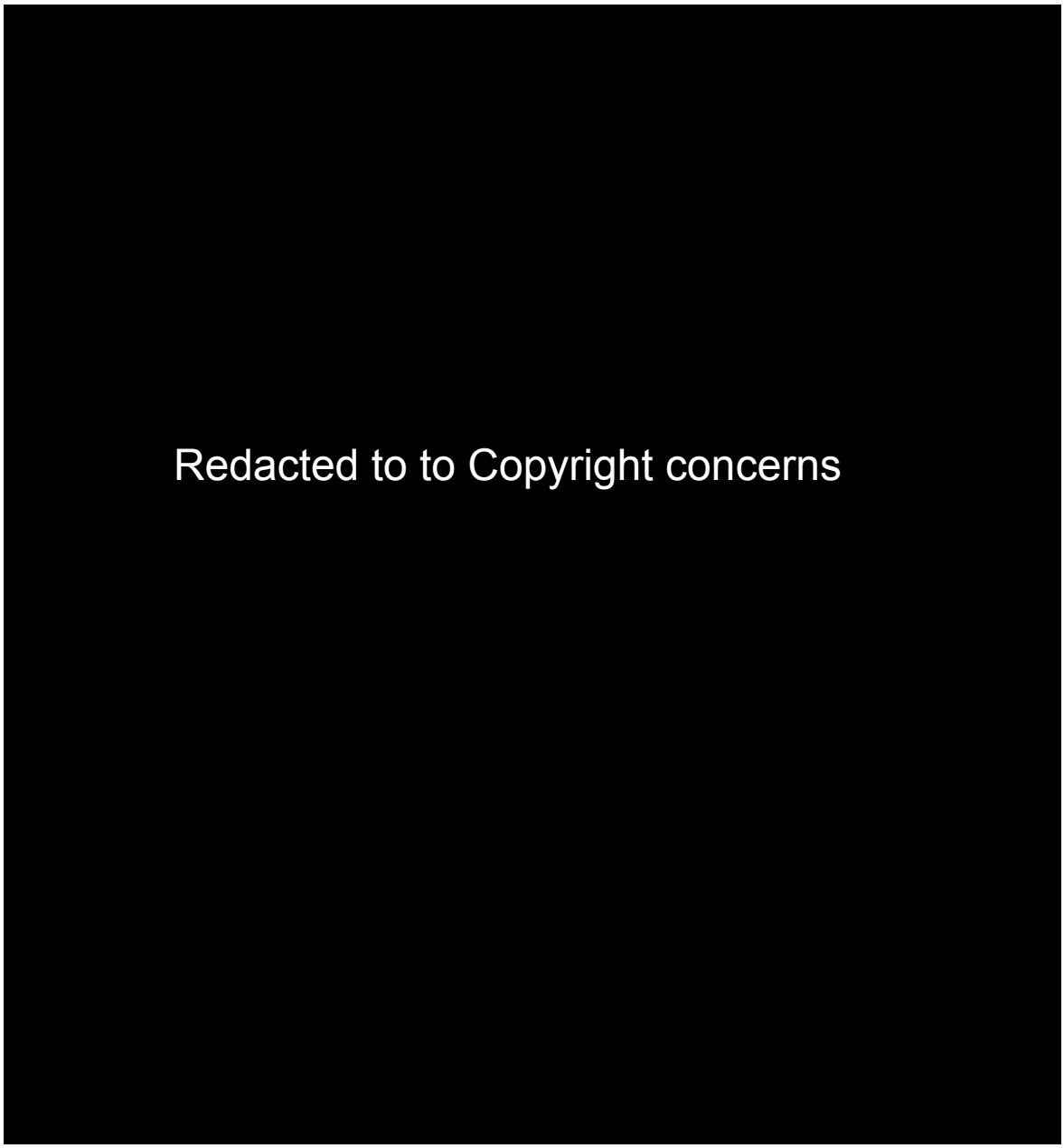

Figure 1.1 A simplified model of the dorsal aspect of the basal ganglia
The nuclei included within the blue box form the basal ganglia. Pathway **1** indicates the direct pathway formed by D_1R-expressing MSNs. Pathway **2** indicates the indirect pathway formed by D_2-R-expressing MSNs. Blue arrows indicate inhibitory GABAergic pathways, red arrows indicate excitatory glutamatergic pathways, yellow arrows indicate dopaminergic pathways and green indicate structures with variable neurochemistry. GPe: external segment of the globus pallidus; STN: subthalamic nucleus; SNr/GPe: substantia nigra pars reticulata and internal segment of the globus pallidus. Modified from Tepper et al (2007)

Figure 1.2 Schematic of formation of SNARE complex in exocytosis
Exocytosis requiresthe formation and dismantling of SNARE complexes to over come the energy barrier of disrupting the energetically stable phospholipid membrane. Transition from the trans-SNARE to cis-SNARE is triggered by Ca^{2+} binding, mediated by the proteins synaptotamin and complexin. Image from Südhof (2013)

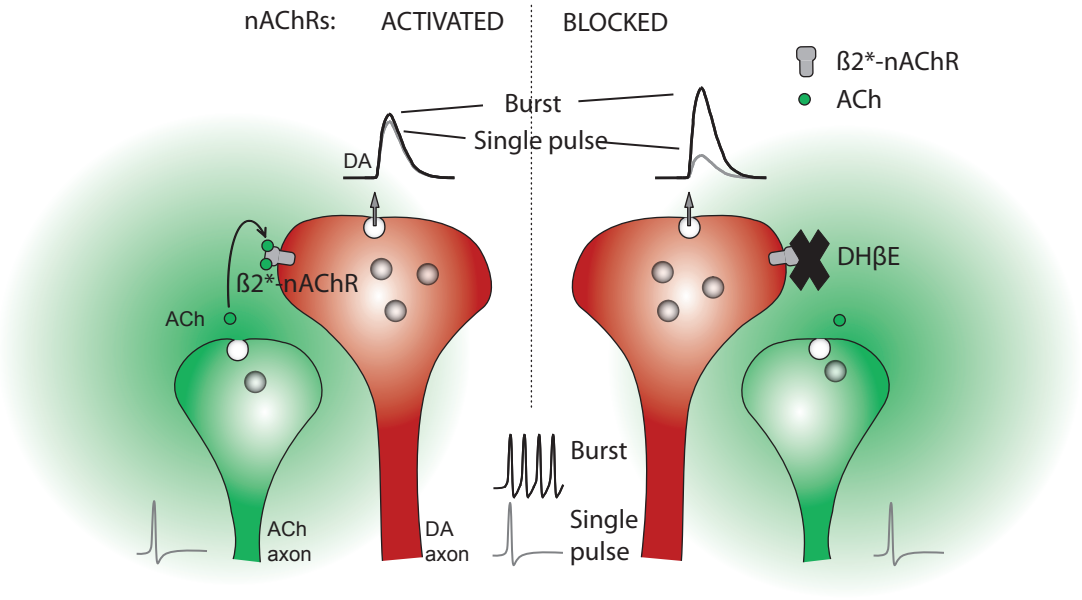

Figure 1.3 ACh modulates the short term plasticity of DA release

ACh released from ChIs acts at nAChRs on DA terminals to control the short-term plasticity of DA release. Activation of nAChRs results in short-term depression of release, resulting in equivalent amounts of DA being released following either a single plulse or a burst of activity. When nAChRs are inhibited (e.g. by DHβE), depression is relieved and burst stimulation evokes significantly more DA release than a single pulse. Modified from Exley et al. 2008.

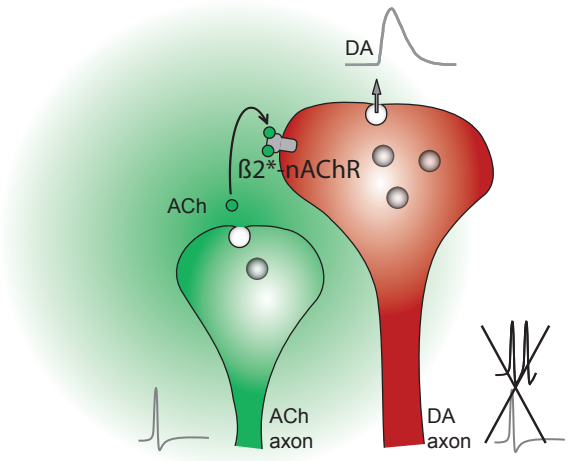

Figure 1.4 ACh directly evokes striatal DA release.

ACh released by synchronous activity in ChIs can act at nAChRs on DA terminals to drive striatal DA release, even in the absence of activity in DA neurons. Modified from Exley et al. 2008

2. Methods

In this chapter I will introduce the methods that are used throughout this thesis, including description and discussions of the model system used, fast-scan cyclic voltammetry (FCV) and immunohistochemistry.

2.1 Murine acute brain slices as a model system for studying DA release

DA neurotransmission is central to motor control and reward-related behaviour, and DA dysfunction is associated with human pathologies including Parkinson's disease (PD) and addiction. Understanding the mechanisms that control DA release could therefore provide insights to help us understand the aetiology, progression and potential therapies for DA related diseases. Due to methodological and ethical constraints, it is not possible to study DA release directly in the human brain, therefore it is necessary to use a model system to investigate the DA system in depth, and following verification, extrapolate our findings to the human brain. Throughout this thesis I have used acute coronal mouse brain sections that contain the striatum, and recorded evoked DA release using (FCV).

The mouse (*Mus muculus*) is an extensively used model organism due to a number of methodological and ethical reasons. For ethical reasons scientists aim to use the simplest (least sentient) animals, which still model the target system, which in this case is the human brain. Non-human primates have brains which are most similar to humans, however they are afforded special protection under the Animal Scientific Procedures Act, therefore unless it is scientifically necessary to use primates, rodents are often used instead. Rodent brains share many of the anatomical and pharmacological features of human brain, and even complex human behaviours can be modelled to a certain extent by rodents. Therefore for many experimental methods, rodents are a preferred model organism over simpler models including worms (*Caenorhabditis elegans*) and flies (*Drosophila melanogaster*). In addition to ethical reasons, rodents including mice make ideal model system for many methodological reasons: Firstly mice have a relatively short life cycle, allowing their physiology at multiple developmental stages to be investigated;

mice also breed easily, and can be ethically housed together and in a relatively small space. A crucial reason why mice are optimal model systems is that they are very amenable to genetic manipulation. The mouse was the first mammal to be genetically modified by targeted gene knock-out (Capecchi, 1989), and now it is possible to genetically manipulate the mouse in a number of ways including conditional knock-out, which allows the mouse to develop with a gene of interest so that when the gene is knocked-out there are limited compensation mechanisms occurring; knock-down allows a gene of interest to be expressed at lower levels by using small interfering RNA (siRNA) technology; transgenic mice express genetic material not endogenous to the mouse, i.e. optogentics, where light activated channels are inserted to allow particular excitable membranes to be activated with light; and targeted mutagenesis that introduces a mutation into a gene of interest, for example a gene related to a specific disease (Miyawaki and Schnitzer, 2007).

The majority of the work in this thesis was conducted in the mouse strain C57Bl6/J, which is a common inbred laboratory mouse strain. This strain is widely used because C57Bl6/J is the background strain for many genetically modified mouse lines, making comparisons between models easier. Some laboratory wild type strains of mice carry a spontaneous deletion of α-synuclein gene (Specht and Schoepfer, 2001), however C57Bl6J mice express the full α-synuclein gene making it our preferred line because we often need to compare our findings to PD model systems that have disrupted α-synuclein expression. In this thesis work I also used two transgenic lines of mice. In the studies discussed in chapter 3 I use a mouse line that expresses Cre-recombinase under the control of the DA transporter (DAT) promoter. These mice are sterotactically injected into the midbrain with a viral vector containing channelrhodopsin 2 (ChR2) gene, resulting in a mouse that selectively expresses ChR2 in midbrain DA neurons; and in chapter 4 I use a transgenic mouse line that expresses high levels of human α-synuclein (*SNACA* OVX) vs. α-synuclein null (*Snca* -/-) littermate controls.

All scientific models have their advantages and disadvantages, therefore it is crucial to use a model whose advantages are most beneficial and the disadvantages least affect the interpretation of the data being gathered. In this thesis work, acute coronal brain slices from the mouse are used as a model system for several reasons. Firstly, the slices are taken from a brain that has reached maturity with all the normal connections and interactions intact. This means that cellular components will have their normal protein expression patterns and that proteins including voltage-dependent calcium channels (VDCCs) will be expressed with their normal accessory subunits so that the role of such channels can be investigated in a near physiological manner. This is an advantage over cultured DA neurons, which lack of the interacting network of cells that are normally present, and therefore could affect their physiology. . Therefore although synaptosome preparations and cultured neurons permit a simplified model, which allow precise manipulation of presynaptic release, it is preferable to investigate how DA release is controlled in a more physiological network because it allows meaningful comparisons between brain regions to be made.

Acute slices also allow application of known drug concentrations, and their effects can be measured on an individual process (i.e. DA release) in a specific anatomical region. This is an advantage over whole animal *in vivo* techniques, because despite *in vivo* techniques benefiting from investigating an intact system, it is harder to dissect out individual factors controlling a complex process such as DA release because drugs are generally applied systemically and will often have many targets and affect a number of processes. to. For example, when investigating the role of a neuromodulator on DA release in a whole animal experimental model, a neuromodulator given systemically will affect numerous targets in the basal ganglia both pre- and post-synaptically which may well feed onto one another. Therefore when investigating the effect of a neuromodulator such as substance P (SP) on the control of DA release it is optimal to use an acute brain slice preparation, where the potential targets are more limited and the actual targets can be determined using pharmacology and by assessing the time course of an effect.

Additionally the effect of a drug, used to probe the role of channel or receptor, may interact with the anaesthesia used during an *in vivo* experiment, which could affect the interpretation of an experiment (McFarlane et al., 1995).

Lastly using acute brain slices also has ethical advantages, because the potential for an animal to suffer pain, distress or lasting harm is greater for *in vivo* work. It is possible to use a single animal for multiple experiments, because approximately five striatal slices (300 µm) can be taken from a single animal, and those slices can be bisected. Performing multiple experiments on a single animal could also enhance the statistical power of an experiment, because it could allow a repeated measures design to be used. However due to the highly heterogeneous nature of the striatum, where site to site differences can account for as much variability as inter-animal differences, such a study would have to be carefully designed. In addition to there being multiple striatal sections in a single animal, it is also possible to use other tissue, even if not answering a related question: For example during my DPhil work, I coordinated with another member of the department so that she could use the heart of a mouse, from which I had already taken the brain. Such cooperation may not be possible if an animal had been under anaesthetic and had systemically applied drugs during an *in vivo* procedure.

In summary I have used acute 300 µm coronal mouse brain slices, which have many of their local striatal networks maintained. Despite the DA axons being severed from their cell bodies in the midbrain, they can still release DA for over nine hours (Bull et al., 1990). The afferent connections to the striatum are also severed but their axons remain, so that interactions between glutamate released from afferent terminals, MSNs, cholinergic interneurons (ChIs), GABAergic interneurons and DA terminals are all preserved (Koós and Tepper, 1999; Avshalumov and Rice, 2003; Rice and Cragg, 2004; Zhang and Sulzer, 2004; Hartung et al., 2011; Threlfell et al., 2012).

2.1.1 Generating slices

All animals were maintained and procedures carried out in accordance with UK Home Office and local guidelines. Most of the experiments in this thesis work used adult (>35 days) male C57Bl6/J mice (wild-type [WT]) (Charles River). In addition to the use of tissue from WT animals, transgenic animals were also used sparingly in this thesis.

In studies described in Chapter 3 an optogenetic approach was used: Heterozygous mice expressing Cre-recombinase under the driver of the DAT promoter (DAT-Cre) on a C57Bl6/J background (bred from stock from Jackson laboratories B6.SJL-*Slc6a3*$^{tm1.1(cre)Bkmn}$/J, stock # 006660) were injected with the Cre-inducible adeno-associated virus serotype 5 (AAV5) containing the ChR2 gene in-frame with coding sequence for enhanced yellow fluorescent protein (eYFP) by Dr Nicola Platt. Mice were injected with 0.5-1.0 µl of virus at a rate of 0.2 µl/min bilaterally in the midbrain in either the VTA (coordinates from Bregma in mm: anterior-posterior (SP) -3.1, medial-lateral (ML) ±0.5, dorsal-ventral (DV) -4.4) or SNc (AP -3.5, ML ±1.2, DV -4.0). The SNc and VTA were targeted in separate hemispheres. Animals were maintained for at least 10 days following surgery to allow time for virus infection and ChR2 expression.

In the studies described in Chapter 4 DA release was studied in a transgenic mouse line that expresses high levels of human α-synuclein (*SNCA* OVX) and α-synuclein null (*Snca* -/-) littermate controls. *SNCA* OVX mice were generated by injecting wild-type C57Bl6 mouse pronuceli with a bacterial artificial chromosome (BAC) that contains the entire human α-synuclein gene locus, including up- and downstream untranslated regions, selected lines were then backcrossed onto *Snca*-/- pure C57Bl6 background for nine generations. The *SNCA* transgene was maintained in a hemizygous state on a pure C57Bl6 background .

Mice were killed by cervical dislocation and their brains were rapidly removed and transferred in to ice-cold HEPES-based buffer solution containing in mM: 120 NaCl, 20 $NaHCO_3$, 6.7 HEPES acid, 5 KCl, 3.3 HEPES salt, 2 $CaCl_2$, 2 $MgSO_4$, 10 glucose, saturated with carbogen. 300 µm thick coronal sections containing both CPu and NAc were cut using a vibrating

microtome(VT1200S; Leica) whilst submerged in ice-cold HEPES-based buffer. Slices were maintained at room temperature in HEPES-based buffer for one hour.

2.2 Fast scan cyclic voltammetry (FCV)

Throughout this thesis work evoked DA release was monitored using FCV at carbon fibre microelectrodes (CFM). FCV is an electrochemical technique that exploits the fact that DA has two hydroxyl groups that oxidise at a specific potential, and that the resultant current from this redox event can be measured and is proportional to the amount of DA present. A triangular waveform of -700 mV to +1300 mV and back, relative to a Ag/AgCl reference electrode, is scanned across the CFM (**Figure 2.1**). DA oxidises to dopamine-o-quinone, and is reduced back to DA on the upwards and downwards sweep of the scan respectively (**Figure 2.2**). The concentration of DA evoked by stimulation of a striatal slice at the electrode surface can be quantified by calibrating the CFM, with a known concentration of exogenous DA and measuring the response of the electrode. The amplitude of the oxidation current detected is directly proportional to the concentration of DA, for the range of DA concentrations typically detected in striatal slices (**Figure 2.3**) (Kelly and Wightman, 1987; Bull et al., 1990).

Much of our understanding of neurotransmitter release is from studying GABA and glutamate release in the hippocampus, where release events are monitored by measuring post-synaptic effects and by measuring Ca^{2+} influx using Ca^{2+} sensitive fluorescent dyes (Reuter, 1995; Emptage et al., 2001; Rusakov, 2006; Myoga and Regehr, 2011; Zhao et al., 2011). However it is not known if DA release, which occurs both synaptically and extrasynaptically via volume transmission is governed by the same rules that apply to classical neurotransmitters in the hippocampus (Cragg and Rice, 2004; Rice et al., 2011; Trueta and De-Miguel, 2012). FCV is an exceptionally powerful technique that allows endogenous DA release to be directly monitored with sub-second temporal resolution in a regionally discrete location. The scan rate of the triangular waveform is fast, occurring at 800 V/s, meaning that the entire sweep takes only 5 ms,

which is on the same temporal scale as physiological transmitter release. The fast scan rate of the waveform allows them to be applied at a high frequency, therefore increasing the resolution of the time course of DA release events. A scanning frequency of 8 Hz is used, permitting the amount of DA to be readout every 0.125 s. The high temporal resolution of FCV is in contrast to microdialysis, which integrates measurements of DA release across several minutes (Salamone, 1996; Robinson and Wightman., 2007). An additional benefit of FCV over microdialysis, is that the CFM used to record DA in FCV is very small, with a diameter of 7-10 µm, compared to a microdialysis probe, which is an order of magnitude higher. The large microdialysis probe can cause significant tissue damage and also does not have the spatial resolution necessary to discriminate between striosome and matrix territories of the striatum, due to striosomes generally being between 100-200 µm across (Bungay et al., 2003).

Amperometry is an alternative electrochemical technique to FCV that can also measure DA release with the same spatial resolution as FCV and better temporal resolution (Michael and Wightman, 1999). However amperometry does not allow the oxidisable molecule to be identified, whereas FCV can discriminate between DA, 5-HT, norepinephrine and epinephrine (Michael and Wightman, 1999). The discrimination between DA, 5-HT and others is possible because the triangular waveform used in FCV produces a characteristic voltammogram, where the oxidisation and reduction peaks occur at particular potentials for different molecules.

Finally recording DA using FCV in acute coronal mouse brain sections is a very stable technique, so that experiments can monitor DA release over several hours with little or no deterioration of the electrode (Bull et al., 1990). Adsorption of DA to the CFM is minimised by the cyclic form of the scanning waveform and that the electrode is switched out of circuit in between scans. When measuring 5-HT release with FCV, adsorption is much more of a problem and is apparent when calibrating CFM with 5-HT, also chronically implanted CFM that are used to measure DA release *in vivo* are also subject to adsorption.

2.2.1 Producing carbon fibre microelectrodes (CFM)

CFMs are produced in house so that each CFM is used for only one experiment; this prevents recordings from being perturbed by changes in electrode kinetics, which can occur when electrodes are used for multiple experiments. A borosilicate glass capillary tube (outer diameter 2.0 mm, inner diameter 1.16 mm, Harvard Apparatus, UK) was filled with acetone to allow an epoxy-free 7 µm diameter carbon fibre (Goodfellow Cambridge Ltd, UK) to be fed through the capillary tube. The acetone also acts to clean the carbon fibre. Epoxy-coated carbon fibres were also trialled, however they were found to be approximately three times less sensitive to DA compared to epoxy-free carbon fibre. Following acetone removal from the capillary tube (either through blotting with filter paper or from evaporation) the capillary tube was pulled into two equal parts under high heat setting using an electrode puller (Narishige, Japan) resulting in a tight seal to be formed around the carbon fibre protruding from one of the capillary tube halves. The heat setting was adjusted so that the seal was sufficiently tight to provide good signal to noise ratio during recordings, but loose enough so that the join between the carbon fibre and glass was visible under 10x objective. The carbon fibre was cut so that the distance from seal to tip was between 50-100 µm. To allow the electrode to be connected to the voltammeter a length of insulated wire is connected to the fibre by forming a conductive connection, by stripping ~0.5 cm of the plastic covering of the wire and dipping the end in conductive paint. The wire is then held in place by using a small drop of superglue to form a seal between the wire and end of capillary tube.

2.2.2 FCV methodology

Acute striatal brains slices (300 µm thick), generated as described above, were transferred into the recording chamber using a dropper pipette. The slices were secured using ~ 8 silver pins and constantly superfused with bicarbonate based buffer aCSF (containing in mM: 124.3 NaCl, 26 $NaHCO_3$, 3.8 KCl, 2.4 $CaCl_2$, 1.3 $MgSO_4$, 1.2 KH_2PO_4, 10 glucose) saturated with 95% O_2 5% CO_2 at a rate of approximately 1.5 mL/min and maintained at 31-33 ^{O}C. A CFM was inserted ~100 µm into

the tissue at a 45^{O} angle in region not intended to be the recording site and left to cycle for 30-60 minutes prior to recording. During this charging period the suitability of the electrode was checked to ensure the electrode has a good seal and tip length by observing that the signal was quiet and the full signal gain was between 3-10 mV/nA respectively. If the electrode was not deemed suitable it was discarded and an alternative selected. A triangular waveform (-700 to +1300 mV and back vs. Ag/AgCl reference electrode, scan rate 800 mV/s) was scanned across the CFM using a Millar voltammeter, and a sampling frequency of 8 Hz was used. It was confirmed that the electroactive molecule being detected was DA by comparing the potentials of the oxidation and reduction peaks of the voltammogram to those seen when a known concentration of DA is applied exogenously during calibration. The oxidation and reduction potentials of DA are +600 mV and -200-250 mV respectively. At the end of each experiment CFMs were calibrated in each of the experimental solutions containing a known concentration of DA (usually 2 μM, because the bigger the signal the more accurately it can be measured, whilst still being in the range of experimental measurements and within the range where $[DA]_O$ is directly proportional to current). The calibration solution was rapidly superfused over the CFM and the signal at the peak oxidation potential was measured. The calibration solutions were made up immediately before use, from stock solutions of 2.5 mM DA in $HClO_4$ stored at $4^{O}C$. Electrodes ranged in sensitivity from 5-25 nA/μM. Electrode sensitivity was affected by extracellular Ca^{2+} concentration, where higher concentrations of calcium made CFMs less sensitive to DA and vice versa (Kume-Kick and Rice, 1998). SNX 482 also could reduce the sensitivity of CFMs to DA by approximately 30%. The DA signals recorded during experiments could be converted into concentrations using the calibration values because the size of the oxidation peak is directly proportional to the DA concentration for range of DA concentrations recorded during experiments.

2.3 Evoking DA release

In our acutely prepared coronal striatal slices the DA axons are severed from their cell bodies, meaning that we do not detect spontaneous DA release, and have to exogenously stimulate the DA terminals either by electrical stimulation of the tissue, which will depolarise all excitable membranes or selectively using an optogenetic strategy. Throughout this thesis work I was interested in comparing the mechanisms controlling DA release in two distinct striatal regions: the dorsolateral caudate putamen (CPu) and a ventral portion of the striatum, the nucleus accumbens core (NAc) (**Figure 2.4**). Therefore DA was locally evoked and locally recorded using either electrical or light stimulations, as opposed to evoking DA in a regionally non-specific manner by application of high concentration of K^+.

2.3.1 Electrically evoked DA

DA release was electrically evoked using a bipolar concentric Pt/Ir stimulating electrode (25 µm diameter, FHC) placed on the surface of the tissue, approximately 100 µm away from the CFM. Stimulation pulses of 200 µs pulse width and perimaximal current of 0.6 mA are delivered using a current stimulator (Digitimer DS3, UK), unless otherwise specified. In some experiments, especially when the DA signals were very small, the recording software (Axoscope 10.2, Molecular Devices, UK) was time locked to the delivery of stimulation pulses using Master-8 stimulator (A.M.P.I, Israel), so that recording started 1 second prior to the delivery of a stimulation, enabling the point at which DA was evoked to be known. The delivery of pulses was also maintained out of phase from the voltage sweeps of the voltammeter to prevent "clashes" between the recording of DA and detection of the stimulation current by the CFM. Stimulations were applied at 2.5 minute intervals, which allows sustained and reliable levels of DA to be evoked and recorded over several hours (<8 hrs.). Data were only included for analysis after $[DA]_O$ was stable and reproducible.

2.3.2 Optically evoked DA

In some experiments it was desirable to selectively stimulate DA terminals, therefore an optogenetic strategy was used: DA was evoked in genetically modified mice, which selectively express the light activated non-selective cation channel channelrhodopsin 2 (ChR2), in midbrain DA neurons. As was explained above, the viral vector AAV5 that contains floxed ChR2 gene was stereotaxically injected into the midbrain of transgenic mice that express the recombinase enzyme Cre, under the DAT-promoter. The striatal subregions of these mice can be stimulated with pulses of blue light to drive exclusively DA release. Two different methods of optical stimulation were used. A laser system, which used a 473 nm diode laser (DL-473, Rapp Optoelectronic) coupled to the microscope via an optic fibre (200 µm multimode, N.A. 0.22). This illuminated 60 µm diameter spot (20x water-immersion objective); and an LED system that used a 470 nm LED (OptoLED, Cairn Research), which illuminated the full-field of view (2.2 mm, 10x water-immersion objective). For both systems the light source was driven by a 2 ms TTL pulse, with perimaximal intensity, which was determined at the start of each experiment. 1, and 5p stimulations (1-25 Hz) were delivered at 2.5 min intervals, which produce reliable DA release sustained over the course of an experiment.

Optically evoked DA release was only used to corroborate findings from electrically evoked DA release in wild-type animals in chapter 3 experiments in which I investigated the role VDCCs in the control DA release, because it is possible that the introduction of foreign ion channels may affect VDCC control DA release due to ChR2 being a non-specific cation channel. The simulation parameters used here are those that have been optimised by other members of the lab (Drs Sarah Threlfell and Nicola Platt) and have been published previously (Threlfell et al., 2012).

2.3 Data analysis

Data were acquired and analysed using Axoscope 10.2 (Molecular devices) or Whole Cell Programme (WCP; University of Strathclyde, Glasgow) and Excel macros written locally. Data are expressed as mean ± standard error of the mean (SEM), where n = number of animals. Data from each animal were calculated by averaging at least 3 recordings at each stimulation frequency, and normalising to control conditions for each animal. Parametric tests were used when raw data passed Shapiro-Wilk normality tests. Statistical analysis was carried out using GraphPad Prism software for both comparison of means and linear and non-linear regression analysis. A significance level of $p<0.05$ is used throughout this thesis. The following symbols have been used to indicate levels of significance *$p<0.05$, **$p<0.01$, ***$p<0.001$.

2.4 Immunohistochemistry

Immunohistochemistry was used for two purposes in this thesis work, firstly to confirm the cell-type specific expression of ChR2 in chapter 3 and secondly to visualise striosome-matrix sub-divisions of the striatum in chapter 5.

2.4.1 Tyrosine hydroxylase (TH) immunoreactivity

The viral construct used to insert ChR2 into midbrain DA neurons contains the ChR2 gene in-frame with the coding sequence for eYFP, which allows all ChR2 expressing cells to be visualised. To confirm that ChR2 insertion was specific to DA neurons the midbrains of injected mice were processed for tyrosine hydroxylase (TH)-immunoreactivity, and co-localisation of eYFP and TH was identified. TH catalyses the rate limiting step of catecholamine synthesis, therefore in many brain regions (where adrenergic and noradrenergic neurons are not present), TH immunoreactivity serves as a selective marker of DA neurons. The midbrains of injected mice (corresponding to between approximately -2.8 and -3.8 mm from Bregma, which contain VTA and SNc) were sectioned at 300 µm using a vibratombe (VT 1200, Leica) then sandwiched between pieces of filter paper to avoid curling and transferred into fixative: Either neutral buffered 10% formalin

solution (NBF) (Sigma); or 4% paraformaldehyde (PFA) dissolved in phosphate-buffered saline (PBS) (120 mM NaCl; 2.7 mM KCl; 10 mM phosphate buffer salts) containing 0.2% picric acid, then stored at 4^{O}C for at least 3 days. Sections fixed in PFA needed to be either re-sectioned after 3 days or transferred into PBS. Formalin fixed slices did not need to be transferred into PBS, because formalin fixation is reversible, and did not appear to suffer from over-fixation (the longest fixation period was ~12 weeks). Post fixation, tissue were washed 3x in PBS then re-sectioned to 40 µm (free floating) using a vibrating microtome (VT1000, Leica). Slices were incubated in PBS containing 0.5% Triton-X-100 (PBS-TX) 10% normal goat serum (NGS) and 10% foetal bovine serum for 30 minutes. Slices were then incubated in PBS-TX, 1% normal goat serum (NGS), 1% foetal bovine serum and 1:2000 primary antibody (rabbit anti-TH, Sigma Aldrich) at 4^{O}C overnight. Slices were then washed in ice cold PBS for 5-10 minutes three times before incubation in PBS-TX, 1% NGS, 1% foetal bovine serum and 1:1000 secondary antibody (Dylight 594 goat anti-rabbit. Jackson) for 2 hours at room temperature. Slices were then washed in ice cold PBS before being mounted on polysine coated slides (VWR) and coverslipped with hard mount Vectashield (Vector labs). Slides were imaged for TH-immunoreactivity (red) and eYFP fluorescence with an Olympus BX41 microscope with Q-Click cooled monochrome CCD camera (Olympus medical). Monochrome images were converted to pseudo-colour images using Q-capture pro7 and images were optimised using histogram equalisation.

2.4.2 µ-opioid receptor (MOR) immunoreactivity

For experiments described in chapter 4 CFM placements were marked and the tissue was processed for MOR immunoreactivity: Following FCV recordings, CFM placement was marked with yellow-green FluoSpheres (1 µm diameter, Invitrogen product number F-13081), then striatal sections were processed for MOR-immunoreactivity to visualise MOR-rich striosome and MOR-poor matrix regions. I developed the following protocol for marking CFM placement sites, and using published literature I optimised a protocol for visualising the striosome-matrix axis via their different expression densities of MOR.

Making the micropipette: A graduated micropipette was pulled to a seal in an electrode puller (Narishige, Japan) at heat setting 5.8-6.2 (arbitrary units), resulting in a tip length of 0.8-1 cm. The sealed tip was cut using scissors, so the tip was ~0.5 cm in length, giving an aperture of ~40 µm. The FluoSpheres were agitated in a sonicator and 0.5-1.0 µL of FluoSpheres were taken up by capillary action into the graduated micropipette. I found that cutting the tip flush, was preferable to a bevelled edge, because a bevelled edge created a streak of FluoSpheres rather than the dense point that can be achieved with a flush cut. Interestingly, cutting the tip of the micropipette so that it was >0.5 cm long (giving a larger aperture) did not seem to increase the area which was marked by FluoSpheres.

Marking recording electrode placement: To indicate the CFM placement, the stimulating electrode was placed on the surface of the tissue, directly above the tip of the CFM, which was disconnected from the circuit. The recording chamber was emptied of aCSF, which prevented the micropipette from emptying as soon as meniscus of the dye contacts aCSF. If the recording chamber was not drained, the micropipette emptied as soon as it enters the bath, and the dye coats the surface of the tissue and the stimulating electrode. The stimulating electrode placement was re-checked before removing the CFM and the surface of the tissue was carefully dried with filter paper. The micropipette was placed in the CFM holder and moved so that it was directly above the stimulating electrode. The stimulating electrode was moved out of the way and the micropipette was rapidly lowered vertically into the tissue to ~ the same depth as the CFM (100 µm) (N.B. the micropipette is mounted in the holder at 45^{O}, and lowered 100 µm into the tissue on the *z*-axis.) If the micropipette was lowered at 45^{O} (i.e. the same path as the CFM) then I found that the tip of the micropipette gets blocked, and the FluoSpheres only labels ~20-40 µm into tissue. I initially used Pontamine sky blue as a dye to mark CFM placements; however the marking did not withstand the fixation, re-sectioning and immunostaining-protocol.

Processing of tissue for μ-opioid receptor (MOR) immunoreactivity: The tissue was transferred into fixative (either PFA of NBF 4% formaldehyde), sandwiched between filter paper to keep it flat. Tissue was kept in fixative for at least 7 days; shorter fixation periods were trialled but were found to be non-optimal. Post fixation, tissue was washed 3x in PBS then re-sectioned to 40 μm (free floating) using a vibrating microtome. Sections were incubated in PBS-TX (0.3%) 20% NGS and 5% foetal bovine serum for 4 hours and then incubated overnight at 4^{O}C in primary antibody for MOR (1:1000 rabbit anti-MOR; Sigma) diluted in PBS-TX with 5% normal goat serum (NGS) and 1% foetal bovine serum. Sections were washed once in PBS then twice more in PBS-TX (0.3%) then incubated for 2 hours at room temperature in secondary antibody (1:1000 DyLight 594 goat anti-rabbit; Jackson) diluted in PBS-TX and 1% NGS and foetal bovine serum. Sections were then washed once in PBS-TX then twice in PBS before being mounted on polysine-coated slides and coverslipped with hard mount Vectashield (Vector labs). Slides were imaged for MOR-immunoreactivity (red) that distinguishes between MOR-rich striosomes and MOR-weak matrix, and FluoSpheres (yellow-green) used to mark the recording site with an Olympus BX41 microscope with Q-Click cooled monochrome CCD camera (Olympus medical). Monochrome images were converted to pseudo-colour images using Q-capture pro7 and images were optimised using histogram equalisation (**Figure 5.2**) On a few occasions CFM placement sites was marked so heavily with FluoSpheres that they were visible when illuminated under the red filter cube, therefore a further optimisation would be to use blue-green FluoSpheres rather than the yellow–green beads used here. It is not immediately clear why the yellow-green FluoSpheres are excited when the red filter cube is being used, as the upper-limit of excitation for the FluoSpheres is 520 nm, whereas the red-filter cube (U-M49008) has an excitation range 540-580 nm.

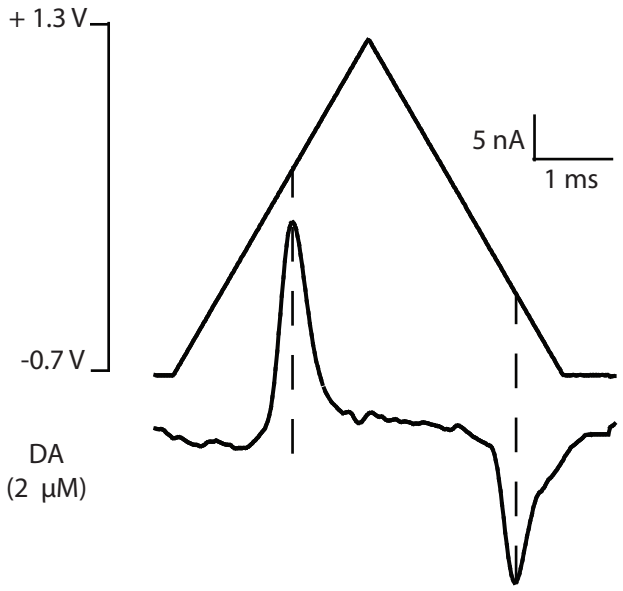

Figure 2.1 Triangular waveform and representitive voltammogram
waveform scan from -1300 mV to +700 mV relative to Ag/AgCl reference electrode. Representative voltammogram of striatal DA evoked by electrical stimulation, showing characteristic oxidation and reduction peaks at +600 mV and -200-250 mV respectively

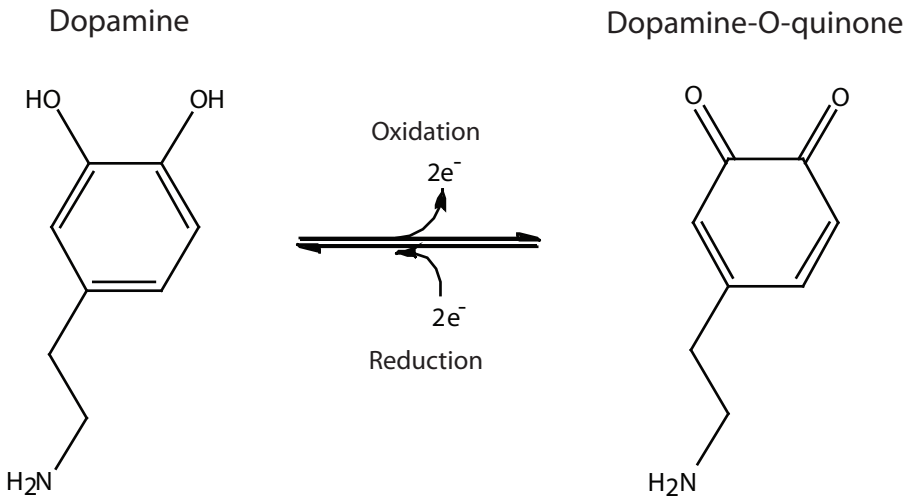

Figure 2.2 Redox reaction of dopamine to dopamine-O-quinone.
On the upward sweep of the triangular waveform, the two hydroxyl groups of DA are oxidised to give dopamine-O-quinone. On the downward sweep of the waveform, dopamine-O-quinone is reduced back to dopamine. The transfer of electrons results in a current that is proportional to DA concentration and, which is detected by the carbon-fibre microelectrode.

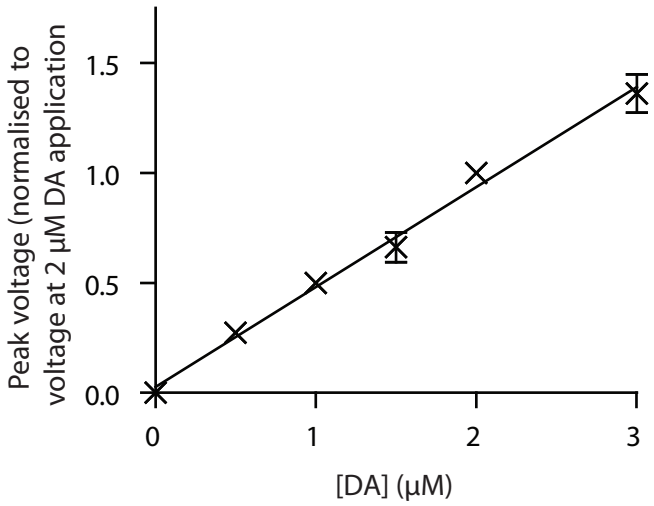

Figure 2.3. Currents recorded at CFMs are directly proportional to [DA] within the relevant experimental range.
Mean peak oxidation currents ±SEM recorded at CFMs, normalised to the current produced by application of 2 µM DA, against concentration of applied DA, across a range of DA concentrations reflecting those seen during electrical stimulation of ex vivo striatal slices. Currents are directly proportional to applied [DA] within this range (R^2=0.96; n = 4).

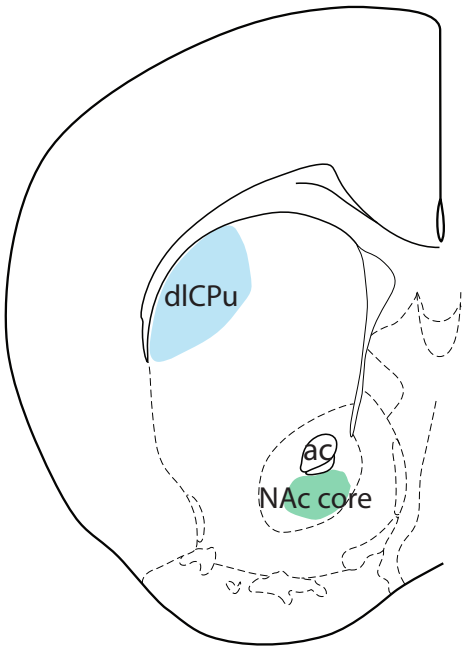

Figure 2.4 Diagram of coronal striatal slice with representative recording sites in dorsal and ventral striatum.
Acute coronal striatal slices were generated containing both dorsal striatum and NAc. When recording in the dorsal striatum, CFM were placed in the dorsolateral quadrant of the CPu (dlCPu) illustrated by the blue area. When recording in the ventral striatum CFM were placed in the NAc core, below the anteriror commisure (ac) shown by the green area.

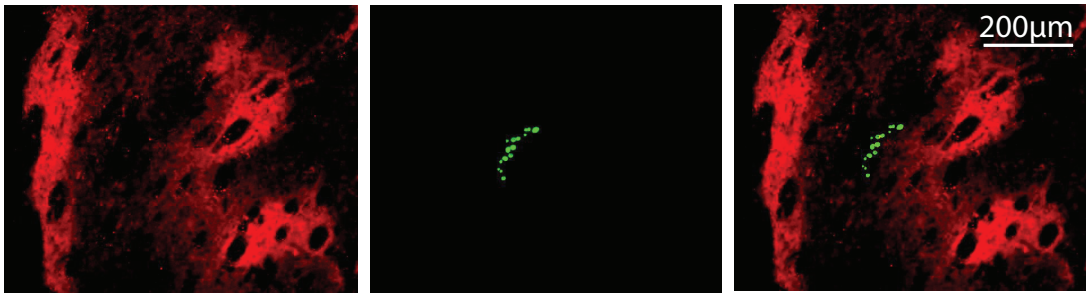

Figure 2.5 CFM placement marked by FluoSpheres and striosomes identifed by high MOR immunoreactivity
Yellow-green FluoSpheres were used to mark CFM placement. MOR-rich strisosomes were visualised by immunohistorchemistry, with DyLight 594 goat-anti rabbit secondary antibodies. Left panels shows MOR-immunoreactivity, which is highest in striosomes. Middle panel shows FluoSpheres indicating CFM placement. Right panel shows merged images. Scale bar 200 µm applied to all panels.

3. Investigating the role of voltage-dependent Ca^{2+} channels (VDCCs) in the control of striatal DA release

3.1 Introduction

3.1.1 The roles of VDCCs in NT release

The Ca^{2+} dependence of exocytosis of neurotransmitters has been long established (Katz and Miledi, 1968) and has led to our appreciation of the importance of understanding how modulation of Ca^{2+} influx at a chemical synapse can influence neurotransmitter release. We now know that many of the properties of excitable cells are governed by voltage-dependent Ca^{2+} channels (VDCCs), a family of ion channels with distinctive pharmacological and biophysical properties as well as varying anatomical distribution and encoded by a number of gene families. The general structure of the channels is however conserved within the family, each member of which is composed of the pore forming α_1 subunit, which confers the pharmacological properties of the channel, β, $\alpha_2\delta$ and γ subunits which are all auxiliary subunits which modulate the trafficking and biophysical properties of the α_1 subunit (Arikkath and Campbell, 2003; Dolphin, 2006).

Multiple VDCCs were first classified through identification of high and low voltage activated currents (Carbone and Lux 1984, Fedulova 1985), which was expanded upon by using pharmacological criteria, broadly defined as dihydropyridine (DHP) sensitive and insensitive Ca^{2+} channels. The discovery of specific toxins that block VDCC allowed further groupings into: DHP, ω-Conotoxin GVIA, high affinity ω-Agatoxin IVA and low affinity ω-Agatoxin IVA sensitive channels (Dolphin, 2006). These classifications are now known to correspond to the L-, N-, P- and Q-type channels respectively, which are defined by their genetic identity. There are 10 known α_1 genes: $Ca_V1.1$-1.4 encode the L-type channels; the P- and Q-type channels are splice variants of the $Ca_V2.1$ gene (Bourinet et al., 1999); $Ca_V2.2$, $Ca_V2.3$ and $Ca_V3.1$-3.3 encode for N-, R- and T-type channels respectively. Despite the channels' properties being predominantly governed by their α_1 subunit, they may be modified by splice variants, post-translational modifications and

associations with accessory subunits (Arikkath and Campbell, 2003; Lipscombe et al., 2004; Kawamoto et al., 2012)

Ca_v2 family of channels are most strongly associated with controlling presynaptic neurotransmitter release (Stanley and Atrakchi, 1990; Dolphin, 2006; Rusakov, 2006). N-, P- and Q-type channels interact directly with the SNARE complex via the synprint domain in a Ca^{2+} dependent manner (Kawamoto et al., 2012). Of the L-type channels the $Ca_V1.2$ and 1.3 subtypes are most widely expressed in the brain (Catterall, 2000).

L-type channels (especially $Ca_v1.2$) are known to couple transcription to depolarisation events and facilitate depolarisation events in the cell body and dendrites of neurons (Guzman et al., 2009). Despite the lack of synprint and low presynaptic expression, there are increasing reports of L-type channels having presynaptic effects (Kato et al., 1992; Bergquist et al., 1998; Bonci et al., 1998; Holmgaard et al., 2009) in addition to being located presynaptically, and interacting with exocytotic machinery (Tippens et al., 2008; Condliffe et al., 2010).

Understanding the role of R-type channels has been hampered by the lack of selective pharmacological agents for R-type channels. Ni^{2+} is often used to block R-type channels and has led to the discovery that R-type channels can control neurotransmission (Wu et al., 1998), however as Ni^{2+} is also reported to block T-type channels at similar concentrations, studies using Ni^{2+} to block R-type channels, rely on biophysical characteristics to distinguish the channel types. A specific but incomplete blocker of R-type channels is SNX-482 (Newcomb et al., 1998; Myoga and Regehr, 2011). Using this drug R-type channels have been reported to couple to SK channels, boosting synaptic potentials (Giessel and Sabatini, 2011), supporting postsynaptic LTP (Myoga and Regehr, 2011) and regulating somatodendritic DA release (Bergquist and Nissbrandt, 2003).

T-type channels represent the low-voltage activating (LVA) group of VDCCs. T-type channels function in controlling low-threshold cell-activity oscillations, hormonal release and cell migration and differentiation (Carbone et al., 2006). However recent evidence reveals a greater

number of roles of T-type channels including initiation of burst firing (Bender et al., 2012) as well as being involved in the control of exocytosis (Li et al., 2005; Carbone et al., 2006; Weiss et al., 2012).

VDCCs control a great number of processes which can affect the control of DA release both directly and indirectly. VDCCs directly controlling DA release will be situated on the DA terminals, where they are opened by membrane depolarisation, permitting Ca^{2+} influx, which triggers exocytosis by the binding of Ca^{2+} to synaptotagmin (Südhof and Rizo, 2011). VDCCs on DA axon terminals will also modulate how an action potential is propagated along the terminals, which may affect DA release (Bean, 2007). It is extremely difficult to determine which VDCCs are present on the axon terminals of DA neurons, as they are so small and much of the surrounding milieu also expresses many VDCCs. Double immunogold labelling would be required for each VDCC sub-type to determine its presence on a TH^{+ve} fibre. However, functions of all the VDCC subtypes have been reported in midbrain DA neurons. Although differences in the roles of VDCCs (L-types) in the cell bodies of SNc and VTA neurons have already been established (Chan et al., 2007; Guzman et al., 2009; Surmeier et al., 2011b) there are no reports of different VDCC expression between these two DA neuron subtypes (Grimm et al., 2004; Chung et al., 2005; Greene et al., 2005; Greene, 2006), however the potential for differential splicing, accessory subunits and localisation to provide diversity between these neuron subtypes is vast.

ChIs are intrinsic to the striatum and are known to powerfully modulate DA release, therefore VDCCs present on ChIs may indirectly control DA release. VDCCs on ChIs may affect DA release by controlling firing or propagation of an action potential in ChIs, or by controlling ACh release. As the ChIs express at least N-, P/Q, L- and R- subtypes of VDCC (Yan and Surmeier, 1996), any of the VDCCs previously identified as controlling DA release may have been acting on the ChIs rather than directly on the DA terminals.

3.1.2 Previous studies of VDCC regulating DA release

Investigating the roles of VDCCs in regulating DA release has long been of interest. As in all areas of science different questions may be best answered with techniques and preparations which will have their own caveats. A range of techniques have been employed to investigate the roles of VDCCs in the regulation of DA release, and have each provided unique and fascinating insights. Early studies using synaptosomes and cell culture allowed the dissection of different release pathways and the biophysical properties of individual ion channels to be established (Ritchie, 1979; Di Virgilio et al., 1987; Carvalho et al., 1995). This work was subsequently built upon by *in vivo* microdialysis studies, which allow all the normal cellular contacts to be maintained and ensure DA is released in a physiological manner, however are hampered by poor temporal resolution and potentially confounding or compensatory effects of surrounding neurons and synaptic contacts, which may also be affected by the drugs applied systemically (Kato et al., 1992; Bergquist et al., 1998). FCV studies using slice preparations allowed DA release to be considered in a more physiological context compared to cell culture, as membrane composition are mature and preserved as well as maintaining many of the network connections, and also benefit from superior temporal resolution to that of *in vivo* microdialysis. The stimulation paradigms used to evoke DA release may be adjusted to investigate interesting mechanistic details and to use physiologically relevant patterns of activity (Phillips and Stamford, 2000b; Chen et al., 2006). Both of these previous studies have advanced our understanding of the roles of VDCCs in DA release by comparing the effects of the channels on DA release in different conditions. Phillips et al compared the roles of N-, P- and Q-type channels in DA release in different areas of CPu at different stimulation frequencies in the rat. Chen et al investigated the differences in Ca^{2+} dependence between striatal and somatodendritic DA release in the guinea pig. Both of these studies provided key insights into how DA release is differentially regulated over different stimulation paradigms and in different areas of the brain. However recent studies have further complicated the picture, as ACh released from striatal ChIs, is now known to act not only as a

modulator of DA release but also as a driver of DA release. Therefore VDCCs present on ChIs are likely to contribute to VDCC regulation of DA release previously identified in these studies. Therefore due to the powerful modulatory effects of ACh on DA release further investigation to determine which VDCCs control DA release at the DA terminals and how this can affect how DA is released across the striatum at different stimulation frequencies is required, because the effect of ACh on DA release changes with stimulation frequency. Another factor which may have confounded Chen et al's results is their inclusion of the DAT blocker GBR 12909, to amplify small signals. Although its inclusion was clearly important to determine if release was abolished or just reduced below detection, new data shows how other uptake blockers (cocaine) change the Ca^{2+} dependence of DA release (Venton et al., 2006), therefore it is possible that GBR 12909 could affect which VDCCs control DA release. In this chapter the role of VDCCs in the control of DA release are determined in the absence of both DAT blockers and the modulatory effects of ACh, to determine which VDCCs control DA release at various stimulation frequencies between CPu and NAc regions of the striatum.

3.1.3 Relevance to Parkinson's disease (PD)

Aberrant DA transmission is linked to many disorders including PD, drug addiction, attention deficit and hyperactivity disorder (ADHD) and schizophrenia (Voorn et al., 2004; Gerfen and Surmeier, 2010; Crittenden and Graybiel, 2011; Surmeier et al., 2011b). In PD the heightened sensitivity of SNc DA neurons to degeneration has been associated with toxicity from Ca^{2+} entry: In PD,DA neurons that originate in SNc are more vulnerable compared to VTA DA neurons that are relatively spared(Grimm et al., 2004; Greene et al., 2005; Surmeier et al., 2011b). Because of the stark contrast of these two apparently similar neuron populations in terms of their vulnerability in PD, comparisons between them provide insights for PD (Grimm et al., 2004; Greene et al., 2005; Chan et al., 2007; Surmeier et al., 2011b). It is now known that SNc but not VTA neurons utilise $Ca_V1.3$ channels to establish Ca^{2+} oscillations to support pacemaking that places an energetic burden on the cells which can combine with other PD susceptibility factors to

promote SNc cell death (Chan et al., 2007; Guzman et al., 2009). This finding illustrates the importance of Ca^{2+} entry in the development of PD, yet the Ca^{2+} entry to the somatodendritic portion of the neuron is a tiny fraction of the cells entire Ca^{2+} load. Nigrostriatal DA neurons form extensive axonal arbors, which in rat are estimated to form >99% of neuron's membrane length. The ratio of membrane length between the somatodendritic region and axons of these neurons, was estimated using the length and volume of axons (Matsuda et al., 2009) and the somatodendritic surface area (Henny et al., 2012). Additionally, the extensive axonal arbors contain as many as 10^5 release sites, all of which will be sites of Ca^{2+} entry (Arbuthnott and Wickens, 2007). These extensive axonal arbors may place significant energetic demands on the neuron (Moss and Bolam, 2010). Therefore Ca^{2+} channels present on DA axons may contribute to the defining physiology and pathophysiology of DA neurons.

3.2 Methods

Methods were carried out as described in chapter 2, unless otherwise described here.

3.2.1 Animals

Experiments in this chapter were mostly performed in wild type (WT) adult male C57Bl6/J mice. For experiments where DA terminals were exclusively activated an optogenetic strategy was used, which required virally injected DAT-cre adult male mice (All viral injections were performed by Dr Nicola Platt). All procedures were carried out in accordance to UK Home Office licence and guidelines.

3.2.2 Slice preparation and maintenance

FCV experiments were carried out on 300 µm acute coronal striatal slices (1.5-0.5 mm from Bregma), which were prepared as previously described. Slices were maintained at $32^{O}C$ and constantly superfused with oxygenated aCSF. Control aCSF contained 2.4 mM Ca^{2+}, in experiments at low extracellular Ca^{2+} ($[Ca^{2+}]_O$) $[Ca^{2+}]$ was reduced to 0.8, 1.0 and 1.2 mM or increased to 3.6 mM by reducing $CaCl_2$ appropriately.

3.2.3 Experimental design

Recordings were obtained from both dorsolateral aspect of the caudate-putamen (CPu) and nucleus accumbens core, directly below the anterior commissure (NAc). DA release was evoked by both electrical and light stimulations.

DA release was evoked by perimaximal local electrical stimulation (200 μs, 0.6 mA) using a bipolar concentric Pt/Ir electrode (25 μm diameter; FHC Inc. ME, USA) placed approximately 100 μm away from the recording carbon fibre microelectrode (CFM). For some experiments the stimulation current was lowered to 200 μA. For optogenetic experiments DA release was driven by a 473 nm diode laser (DL-473, Rapp Optoelectronic), coupled to the microscope with a fibre optic cable (200 μm multimode; NA 0.22), which illuminated a 60 μm diameter spot (10x water immersion objectives). TTL-driven laser pulses (2ms duration, ~40 mW/mm2 at specimen) were delivered at frequencies up to 25Hz.

DA neurons exhibit both tonic and phasic firing patterns, whereby tonic pacemaker firing occurs at 2-5 Hz and phasic burst firing is >15 Hz (Grace and Bunney, 1984a, 1984b; Hyland et al., 2002). The stimulation paradigms: A single pulse (1p) or 5 pulses at 5, 25, 40 and 100 Hz were chosen to span a full range of firing frequencies. The mean peak $[DA]_O$ evoked by 1p is equivalent to that of 5p at 1 Hz. 100 Hz stimulation frequency is a particularly useful in exploring differences in release probability(Rice and Cragg, 2004). Both electrical and light stimulations were repeated at 2.5 minute intervals, which allow stable release to be sustained over several hours. Each stimulation paradigm was recorded in triplicate in a random order per slice. At least three 1p stimulations were given to ensure a stable baseline prior to drug wash on. Data was only included in analysis once 1p $[DA]_O$ was stable.

3.2.4 Drugs

Dihydro-β-erythroidine (DHβE) was purchased from Tocris or Ascent scientific. NNC 55-0396 and isradipine were purchased from Tocris. ω-Conotoxin GVIA, ω-Agatoxin IVA were purchased from

Ascent scientific. $NiCl_2$ was purchased from Sigma Aldrich. Stock solutions of DHβE, ω-conotoxin GVIA and NNC 55-0396 were dissolved in dH_2O to 1000-2000x final concentrations and stored at -20^{o}C. Isradipine was dissolved in DMSO. Drugs were diluted in oxygenated aCSF immediately prior to use to final concentrations required. Drug concentrations were chosen in accordance with previous studies (Phillips and Stamford, 2000b; Chen et al., 2006; Guzman et al., 2009; Tai et al., 2011)

3.2.5 Data analysis

Data were acquired and analysed using Axoscope 10.2 (Molecular devices) or Whole Cell Programme (WCP; University of Strathclyde, Glasgow) and Excel macros written locally (Drs S Cragg and K Jennings). Data are expressed as mean ± standard error of the mean (SEM), where n = number of animals. Data from each animal were calculated by averaging at least 3 recordings at each stimulation frequency and normalised to control conditions for each animal. Data from at least 3 animals were averaged to give mean values for each drug and protocol condition. Means were compared using two-way ANOVA with post-hoc Bonferroni's t-test where appropriate, using GraphPad Prism. Parametric tests were used as raw control data passed Shapiro-Wilk normality test (*p=0.34)*.

3.3 Results

3.3.1 Role of N-type VDCCs

As has been earlier described, in addition to ACh being able to drive DA release independently from activity in DA neurons it also has profound regulatory effects on DA release. When nAChR are active, DA release is only slightly sensitive to firing frequency; whereby DA release shows and inverted U relationship, with greatest DA release at 25Hz. NAc is slightly more sensitive to frequency than CPu. In the presence of DHβE (1 μm), which blocks nAChRs, DA release is greater following high frequency stimulations than following a single stimulation pulse (1p). In CPu, DA release increases approximately exponentially with stimulation frequency up to 100Hz, whereas

in NAc, DA release approaches a plateau at approximately 40Hz. In both regions, the mean peak $[DA]_O$ following 1p is equivalent to that following 5p 1 Hz stimulation.

In the experiments described in the next section control conditions are in the presence of DHβE (1 μM) to block nAChRs. Under these control conditions, peak evoked $[DA]_O$ varied with stimulus frequency in CPu (**Figure 3.1a**; 1-way ANOVA, $F_{4,26}$=62.7, *p<0.001*) and NAc (**Figure 3.1 b**; 1-way ANOVA, $F_{4,14}$=36.26, *p<0.001*) as shown previously during nAChR inhibition (Rice and Cragg, 2004; Exley and Cragg, 2008; Exley et al., 2012). Single pulses evoked a mean peak $[DA]_o$ of 0.97 ± 0.10 μM in CPu and 0.67 ± 0.10 μM in NAc, in line with previous studies (Threlfell et al., 2010; Hartung et al., 2011).

Application of the N-type blocker ω-conotoxin GVIA (100 nM) dramatically decreased peak $[DA]_o$ evoked by all stimuli in CPu (**Figure 3.1 a**, 2-way ANOVA, effect of drug $F_{1,20}$=121.51, *p*<0.001) and NAc (**Figure 3.1b**, 2-way ANOVA effect of drug $F_{1,20}$=210.06, *p*<0.001) to ~15-50% of control $[DA]_o$, depending on stimulus frequency (CPu, **Figure 3.1a**, 2-way ANOVA, drugXfrequency interaction $F_{4,44}$=5.3, *p<0.01;* NAc, **Figure 3.1b**, 2-way ANOVA, drugXfrequency interaction $F_{4,20}$=6.6, *p<0.001*). The percentage reduction of evoked $[DA]_O$ by N-type channel blockade was greater at lower frequency stimulations (**Figure 3.1a,b,c**), and was greater in CPu than NAc (**Figure 3.1c**; 2-way ANOVA, region: $F_{1,20}$=13.70, *p*<0.01). The effect of ω-Conotoxin GVIA was found to be maximal at 100 nM. Reducing the concentration of ω-Conotoxin GVIA to 50 nM, increased the time taken to achieve a stable effect. Doubling ω-Conotoxin GVIA to 200 nM had the same effect at 100 nM (**Figure 3.1d**).

To investigate if N-type channels contribute to the modulatory effect of ACh on DA release I repeated the N-block experiment without DHβE present, so nAChR were active. In agreement with Phillips et al (2000) and Chen et al (2006), when nAChR are active (without DHβE) ω-Conotoxin GVIA (100 nM) dramatically decreased 1p DA release in both regions, however 1p evoked DA was still apparent following N-block (**Figure 3.2 a**), blockade of nAChR (1 μM DHβE)

following N-block had no effect on 1p evoked $[DA]_O$ (**Figure 3.2 a**). In agreement with previous studies the percentage effect of N-block on DA release was greatest at low frequencies (**Figure 3.2b** 2-way ANOVA effect of frequency $F_{1,16}$=28.24 *p<0.001*) and I found that similarly to when nAChR are blocked, N-type block has a greater effect on DA release in CPu than NAc (**Figure 3.2b** 2-way ANOVA effect of region: $F_{1,16}$=37.96 *p<0.001*). When DHβE (1 μM) was applied following N-block it had no effect at low frequency stimulations, but 5p 100 Hz evoked $[DA]_o$, DHβE increased DA release to levels equivalent to pre-drug conditions (**Figure 3.2c** 2-way ANOVA drugxfrequency interaction CPu: $F_{6,24}$=23.6 *p<0.001*, and NAc: $F_{6,24}$=15.2 *p<0.001*) postests show *p>0.05* at frequencies 1-40 Hz but *p<0.001* at 100Hz, between ω-Conotoxin GVIA and DHβE conditions). It could be seen the effect of N-type channel blockade on 5p 100Hz DA release can be reversed by subsequent blockade of nAChR, however it is also possible that the large increase in 5p 100Hz DA release following blockade of nAChR just happens restore DA to pre-drug levels, but at different stimulation paradigms DA release between N-block and N-block+nAChR block would diverge. Therefore 5p, 10p and 20p at 100Hz evoked DA release was compared between drug free and N-block+nAChR conditions. In both CPu and NAc there was no significant difference between 5p, 10p and 20p 100Hz DA release in drug-free control conditions and when nAChR and N-type calcium channels were blocked (**Figure 3.2 d** 2-way ANOVA effect of drug CPu: $F_{2,15}$=0.1 *p>0.05*; NAc $F_{2,15}$=0.2 *p>0.05*). The effect of other VDCC subtypes were not tested when nAChR were active.

3.3.2 Role of P/Q-type VDCCs

Experiments in this section were done in the presence of DHβE to block nAChR. P-type VDCCs can be exclusively blocked (as opposed to both P and Q-type channels) with a low concentration of ω-Agatoxin IVA (15 nM). At this concentration ω-Agatoxin IVA had no effect on DA release in either CPu (**Figure 3.3 a**: 2-way ANOVA effect of drug $F_{1,20}$=3.69 *p=0.069*) or NAc (**Figure 3.3b**: 2-way ANOVA effect of drug $F_{1,20}$=1.20 *p=0.29)* at any frequency. Blockade of P-type channels by ω-

Agatoxin IVA (15 nM) can be overcome by strong membrane depolarisations (McDonough et al., 1997), therefore experiments were repeated using a low stimulation current (0.2 mA). ω-Agatoxin IVA (15 nM) still had no effect on DA release in either region under low current stimulation conditions (**Figure 3.3c** 2-way ANOVA $F_{1,20}$=0 *p>0.05* and **Figure 3.3d** $F_{1,20}$=1.43 *p>0.05*). It is possible that blocking Ca^{2+} entry via P-type channels does not reduce Ca^{2+} entry sufficiently below a threshold to affect DA release, or other VDCC sub-types may compensate for a reduction in Ca^{2+} availability, therefore the effect of blocking P-type channels on a background of N-type blockade was examined. When N-type channels were blocked with ω-Conotoxin GVIA (100 nM) and then P-type channels were subsequently blocked there was still no effect of ω-Agatoxin IVA (15 nM) on DA release in either CPu (**Figure 3.3e**: 2-way ANOVA effect of drug $F_{1,20}$=0.78 *p=0.39*) or NAc (**Figure 3.3f**: 2-way ANOVA effect of drug $F_{1,20}$=0.60 *p=0.45)* at any frequency.

A higher concentration of ω-agatoxin IVA (200 nM) was subsequently used to block P+Q type channels, which may be assumed to reveal the role of Q-type channels, and significantly decreased peak evoked $[DA]_o$ in CPu (**Figure 3.4a**, 2-way ANOVA, effect of drug $F_{1,40}$=93.68, *p*<0.001) and NAc (**Figure 3.4b**, 2-way ANOVA, effect of drug $F_{1,40}$=24.05, *p*<0.001). Evoked $[DA]_o$ was decreased by Q-block to ~30-50% of control in CPu, depending inversely on stimulation frequency (**Figure 3.4a**; 2-way ANOVA, drugXfrequency interaction $F_{4,40}$=3.8 *p<0.05*) but was decreased only to ~70-80% of control in NAc which did not vary significantly with stimulation frequency (**Figure 3.4b**; 2-way ANOVA, drugXfrequency interaction $F_{4,40}$=0.9, *p>0.05*). The effect of P/Q type channel blockade on $[DA]_O$ was significantly different between CPu and NAc (**Figure 3.4c**; 2-way ANOVA, region: $F_{1,40}$=29.34, *p*<0.001).

3.3.3 Role of T-type VDCCs

Experiments in this section were done in the presence of DHβE. Ni^{2+} (100 µM) is commonly used to block T-type channels (Wolfart and Roeper, 2002; Chen et al., 2006). The effect of Ni^{2+} (100 µM) on DA release was initially used to probe the role of T-type channels. Application of Ni^{2+} resulted in a reversible increase in DA release in both CPu and NAc. The DA transients for CPu and NAc are shown in the left panels of **figure 3.5a and b** respectively. Here it can be seen that Ni^{2+} both increases DA release and delays clearance of DA, with the peak $[DA]_O$ occurring 0.125 s later than control conditions. For 5p 5Hz in NAc, Ni^{2+} also changes the time course of DA release, where the transient has a much more pronounced plateau phase. Ni^{2+} significantly increases the peak max $[DA]_O$ in both CPu (**Figure 3.5a** 2-way ANOVA $F_{1,20}$=10.9 *p=0.004*) and NAc (**Figure 3.5b** 2-way ANOVA $F_{1,20}$=18.9 *p<0.001)*. This increase in mean peak DA and delayed clearance of DA transients caused by Ni^{2+} is highly reminiscent of the effect of cocaine and other DAT blockers. To investigate this further Ni^{2+} was applied following cocaine (5 µM) using a truncated stimulation protocol of 1p, 5p at 5 and 100Hz. On a background of cocaine, Ni^{2+} application decreased 1p evoked DA release but not 5p 5Hz or 5p 100Hz release in CPu (**Figure 3.5c** 2-way ANOVA $F_{1,12}$=11.9 *p<0.01*). In addition to the reduction in 1p evoked DA, Ni^{2+} also significantly slowed the decay phase of DA transients at all stimulation frequencies, shown by the increase in half-lives (**Figure 3.5d** CPu: 2-way ANOVA effect of drug $F_{1,8}$=64.07 *p<0.001*). The effect of Ni^{2+} on a background of cocaine in NAc was analogous to the effects in CPu, whereby Ni^{2+} only decreased 1p DA release (**Figure 3.5e** 2-way ANOVA $F_{1,12}$=9.32 *p<0.05)*, but the decay phase of the DA transients to all stimulation frequencies were much slowed (**Figure 3.5f** 2-way ANOVA : $F_{1,8}$=85.76 *p<0.001)*. As the peak max of 1p evoked DA release was decreased by Ni^{2+} it was not possible to compare $t_{1/2}$ of 1p release statistically as they were not concentration matched, however, by eye it seems that the time course of the 1p transients were also much slowed. Ni^{2+} did not change the calibration values of any of the electrodes used.

Ni^{2+} appeared to have non-specific actions, putatively acting on the DAT, therefore a more selective T-type channel was chosen. Mibefradil is a selective T-type channel blocker, but has previously been reported to interact with CFMs, making them insensitive to DA (Chen et al., 2006). NNC 55-0396 is a non-hydrolysable derivative of mibefradil, which has greater selectivity for T-type channels over L-type channels than mibefradil (Li et al., 2005). NNC 55-0396 has previously been used in slice preparation assays at 10 µM (Tai et al., 2011). To ensure the most appropriate concentration of NNC 55-0396 was being used, the effect of NNC 55-0396 on DA release was tested at 0.1, 1 and 10 µM. The effect of NNC 55-0396 was found to be maximal at 1 µM, and was chosen as the most appropriate concentration to be used (data not shown). NNC 55-0396 did not change the calibration factors of any of the electrodes used.

Application of NNC 55-0396 (1 µM) significantly decreased mean peak evoked $[DA]_O$ in CPu (**Figure 3.6 a**; 2-way ANOVA; drug: $F_{1,20}$=28.68, p<0.001), but not in NAc (**Figure 3.6 b**; 2-way ANOVA; drug: $F_{1,20}$=0.03, *p>0.05*); these effects in CPu and NAc were significantly different from each other (**Figure 3.6** c, 2-way ANOVA; region: $F_{1,20}$=37.94, p<0.001). Higher drug concentrations (10 µM, NNC 55-0396) had no further effect (data not illustrated). The reduction of evoked DA by T-type channel blockade in CPu was to 57-65% peak $[DA]_o$ of control levels which did not vary significantly with stimulation frequency (**Figure 3.6 a**; 2-way ANOVA, drug x frequency interaction $F_{4,20}$=2.1 *p>0.05*).

.

3.3.4 Role of L-type VDCCs

Experiments in this section were done in the presence of DHβE. In CPu, blockade of L-type Ca^{2+} channels with isradipine (5 µM) modestly but significantly decreased electrically evoked DA release, to ~75% of controls in CPu (**Figure 3.7 a,b** ; 2-way ANOVA, $F_{1,30}$=20.38, *p<0.001*), invariantly with stimulation frequency (**Figure 3.7 a,b**; no drug x frequency interaction, 2-way ANOVA, $F_{4,30}$=1, *p>0.05*). These effects were reversible on drug washout (**Figure 3.7 c**). By

contrast, isradipine did not modify evoked $[DA]_o$ in NAc (**Figure 3.7d,e**; 2-way ANOVA, $F_{1,20}$=1.18 *p>0.05*). Higher drug concentrations (10 µM isradipine) had no further effect (data not illustrated). These outcomes of L-block were statistically different in CPu and NAc (**Figure 3.7f;** 2-way ANOVA; region: $F_{1,20}$=206.67, *p*<0.001).

To confirm that the L-type channels regulating DA release in CPu are expressed within the DA terminals rather than on other potential neuromodulatory circuits that might be driven by the electrical stimulus, we used an optogenetic approach to drive DA axons exclusively, with pulses of blue light (2 ms). ChR2-eYFP was expressed by DA neurons and axons after injection of a Cre-inducible floxed construct into the SNc of DAT-Cre mice (**Figure 3.7g**), as previously described (Threlfell et al., 2012). In drug-free control conditions in CPu, light pulses (1p, or 5p at 5Hz or 25Hz) evoked peak $[DA]_o$ of ~0.75-1.5 µM, equivalent to those evoked by local electrical stimuli in the presence of DHβE. Isradipine (5 µM) significantly reduced light-evoked DA release to ~75% of control level (**Figure 3.7 h,i**; 2-way ANOVA, $F_{1,6}$=23.59, *p*<0.01) invariantly with stimulus frequency (**Figure 3.7 i**; 2-way ANOVA no drugxfrequency interaction $F_{2,12}$=0.3 *p>0.05*). These data corroborate a role for L-type VDCCs expressed by DA axons in DA release.

L-type channels are not classically thought of as acting presynaptically, therefore the finding that L-type channel blockade decreased DA release in a presynaptic manner needed to be verified by using an alternate L-type blocker. Nifedipine is another L-type channel blocker that has a similar preference for $Ca_v1.3$ over $Ca_v1.2$ subtypes. Initially an optogenetic approach was chosen to replicate the effects of isradipine with nifedipine. However nifedipine (10 µM) appeared to be photoactive: light activation of DA terminals caused a large broad oxidation peak, which was positively shifted (720 mV) compared to DA (600 mV) (**figure 3.7j**), which got progressively larger and broader with successive stimulations. The reduction peak appeared to be normal. Studies have shown that nifedipine is photoactive, forming an aromatic product with multiple oxidisable groups (Li et al., 2011).

To avoid the photoactive properties of nifedipine, electrical stimulation of DA release was used to replicate the effect of isradipine. In a single pilot study (n=1 animal, 3 observations per stimulation protocol in each drug condition) nifedipine (10 μM) reduced DA release across all stimulation protocols to 70% of control in CPu, which is analogous to the effect of isradipine (**Figure 3.7 k**).

3.3.5 Role of R-type VDCCs

Experiments in this section were done in the presence of DHβE. R-type channels were blocked with SNX 482 (100 nM), which resulted in a significant increase in DA release in both regions that did not vary with stimulation frequency. (**Figure 3.8a** CPu: 2-way ANOVA, $F_{1,20}$=58.47 *p<0.001,* no drugXfrequency interaction $F_{4,20}$=1.54 *p>0.05* **Figure 3.8b** NAc: $F_{1,20}$=27.61 *p<0.001 ,* no drugXfrequency interaction $F_{4,20}$=1.96 *p>0.05)* The effect of R-block was not significantly different between CPu and NAc (**Figure 3.8c**; 2- way ANOVA; region: $F_{1,20}$=1.31 *p*=0.27). Because it seems unlikely that blocking Ca^{2+} entry to the terminals would increase DA release, pilot data (n=1) were obtained in GABA and glutamate blockade (MCPG (200 μM), GYKI (10 μM), D-AP5 (50 μM), bicuculline (10 μM) and saclofen (50 μM)), to assess whether the increase in DA release following SNX 482 was indirectly mediated by R-type channels present on glutamate or GABA afferents in the striatum, resulting in disinhibition. An increase in DA following SNX 482 application was still apparent in the presence of glutamate and GABA block (data not shown).

SNX 482 decreased the sensitivity of the CFM in four out of six experiments, which suggests that SNX 482 is interacting with the electrode, and therefore the increase in signal observed may be an electroactive effect, rather than a receptor-drug interaction. To further investigate if the increase in signal is due to a rise in $[DA]_O$ or a change in electrode sensitivity, it was explored whether the increase in DA following SNX-482 remained when DHβE was absent (meaning nAChR were active), because if the increase was only due to a change in electrode sensitivity you would expect the increase to be unaffected by the presence or absence of DHβE.

In the absence of DHβE, and SNX 482 no longer had an effect on DA release in CPu (**Figure 3.8d**: 2-way ANOVA $F_{1,20}$=3.62 *p>0.05*) but SNX-482 still increased DA release in NAc (**Figure 3.8e**: 2-way ANOVA $F_{1,20}$=8.48 *p>0.01*), albeit to a lesser extent than when nAChR were blocked with DHβE. Therefore it seems that SNX 482 is having a real effect on DA release, and that the increase in signal was not just due to an electroactive artefact of SNX 482.

3.3.6 Investigating the frequency-dependent nature of VDCCs

Previous studies have suggested that the function of individual types of VDCCs in the control of DA transmission is variable depending on stimulation frequency (Phillips and Stamford, 2000b; Chen et al., 2006), suggesting that the kinetics of VDCC activation/inactivation may be exploited by DA axons to tune DA transmission with particular VDCCs acting at particular subsets of phasic or tonic frequencies of neuron activity. However, the results of previous studies may be due predominantly to the effects of VDCC blockers on ACh release which acts at nAChRs to modify DA release powerfully and in a frequency-dependent manner (Zhou et al., 2001; Rice and Cragg, 2004; Zhang and Sulzer, 2004; Threlfell et al., 2012). Throughout this study, we excluded the effects of ACh by conducting experiments in the presence of nAChR antagonists. Nonetheless, we detected some variation in effects of given VDCC blockers with stimulus frequency (e.g. N- and P/Q-type **Figures 3.1 a,b and,3.4 a**): effects of N- and P/Q blockers were greatest at lowest stimulation frequencies and more limited at higher frequencies. We noted that this variable effect for P/Q block was significant in CPu but not NAc, suggesting it was not intrinsic to the channel properties, and noted furthermore that this variation was most prominent where blockers caused a large (>50%) suppression of DA release evoked by single pulses, suggesting that the frequency specificity of VDCC block may arise from an inverse relationship between initial DA release probability (P_R) and its short-term plasticity (STP) that can be governed by Ca^{2+}-availability (Cragg, 2003).

To explore whether the apparent frequency-specificity of VDCC blockade on DA release in the presence of DHβE could be due to a Ca^{2+}-limited change in P_R and STP, we first compared the effect of VDCC blockade to that of decreased extracellular Ca^{2+}, on frequency dependence of DA release. A reduction of extracellular Ca^{2+} to 1.0 mM (from 2.4 mM) had similar effects to N-block (as shown previously in **Figure 3.1**): it reduced peak $[DA]_o$ evoked by all stimuli, and to a greater extent for single pulses and lower frequencies, in CPu (**Figure 3.9 a,b**, 2-way ANOVA effect of Ca^{2+}: $F_{1,20}$=1.16, *p>0.05;* effect of frequency: $F_{4,20}$=10.21, *p<0.001*) and NAc (**Figure 3.9 c,d**, 2-way ANOVA effect of Ca^{2+}: $F_{1,20}$=3.75, *p>0.05*; effect of frequency: $F_{4,20}$=7.12, *p<0.01*). We next explored whether there was an overall relationship between the degree of frequency dependence and release by 1p that could describe the data set as a whole, using data for all VDCC blockers as well as a range of $[Ca^{2+}]_o$. We plotted the ratios of $[DA]_o$ evoked by 5p/100Hz:1p (5p:1p ratio) as a measure of frequency dependence, against the $[DA]_o$ evoked by 1p (a measure of initial P_R) for all individual experiments with VDCC blockers and with a range of $[Ca^{2+}]_O$ (2.4 mM control, 1.0 mM and 0.8 mM) (**Figure 3.9e**). These combined data could be described by a continuous inverse relationship between 5p:1p ratio and 1p $[DA]_o$ in CPu, and also in NAc (**Figure 3.9e**: e.g. two-phase exponential curves, CPu, R^2=0.73; NAc, R^2=0.76). These plots show that where DA P_R (1p $[DA]_o$) is high, e.g. in control conditions of 2.4 mM $[Ca^{2+}]_o$ in the presence of DHβE but without VDCC blockade; or is only mildly decreased (L- or T-block in CPu, or P/Q block in NAc), the 5p:1p ratio remains at ~4-5, i.e. release nearly linearly reflects pulse number. As DA P_R (1p $[DA]_o$) becomes reduced further, by low $[Ca^{2+}]_o$ or N-block (and P/Q block in CPu) the 5p:1p ratios become correspondingly greater, such that when 1p $[DA]_o$ release is reduced to the lowest quartile of release levels, there is short-term facilitation (STF) where 5p:1p ratio >> 5. These data support the hypothesis that the apparent frequency specificity of some VDCC blockers results from significantly reduced Ca^{2+} entry and DA P_R with inverse consequences for Ca^{2+} -limited STF.

Thirdly, we tested whether a channel that did not ordinarily show frequency-specific modulation of DA release (e.g. L-type, see Figs 3.7), could be made to show this dynamic property

by a prior reduction in DA P_R. Any further reduction in P_R (leftward shift in Fig 3.5e) by subsequent channel block should increase the 5p:1p ratio if this prediction is correct. Indeed, in CPu, in the presence of N-type blocker (ω-conotoxin IVA 100 nM), when DA P_R is compromised and 5p:1p ratio is > 10 (**Figure 3.9 e**), the subsequent application of L-blocker isradipine (5 µM) further decreased $[DA]_O$ evoked by 1p (by ~50%) but not by 5p 100Hz, resulting in a significant increase in 5p:1p ratio (**Figure 3.9 5 f**, linear regression R^2=0.79, *p<0.05*). Therefore, we show here that the dynamic effects of VDCCs are due to a causal relationship between release probability and its short-term plasticity, rather than other specific attributes of VDCC subtype activation/inactivation. Note, in NAc, L-type blockade following N-type blockade had no effect on DA release (data not illustrated).

To better understand why NAc DA release was consistently more resistant to reducing Ca^{2+} availability than CPu (e.g. Figure 3.4c) calcium response curves (CRC) of 1p mean peak max $[DA]_O$ were determined for both CPu and NAc. From this we can see that the two regions differ in their relationship between DA release and Ca^{2+} availability (**Figure 3.9g**: Comparison of fits test between CPu and NAc variable slope sigmoidal curve: $F_{4,76}$=9.5 *p<0.001* CPu R^2=0.76 NAc R^2=0.90). In CPu, DA release is most sensitive to changes in Ca^{2+} availability below 2.4 mM Ca^{2+}, whereas NAc is most sensitive to changes in Ca^{2+} availability between 5 and 2.4 mM.

3.4 Discussion

The recent discovery that DA release can be driven by the cholinergic system, made it apparent that our understanding of the VDCCs that control DA release is incomplete. In this chapter I have shown that in CPu, DA release is directly controlled by N>P/Q>T>L- VDCC types, whereas in NAc only N- and P/Q-types appear to control release. It is apparent that CPu DA release is more sensitive to VDCC inhibition than NAc, and in both regions the frequency response of DA release is a function of its initial release.

3.4.1 DA release in dorsolateral CPu is regulated by more VDCCs than NAc.

In both CPu and NAc, N-type VDCC blockade reduces 1p evoked DA release more than any other VDCC type blockade, indicating that N-type VDCCs exert the greatest control over DA release in these regions. P/Q-type blockade also dramatically reduces DA release; however the reduction in DA release in CPu is much more marked than in NAc. It appears that in CPu, N-and P/Q-type VDCCs are equivalent in their control of DA release, whereas in NAc N-type VDCCs control DA release to a greater extent than P/Q-type VDCC.

I have identified roles for L- and T-type VDCCs in the control of DA release in dorsolateral CPu but not NAc. The effect of L-type VDCC blockade in CPu is of particular interest, due to the involvement of L-type VDCC in the somatodendritic regions: SNc DA neurons express $Ca_V1.3$ (L-type) which drive Ca^{2+} oscillations, leading to increased intracellular Ca^{2+} levels and mitochondrial oxidative stress (Guzman et al., 2010). By contrast VTA DA neurons do not utilise the $Ca_V1.3$, instead using monovalent cations to generate their pacemaker action potentials (Chan et al., 2007). The roles of L-type Ca^{2+} channels throughout the entire neuron will be important when considering treatments of PD. Most work on L-type VDCCs has focused on their roles in the somatodendritic region of neurons, where they are known to regulate transcription and firing patterns of neurons (Bean, 2007; Guzman et al., 2009; Putzier et al., 2009; Schlick et al., 2010). Data shown here indicates that L-type VDCCs also have a presynaptic role in CPu. L-type VDCCs are not classically thought to control presynaptic neurotransmitter release as they are high-voltage activating and have slow activation kinetics. However, L-type VDCCs have been identified as existing presynaptically in hippocampal neurons and in controlling release in DA neurons both *in vivo* and in cell culture (Bergquist et al., 1998; Tippens et al., 2008; Holmgaard et al., 2009; Subramanian and Morozov, 2011). Moreover data are increasingly pointing to a great deal of functional diversity among the L-type VDCCs including: varying dihydropyridine sensitivity; fast activation kinetics and activation over a range of voltages (Lipscombe et al., 2004). A large number of splice variants for the four different L-type VDCCs and their associations with different

regulatory subunits may underpin the range of characteristics and corresponding functions of the L-type VDCCs. There are no reported differences in transcription levels of the different VDCC subtypes between SNc and VTA DA neurons (Grimm et al., 2004), therefore it is unclear why the T- and L-type channels only appear to control DA release in CPu, however factors including trafficking to the membrane and posttranslational modifications would explain why there is a discrepancy between differences in functionality but similarities at the transcriptional level.

3.4.2 Ca^{2+}availability affects the frequency sensitivity of DA release

It is intuitive that reducing Ca^{2+} entry to the terminals would both reduce initial release of DA, and increase burst ratio; as subsequent action potentials could overcome the shortage of Ca^{2+} and lead to the release of available DA. We show that DA released to 1p is inversely proportional to the burst ratio. Therefore in contrast to Phillips et al, we find that instead of a subset of channels being more instrumental in controlling release to a burst vs. discrete stimulations, there is a dynamic relationship between the initial release and burst stimulations, which can be shifted by manipulating calcium entry. N-type blockade causes a greater percentage reduction of DA in response to low rather than high frequency stimulations, not because N-type VDCCs preferentially control low-frequency release, but rather the reduction in 1p evoked DA is large enough to shift the relationship between 1p and burst release along an existing continuum.

DA release in CPu is more sensitive to reducing extracellular Ca^{2+} below 2.4 mM which supports the finding that VDCC blockade consistently reduces DA release in CPu to a greater extent than in NAc. However the steepest phase of the calcium response curve in NAc is between 2.4 mM Ca^{2+} and 3.6 mM. This may suggest that the reduced sensitivity of VDCC blockade in NAc is due a lack of “dynamic working range” of DA release in NAc, rather than an absence of the channels (L- and T-type VDCCs). Pilot data indicates that at 3.6 mM extracellular Ca^{2+} DA release in NAc is reduced by application of

both T- and L-type blockers. This would suggest that the channels are present on DA terminals in NAc, but DA release is not responding to changes in Ca^{2+} availability in this range.

3.4.3 The role of VDCCs in the control of DA release has been confounded by the powerful modulatory effects of ACh

Previous studies which have looked at the VDCCs involved in DA release in the striatum, have been confounded by the influence of ACh (Phillips and Stamford, 2000b; Chen et al., 2006). Therefore the VDCCs identified as controlling DA release would have also been those on the ChI. When nAChR are active, ACh driven DA release appears to be a major component of total electrically evoked DA release, because the release is frequency insensitive and when nAChR are blocked 1p evoked DA release is approximately halved. Despite the confounding effects of ACh present in previous studies, we also find N- and P/Q-type channels to be the predominant VDCC types in controlling DA release in the striatum. Yet by removing the confounding effects of ACh, we have also exposed roles for L- and T-type VDCCs in controlling DA release in CPu but not NAc. There are several possibilities for why the role of L- and T-type VDCCs in controlling DA release are only apparent in the absence of nAChR activation. It could be that there is sufficient Ca^{2+} entry through nAChR to make L- and T-type VDCCs superfluous. However this seems unlikely as the α7 containing nAChRs have the greatest permeability to Ca^{2+} ions, and these channel compositions are not present in the striatum, the β2-containing nAChR, which are present in the striatum have very low Ca^{2+} permeability (Exley and Cragg, 2008; Wu et al., 2009). Alternatively, it could be that cholinergic driven DA release occurs downstream of where L- and T-type modulates DA release (i.e. they function to shape action potential, or change the membrane properties etc), meaning they no longer modulate DA release. The experiments discussed in this chapter builds upon the work of Phillips et al (2000) and Chen et al (2006), providing further evidence for how the roles of VDCCs in DA release vary between brain regions. Furthermore, by comparing the VDCCs that control DA release when nAChR are active (Phillips et al and Chen et al)

and blocked (experiments discussed in this chapter) could provide insights for the mechanisms by which nAChR activation modulates and drives DA release.

3.4.4 Pharmacological issues

In this thesis work I used a pharmacological approach to dissect the roles of VDCCs that operate on DA terminals to control striatal DA release in the absence of the confounding effects of ACh. Many of the drugs used in this chapter have exquisite selectivity and efficacy for their specific channels (namely ω-Conotoxin, ω-Agatoxin), however some of the drugs are far less specific. One of the pharmacological issues which has confounded our understanding of the roles of VDCCs in neuron physiology is the finding that at high concentrations (>20 μM) isradipine can block Na^+ channels as well as the L-type channels, in this thesis I therefore used a lower concentration that is still sufficient to penetrate the tissue in a reasonable time course but remains specific for L-type channels (Guzman et al., 2009).

Within this thesis work I identified further pharmacological issues. Firstly, Ni^{2+} was found to be an unsuitable blocker of T-type channels due to it having apparent interactions with the DAT. Therefore caution should be taken when interpreting data that has used Ni^{2+} as a VDCC when DAT or other monoamine transporters are present. Therefore for experiments investigating the roles of T-type channels I used NNC 55-0396, as a more suitable T-type blocker. Mibefradil and TTA-P2 are alternative specific T-type blockers, however these drugs were not used here as mibefradil makes CFM insensitive to DA (Chen et al., 2006) and TTA-P2 is not commercially available.

Investigating the role of the R-type channels in DA release was also limited by suitable pharmacological agents for two reasons. Firstly there are no alternative R-type channel blockers to confirm that the unexpected effect of SNX-482 causing an increase in DA release are mediated by R-type channels and secondly SNX-482 altered the sensitivity of the CFM, which introduced the possibility that the increase in signal was an electrochemical artefact rather than a real increase in

$[DA]_O$. However taking into account the fact that the increase in signal remains even if the calibration factor is not altered; the effect of SNX-482 is different in the absence and presence of DHβE and that the effect of ω-Conotoxin is altered following SNX-482 application all support the idea that SNX-482 is having a real effect on DA release and not just altering electrode sensitivity.

The final example of imperfect pharmacology discussed here is the finding that nifedipine is photoactive, that produces an electroactive product. The identification of photoactive properties of drugs could cause significant issues with the advent of optogenetic technologies. Nifedipine may be less susceptible to photoreactions when local spot illumination (with a laser) rather than a full-field LED illumination is used, however this was not investigated here. The electroactive breakdown product may not cause a problem for other techniques (i.e. whole cell recordings) but it isn't known the degree to which nifedipine is broken down, so it is possible that it could change the concentration of the drug at the tissue, which may have to be considered, especially in long experiments.

3.4.5 Implications for PD

The motor symptoms of PD are predominantly due to the death of SNc DA neurons, which innervate the dorsal striatum, leading to a loss of striatal DA. One of the reasons that SNc DA neurons are thought to be especially sensitive in PD is the extra Ca^{2+} load caused by their recruitment of Cav1.3 (L-type) SOP, which support pacemaker activity. Therefore it has been suggested that one of the reasons for the different susceptibilities of VTA and SNc DA neurons in PD is due to differential recruitment of VDCCs. In this chapter I have concluded that the terminal fields of SNc and VTA neurons, which innervate CPu and NAc regions of the striatum respectively also have different dependencies on VDCC subtypes for controlling DA release. Therefore the potentially toxic effects of Ca^{2+} entry though Cav1.3 channels in SNc DA neurons may not be limited to the cell bodies, and may actually extend throughout the extensive axonal arbors of these neurons.

Antagonism of the $Ca_V1.3$ with isradipine is being tested in PD patients to reduce the Ca^{2+} oscillations and subsequent mitochondrial oxidative stress, to prevent SNc neuron degeneration (Simuni et al., 2010; Rees et al., 2011). However because isradipine can also reduce CPu DA release, it is possible that isradipine will inhibit DA release in the already DA depleted brains of PD patients. If isradipine does further reduce DA release in PD patients, it is unclear if this negative effect would be offset by any protective effect in the cell bodies. Alternatively it may be true that Ca^{2+} entry through L-type channels in the terminals also gives rise to oxidative stress, which could mean that isradipine treatment protects both the cell body and axonal regions from oxidative stress.

The control that L and T-channels exhibit in DA terminals of the dorsal striatum, may be small but the extra Ca^{2+} they supply over a lifetime could well contribute to the extra Ca^{2+} burden of the SNc DA neurons, thought to be key to their heightened sensitivity to PD. It has recently been shown that entry of Ca^{2+} via L-type channels results in more oxidative stress in dendrites than is seen in the soma (Dryanovski et al., 2013). It may be theorised from this work, that because the axons are even further from the soma than the dendrites are, the oxidative stress arising from L-type Ca^{2+} entry may be even more marked than seen in the dendrites. Additionally the role of the L- and T-type channels in controlling DA release may be illustrating an interesting difference in the mechanism of controlling DA release in the two neuron types. The differing functional roles of L- and T-type channels in supplying the terminals with Ca^{2+} in the CPu but not NAc may provide insights into the increased sensitivity of SNc over VTA DA neurons to PD, especially as there are no reported differences in transcription levels of the different VDCC subtypes between SNc and VTA DA neurons (Grimm et al., 2004).

The contribution of the huge axonal arbour to the metabolic state of the cell is especially important if PD progresses in a “dying back mechanism” (Hornykiewicz, 1998;

Cheng et al., 2010). The idea that axonal degeneration occurs via different mechanisms to that of programmed cell death of the soma, is supported by evidence which suggests that the terminals are more sensitive to mitochondrial stress than the cell body (Pickrell et al., 2011). If the axons are more sensitive to oxidative stress then the cell body, and Ca^{2+} entry via VDCCs causes oxidative stress then, understanding the roles of VDCCs controlling DA release should be a priority. Identifying different requirements for Ca^{2+} entry via VDCCs between terminals of SNc and VTA dopaminergic neurons may be of significance to understanding why SNc neurons are so sensitive, especially when considered in conjunction with other known risk factors such as α-synuclein.

3.4.6 Summary

DA release was consistently shown to be more sensitive to Ca^{2+} challenge in CPu than NAc. This was particularly pronounced for P/Q blockade, where DA release was reduced to ~33% and 70% to that of control conditions in the CPu and the NAc respectively. In NAc only N- and P/Q-type VDCCs appear to control DA release, whereas in CPu N>P/Q>T>L-type VDCCs control DA release. The sum of the percentage effects of N and P/Q-type blockade in the NAc is ~100%, possibly indicating that the N and P/Q type channels control the release of separate pools of DA. In CPu the percentage effect of the different channel blockers exceeds 100%. This may indicate co-operativity between the VDCCs in the CPu, whereby some pools of DA may require multiple VDCC types to facilitate release. DA release in CPu may be more sensitive to a Ca^{2+} challenge because a higher Ca^{2+} threshold is necessary to trigger exocytosis. Higher extracellular Ca^{2+} may be required if the exocytosis complex in CPu requires more Ca^{2+} to be bound or if the coupling between Ca^{2+} entry and its binding to the exocytosis complex is less efficient in comparison to those of NAc. And finally the frequency dependent nature of certain VDCCs previously reported was further investigated and found to be due to a dynamic relationship between initial release and re-release that could be altered by changing calcium availability, rather an intrinsic property of certain VDCC subtypes.

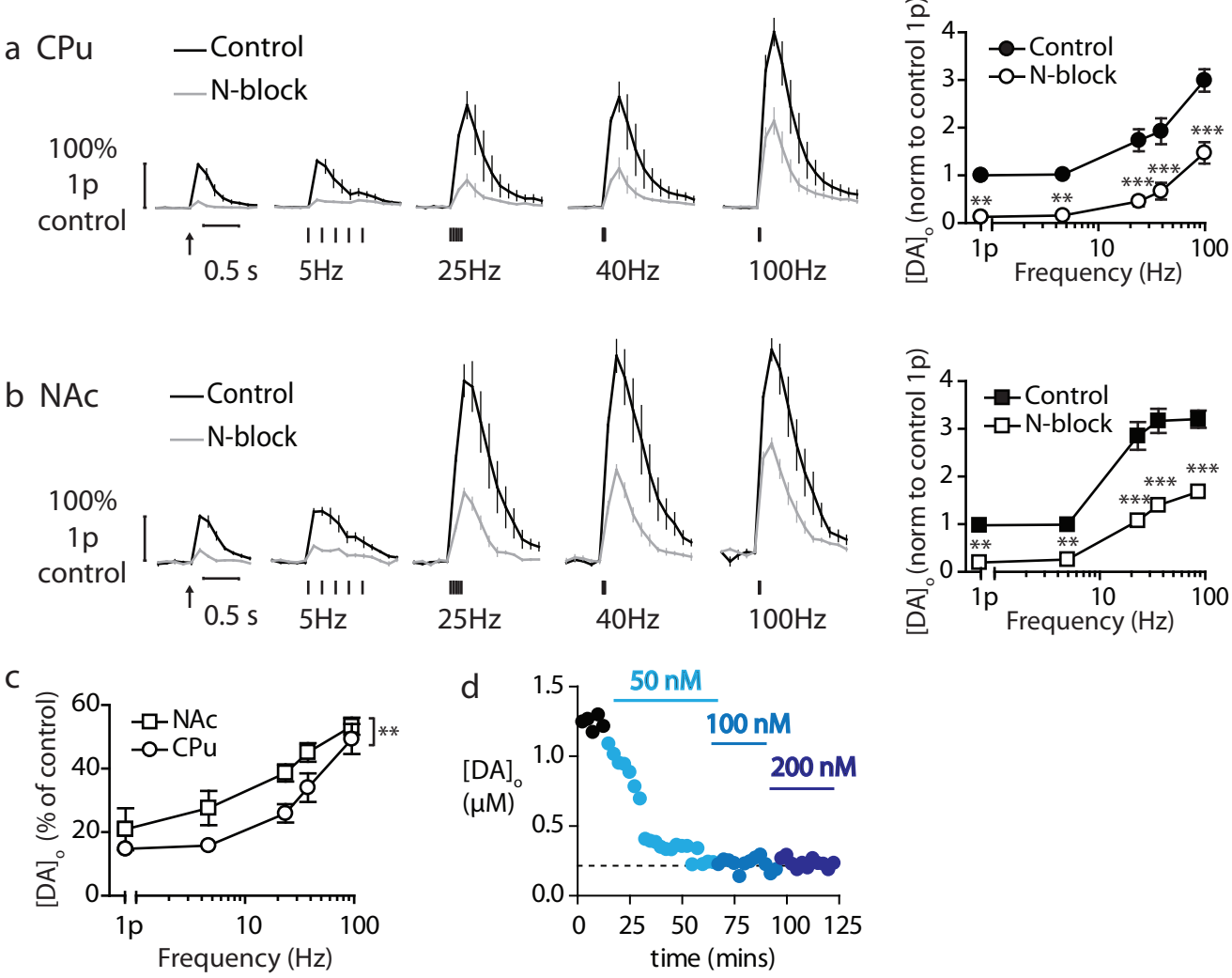

Figure 3.1 N- blocker ω-conotoxin GVIA (100 nM) reduces DA release in CPu and NAc
Control conditions are in the presence of DHβE (1 μM). (a, b Left panel) Mean $[DA]_o$ ± SEM vs time post stimulation, data are normalised to peak $[DA]_o$ evoked by 1p in control conditions. Control conditions (black lines), N-block (grey lines). (a,b Right panel) Mean peak $[DA]_o$ ±SEM vs frequency at 1p or 5p. Control conditions (filled shape) and N-block (unfilled shape). (a) are data from CPu, (b) are data from NAc . (c) N-block has a greater effect in CPu than NAc: Mean peak [DA]O expressed as percentage of control ± SEM vs frequency at 1p or 5p in CPu (unfilled circle) and NAc (unfilled square). (d) ω-conotoxin GVIA has its maximal effect at 100 nM. Data are 1p peak max $[DA]_o$ (μM) collected at 2.5 min intervals. n=3 animals.

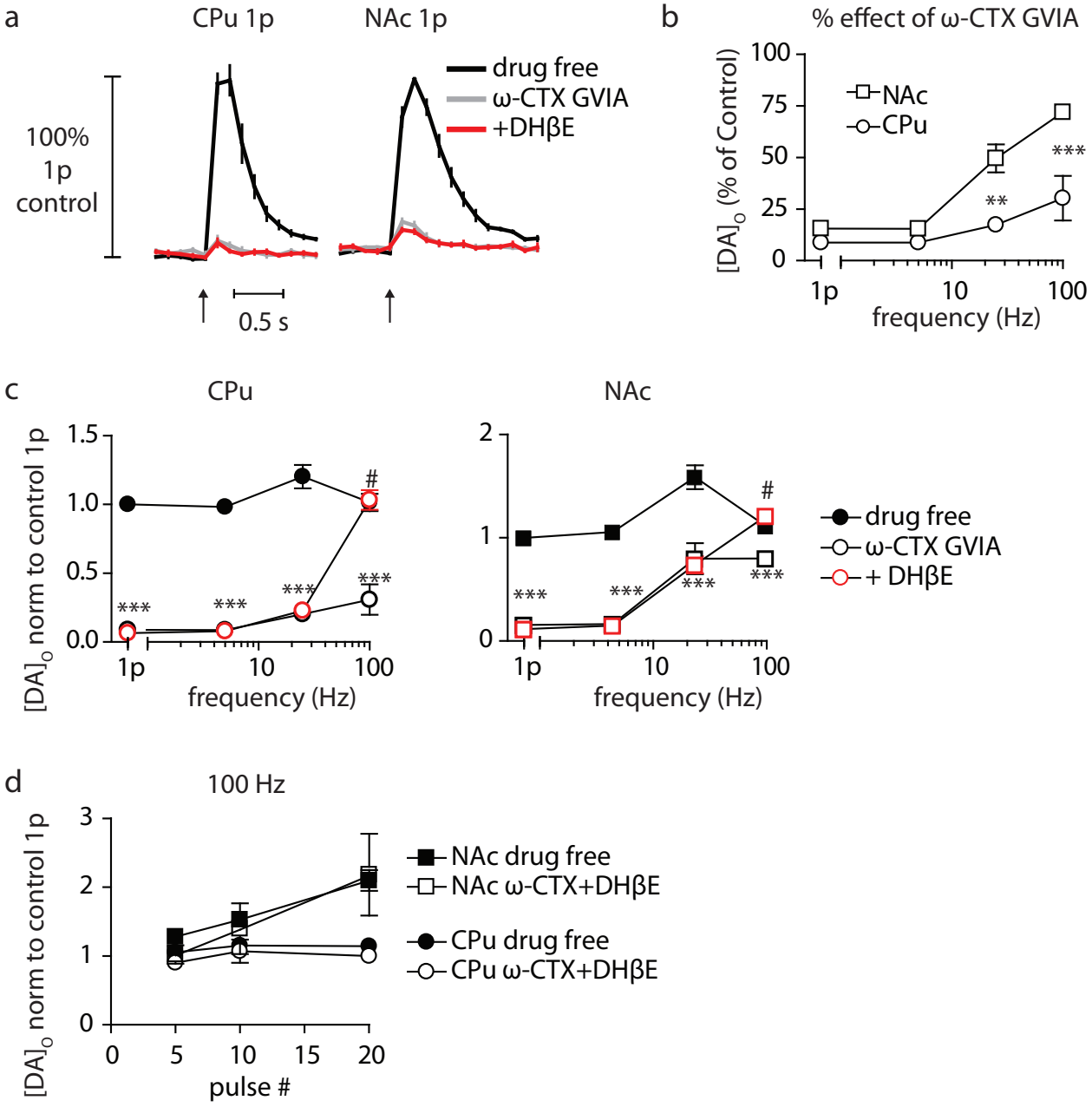

Figure 3.2 N-block reduces DA release in CPu and NAc when ChIs are active.
(a) Mean $[DA]_O$ SEM vs time post stimulation, data are normalised to peak $[DA]_O$ evoked by 1p in control conditions. Drug free conditions (black lines), N-block (grey lines), N-block+DHβE (red lines). (b) N-block has a greater effect in CPu than NAc: Mean peak $[DA]_O$ expressed as percentage of control ± SEM vs frequency at 1p or 5p in CPu (unfilled circle) and NAc (unfilled square). (c) DHβE has no effect following N-block at low frequencies, but reverts 5p 100 Hz $[DA]_O$ to drug free levels. Mean peak $[DA]_O$ ±SEM vs frequency at 1p or 5p. Drug free (filled shape), N-block (unfilled shape), N-block+DHβE (red outline shape) n=3 animals. (d) DHβE returning 5p 100 Hz $[DA]_O$ to drug free conditions is not a coincidental cross over. Mean peak $[DA]_O$ ±SEM vs number of pulses at 100 Hz. Control conditions (filled shape) and N-block+DHβE (unfilled shape) n=3 animals

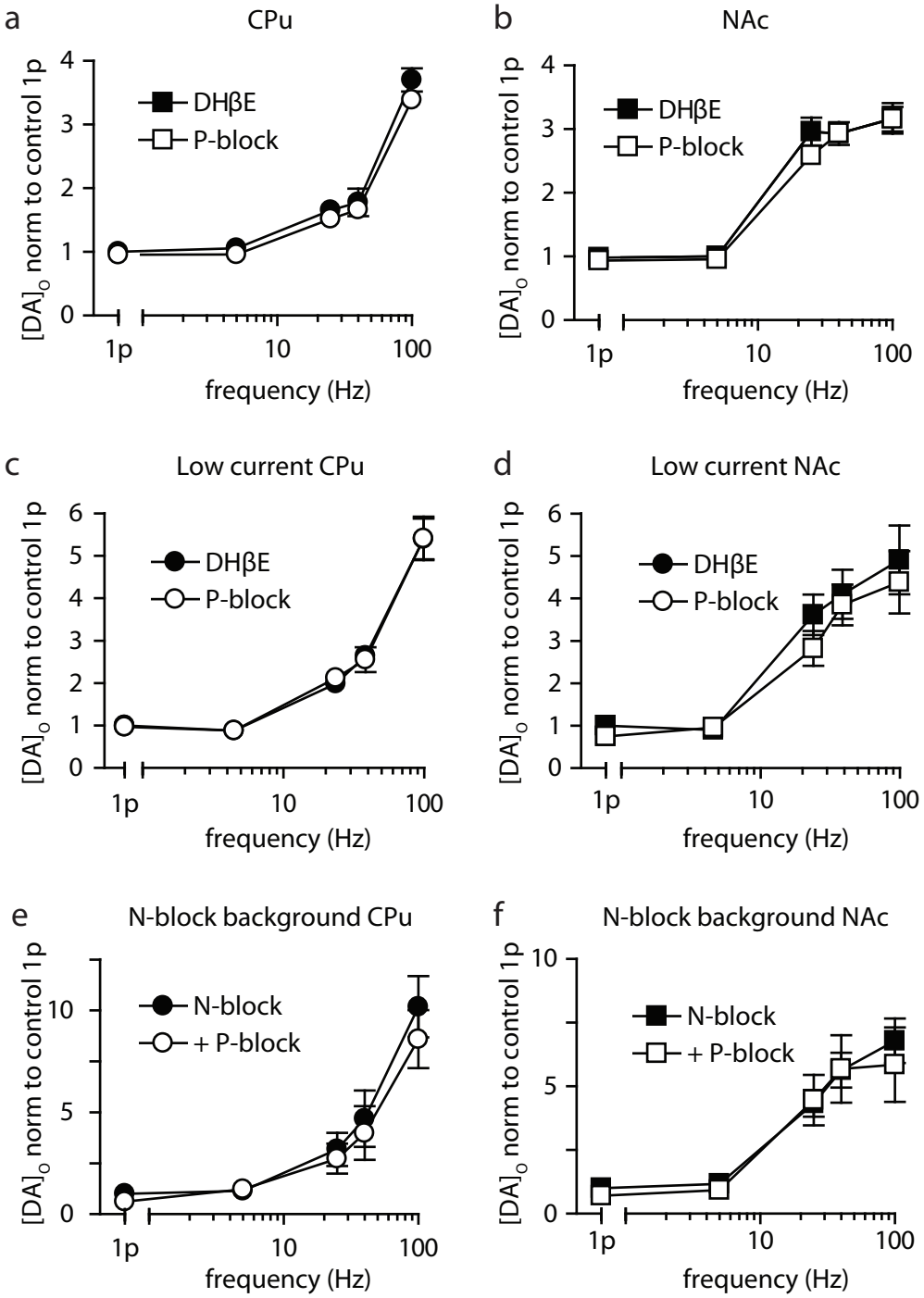

Figure 3.3 P-blocker ω-agatoxin IVA (15 nM) has no effect on DA release in CPu or NAc
Control conditions are in the presence of DHβE (1 μM). (a,b,c,d) Mean peak $[DA]_O$ ±SEM vs frequency at 1p or 5p. Control conditions (filled shape) and P-block (unfilled shape) data are normalised to peak $[DA]_O$ evoked by 1p in control conditions. (e,f) Mean peak $[DA]_O$ ±SEM vs frequency at 1p or 5p. Control conditions are in the presence of N-block (filled shape) and P-block (unfilled shape) data are normalised to peak $[DA]_O$ evoked by 1p in N-block. n=3 animals.

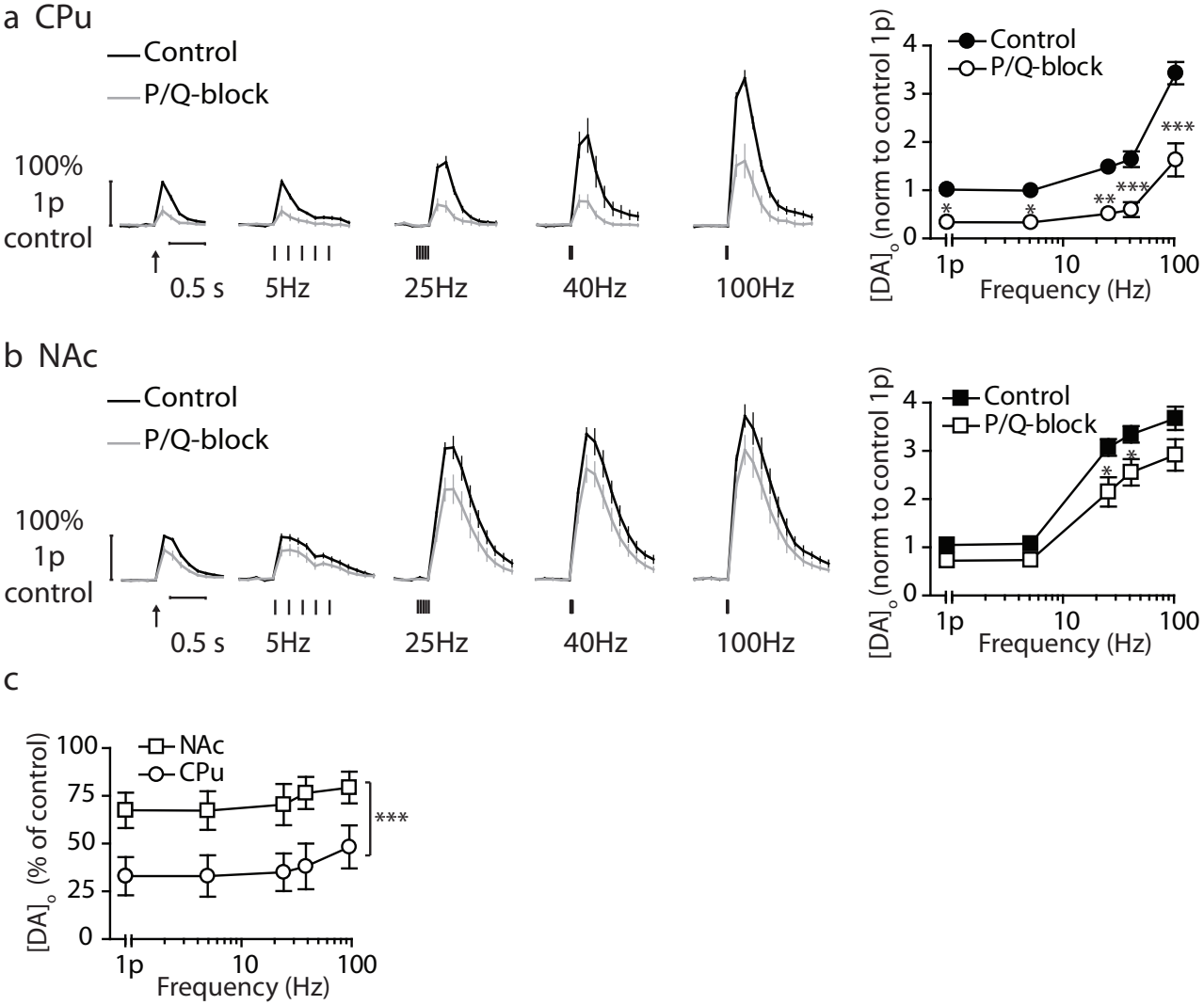

Figure 3.4 P/Q-blocker ω-agatoxin IVA (200 nM) reduces DA release in CPu and NAc
Control conditions are in the presence of DHβE (1 μM). (a,b Left panel) Mean [DA]O ± SEM vs time post stimulation, data are normalised to peak $[DA]_o$ evoked by 1p in control conditions. Control conditions (black lines), P/Q-block (grey lines). (a,b Right panel) Mean peak [DA]O ±SEM vs frequency at 1p or 5p. Control conditions (filled shapes) and P/Q-block (unfilled shapes). (c) P/Q-block has a greater effect in CPu than NAc: Mean peak [DA]O expressed as percentage of control ± SEM vs frequency at 1p or 5p in CPu (unfilled circles) and NAc (unfilled squares) n=5 animals.

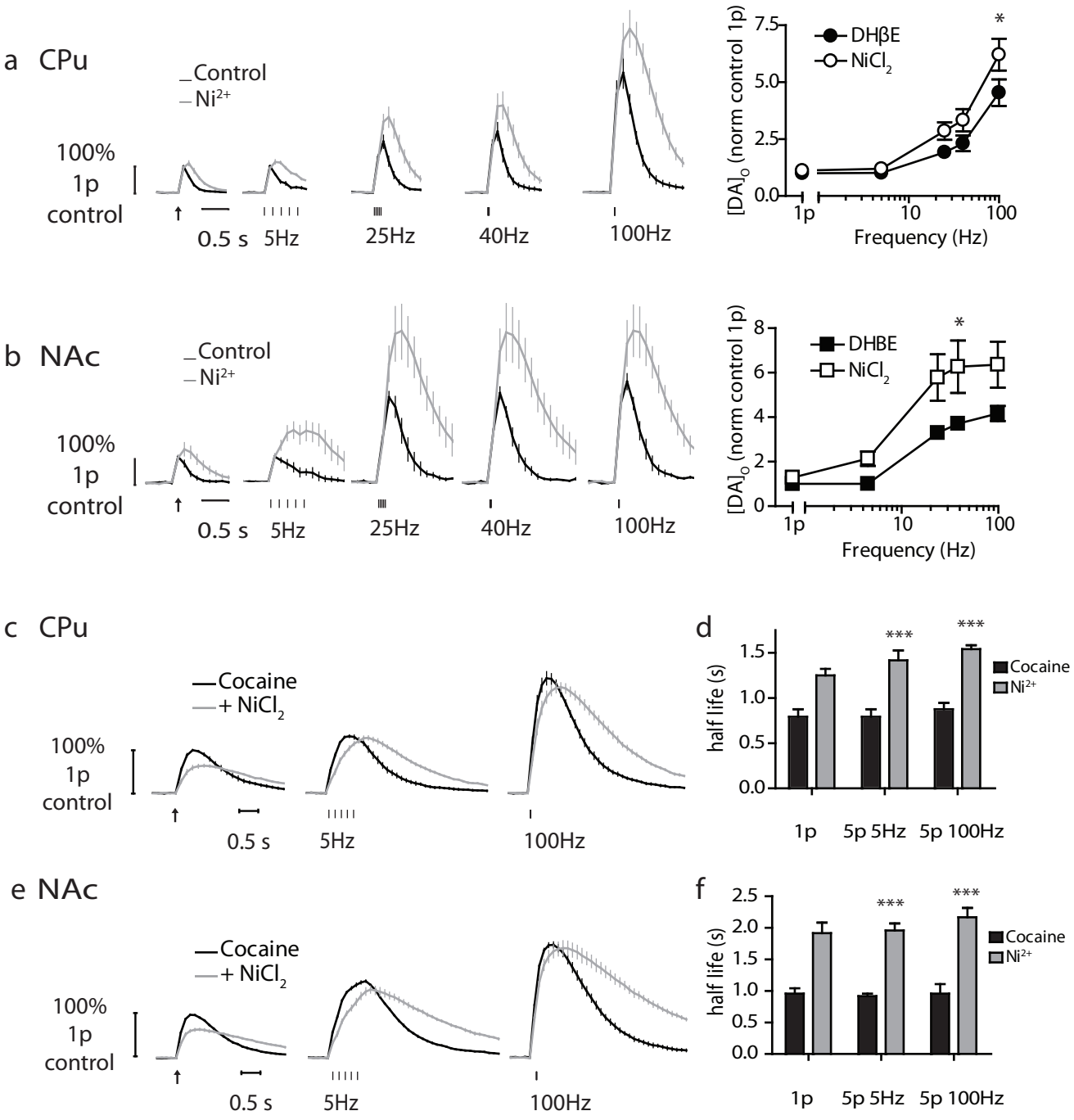

Figure 3.5 Ni^{2+} (100 µM) is not a suitable T-type channel blocker due to putative interactions with the DAT

Control conditions are in the presence of DHβE (1 µM). (a, b Left panel) Mean $[DA]_O$ ± SEM vs time post stimulation, data are normalised to peak $[DA]_O$ evoked by 1p in control conditions. Control conditions (black lines), Ni^{2+} (grey lines). (a,b Right panel) Mean peak $[DA]_O$ ±SEM vs frequency at 1p or 5p. Control conditions (filled shape) and N-block (unfilled shape). (a) are data from CPu, (b) are data from NAc. (c,d,e,f) Ni^{2+} affects the time course of DA release when DAT is blocked with cocaine. (c,e) Mean $[DA]_O$ ± SEM vs time post stimulation, data are normalised to peak $[DA]_O$ evoked by 1p in the presence of cocaine. Cocaine (black lines), Ni^{2+} (grey lines). (d,f) Ni^{2+} increases the half-life of DA transients. Half-life is the time (s) taken for the $[DA]_O$ to reach half the peak max $[DA]_O$ levels.

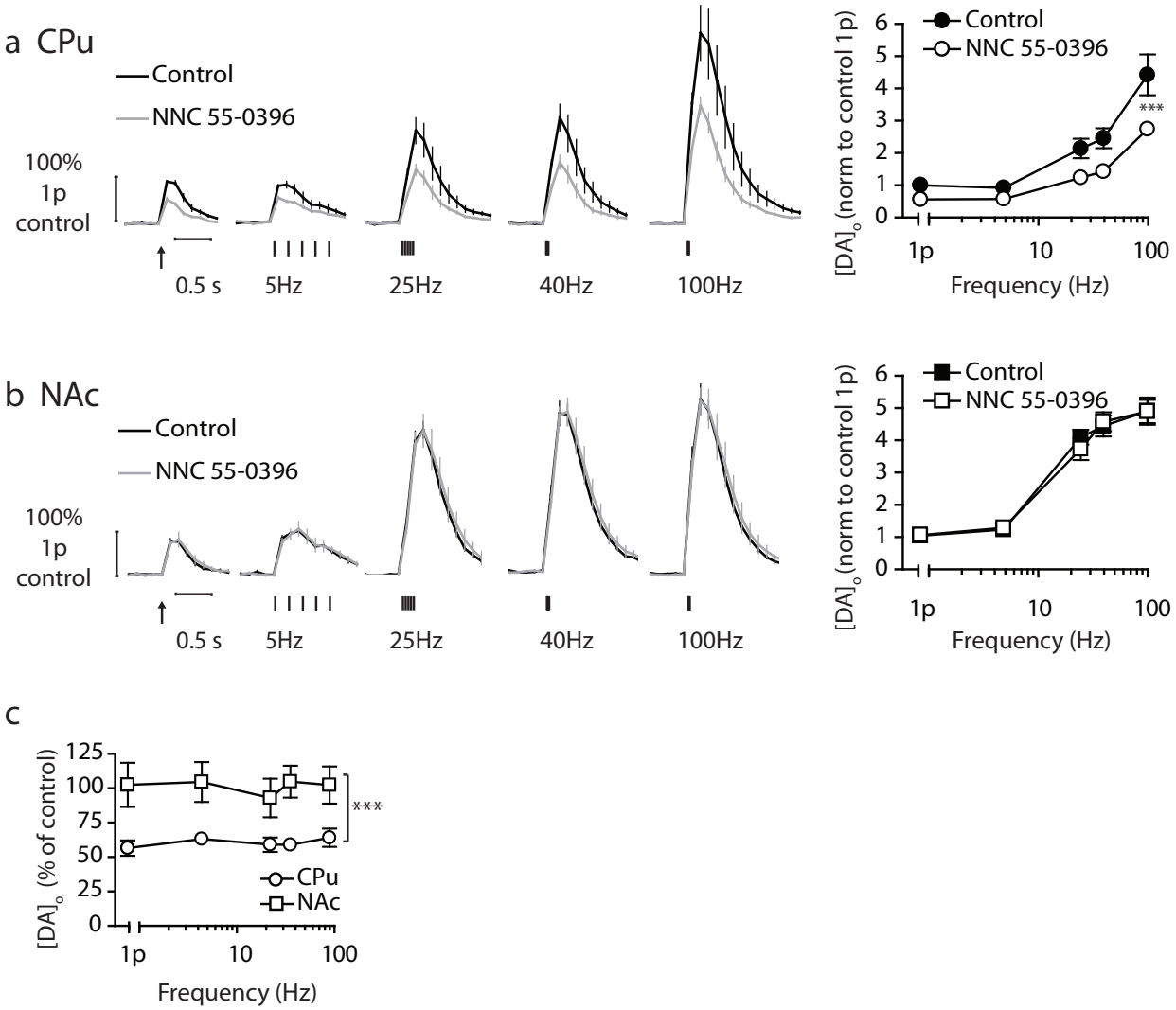

Figure 3.6 T-type blocker NNC 55-0396 (1 µM) reduces evoked DA in CPu but not NAc.
Control conditions are in the presence of DHβE (1 µM). (a, c) Mean $[DA]_o$ ± SEM vs time post stimulation, data are normalised to peak $[DA]_o$ evoked by 1p in control conditions. Control conditions (black lines), T-block (grey lines). (b, d) Mean peak $[DA]_o$ ±SEM vs frequency at 1p or 5p. Control conditions (filled shapes) and T-block (unfilled shapes). a&b are data from CPu, c&d are data from NAc. (e) T-block has a greater effect in CPu than NAc: Mean peak $[DA]_o$ expressed as percentage of control ± SEM vs frequency at 1p or 5p in CPu (unfilled circles) and NAc (unfilled squares) n=3 animals.

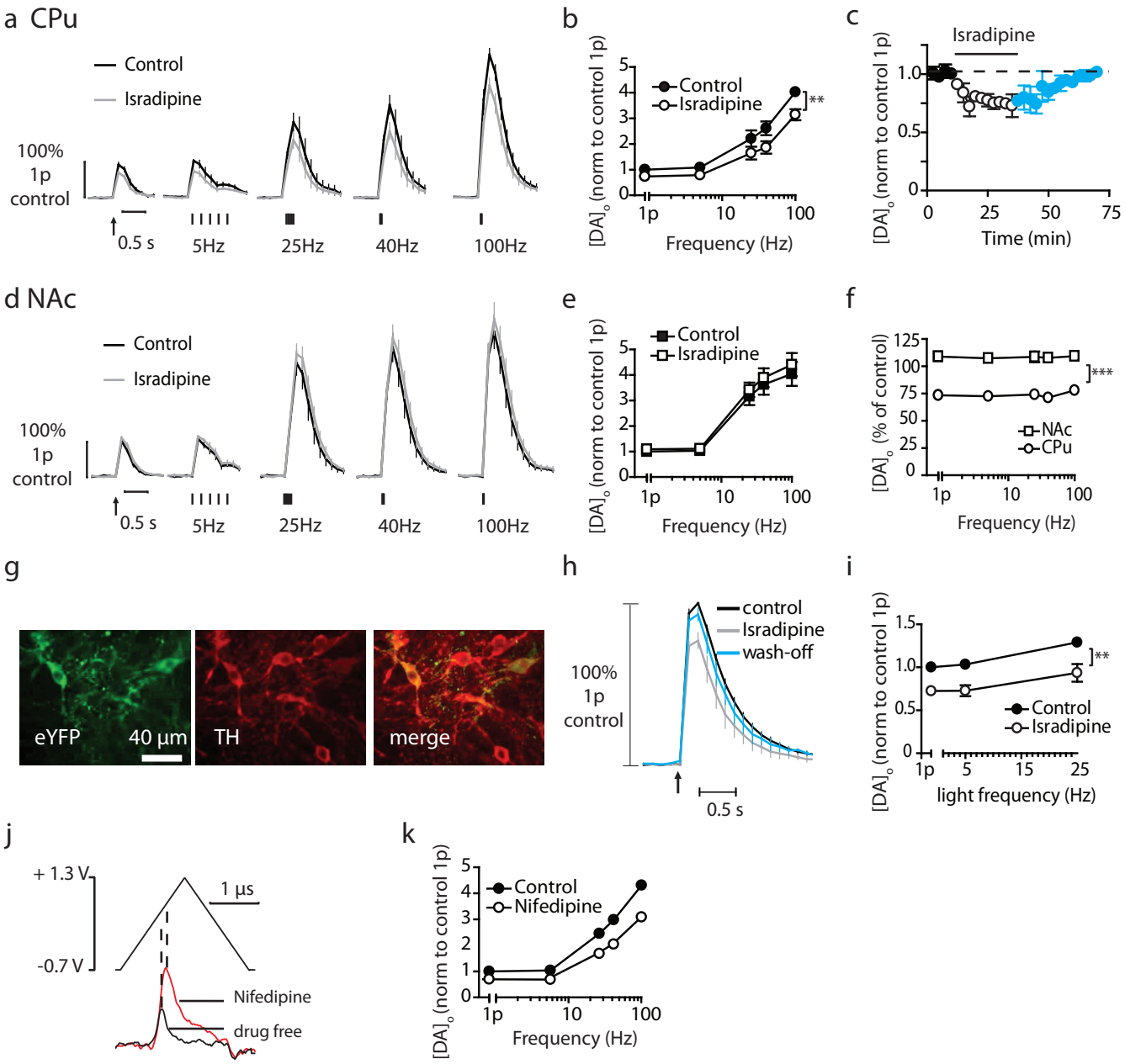

Figure 3.7 L-type blocker Isradipine (5 µM) reduces evoked DA in the CPu but not NAc

Control conditions are in the presence of DHßE (1 µM). (a, d) Mean $[DA]_o$ ± SEM vs time post electrical stimulation, data are normalised to peak $[DA]_o$ evoked by 1p in control conditions. Control conditions (black lines), isradipine (grey lines). (b, e) Mean peak $[DA]_o$ ±SEM vs frequency at 1p or 5p. Control conditions (filled shapes) and isradipine (unfilled shapes). (c) The effect of isradipine is reversible following washing 1p peak $[DA]_o$ in control (black circles), the duration of isradipine (unfilled circles) is shown by the black bar, and following wash off (blue circles). isradipine has a greater effect in CPu than NAc: (f) Mean peak $[DA]_o$ expressed as percentage of control ± SEM vs frequency at 1p or 5p in CPu (unfilled circles) and NAc (unfilled squares). n=4 animals in CPu, n=3 animals in NAc. The effects of isradipine are replicated when DA terminals are exclusively activated using optogentic techniques (g) Fluorescence shows ChR2-eYFP expression (left panel), Tyrosine hydroxylase (TH) positive cells (middle panel) and merged images (right panel) scale bar (40 µm) applies to all panels. The image shows co-labelling of TH and eYFP from the lateral aspect of the SNc (h) Mean $[DA]_o$ ± SEM vs time post stimulation, data are normalised to peak $[DA]_o$ evoked by 1p in control conditions. Control conditions (black lines), isradipine (grey lines) wash-off (blue line) (i) Mean peak $[DA]_o$ ±SEM vs frequency at 1p or 5p. Control conditions (filled circles) isradipine (unfilled circles) n=3 animals. (j)Nifedipine (10 µM) is photoactive: DA oxidation peak is broad and right shifted in the presence of nifedipine following stimulation with LED (k) Pilot data shows nifedipine (10µM) replicates the effect of isradpine on electrically evokd DA (n=1) in CPu.

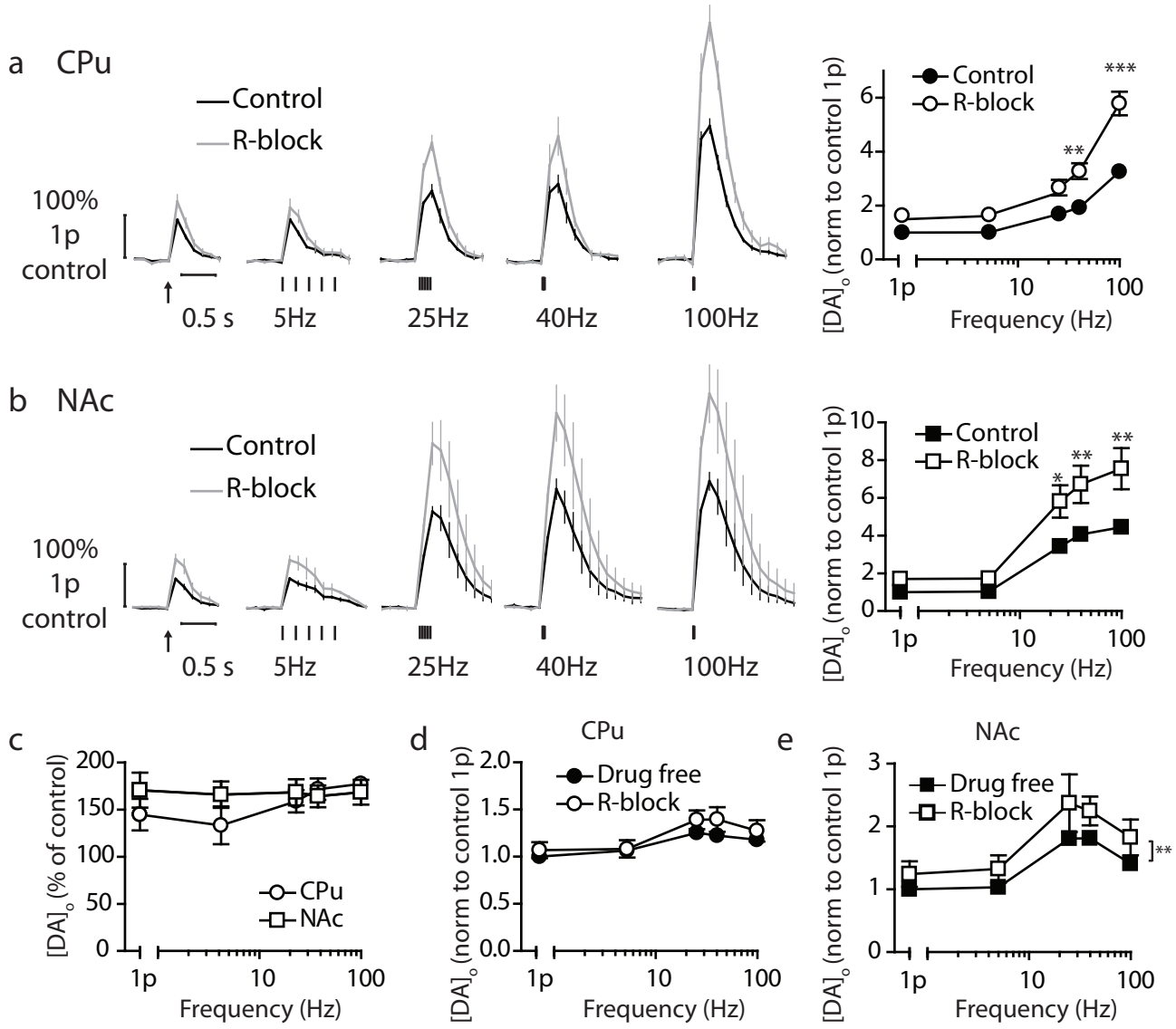

Figure 3.8 R-blocker SNX 482 (100 nM) increases evoked DA in CPu and NAc.
Control conditions are in the presence of DHßE (1 µM). (a,b Left panel) Mean $[DA]_o$ ± SEM vs time post stimulation, data are normalised to peak $[DA]_o$ evoked by 1p in control conditions. Control conditions (black lines), R-block (grey lines). (a,b Right panel) Mean peak $[DA]_o$ ±SEM vs frequency at 1p or 5p. Control conditions (filled shapes) and R-block (unfilled shapes). (c) R-block has the same effect in CPu and NAc: Mean peak $[DA]_o$ expressed as percentage of control ± SEM vs frequency at 1p or 5p in CPu (unfilled circles) and NAc (unfilled squares). (d,e) R-block has no effect on $[DA]_o$ when ChIs are active in CPu, but still increases $[DA]_o$ in NAc: Mean peak $[DA]_o$ ±SEM vs frequency at 1p or 5p. Drug free (filled shapes) and R-block (unfilled shapes) data are normalised to peak $[DA]_o$ evoked by 1p in drug free conditions.

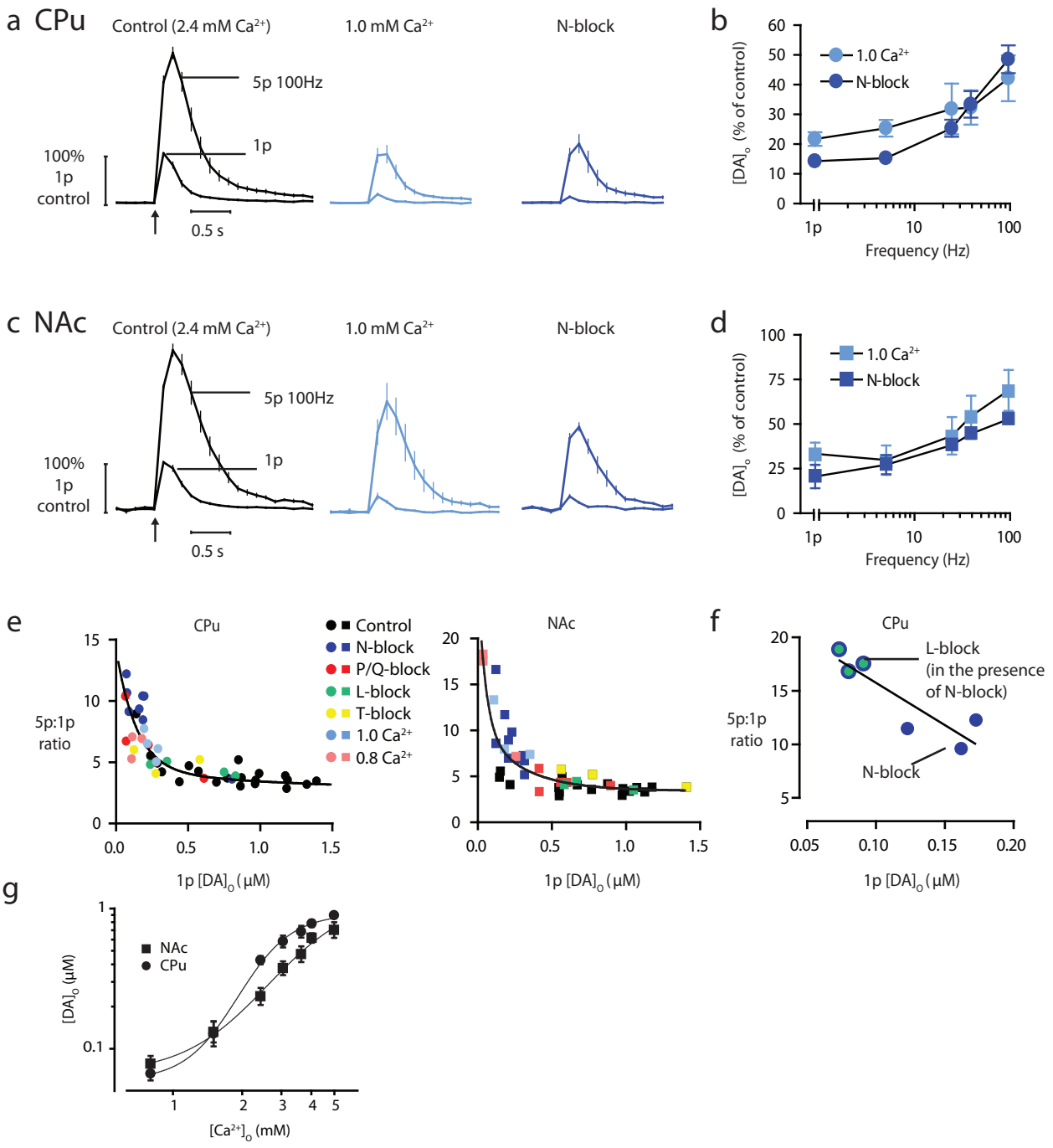

Figure 3.9 The frequency dependency of evoked $[DA]_o$ is dependent on initial release levels. Control conditions are in the presence of DHßE (1 μM). Reducing $[Ca^{2+}]_o$ to 1.0 mM reduces DA release at all frequencies in both regions in a manner similar to N-type VDCC block in CPu (a, b) and NAc (c, d). Data are: (a, c) The profile of mean $[DA]_o$ ± SEM vs time. (b, d) mean peak $[DA]_o$ expressed as percentage of control ± SEM vs frequency at 1p or 5p for 1 mM extracellular Ca^{2+} (light blue) or N-block (dark blue). (e,f) Data are $[DA]_o$ released to 1p plotted against 5p:1p ratio for CPu (left panel) and NAc (right panel), and (f) CPu for the effect of L-block following N-block , each colour shape shows the manner in which Ca^{2+} availability was altered: control are 2.4 mM extracellular Ca^{2+}. (g) CPu shows a steeper 1p $[DA]_o$ response between 0-2.4 mM Ca^{2+}, NAc is steeper >2.4 mM Ca^{2+}. Data are mean peak 1p evoked $[DA]_o$ ± SEM vs extracellular $[Ca^{2+}]$ for CPu (circles) and NAc (squares).

4. Investigating the effect of α-synuclein on the control of striatal dopamine by voltage-dependent Ca^{2+} channels (VDCCs)

4.1 Introduction

4.1.1 Role of Ca^{2+} in Parkinson's disease (PD)

Aberrant DA transmission is linked to many disorders including Parkinson's disease (PD), drug addiction, attention deficit and hyperactivity disorder (ADHD) and schizophrenia (Voorn et al., 2004; Gerfen and Surmeier, 2010; Crittenden and Graybiel, 2011; Surmeier et al., 2011b). The motor symptoms of PD are thought to be due to a loss of striatal DA, especially in the dorsolateral striatum, which is innervated by calbindin negative dopaminergic cells of the SNc (Lavoie and Parent, 1991; Iacopino et al., 1992).

In PD, DA neurons that originate in SNc are more vulnerable compared to VTA DA neurons, which are relatively spared (Grimm et al., 2004; Greene et al., 2005; Surmeier et al., 2011b). Because of the stark contrast of these two apparently similar neuron populations in terms of their vulnerability in PD, comparisons between them may provide great insights for understanding the factors that govern vulnerability in PD (Grimm et al., 2004; Greene et al., 2005; Chan et al., 2007; Surmeier et al., 2011b). Many of the identified differences between these two neuron populations occur in the somatodendritic portion of the neurons, which are situated in the midbrain. For example, it is now known that SNc but not VTA DA neurons utilise $Ca_V1.3$ channels to establish Ca^{2+} oscillations to support pacemaking, which places an energetic burden on the cells that can combine with other PD susceptibility factors (Chan et al., 2007; Guzman et al., 2009). This finding illustrates the importance of Ca^{2+} entry in the development of PD. However the Ca^{2+} entry to the somatodendritic portion of the neuron is a tiny fraction of the cells entire Ca^{2+} load. Both SNc and VTA DA neurons form extensive axonal arbors in the striatum, which in rat are estimated to form >99% of neuron's membrane length. The ratio of membrane length between the somatodendritic region and axons of these neurons, was estimated using the length and volume of axons (Matsuda et al., 2009) and the somatodendritic surface area (Henny et al., 2012). These extensive axonal arbors will have VDCCs positioned to regulate DA exocytosis

at each of 10^5 release sites per neuron (Arbuthnott and Wickens, 2007; Moss and Bolam, 2010). Therefore Ca^{2+} entry in the axonal arbors of DA neurons may well contribute to the toxic Ca^{2+} load. In chapter 3 of this thesis I identified that L-type channels modulate DA release in the dorsal striatum but not ventral striatum, which illustrates that differences between SNc and VTA neurons differ in their utilisation of VDCCs in both axonal and somatodendritic parts of the neuron.

4.1.2 α-synuclein

The multiple hit hypothesis of PD suggests interactions between DA, Ca^{2+} entry via L-type VDCCs and α-synuclein promote a PD vulnerable environment, which makes SNc DA neurons especially vulnerable (Sulzer, 2007; Mosharov et al., 2009; Collier et al., 2011). α-synuclein belongs to a family of structurally related proteins; in addition to α-synuclein there are two other synucleins,β and γ-synuclein. The synuclein family have strong homology in the N-terminus of the peptides, with high variability in the C-terminus (Senior et al., 2008). α-synuclein is genetically linked to developing both rare-inherited and sporadic PD: Both duplication and triplication of the *SNCA* locus are causal factors in the development of PD in humans, in a dose dependent manner, where PD patients with triplications have a more severe phenotype that and an earlier onset than duplications, both duplications and triplications of *SNCA* are fully penetrant (Singleton et al., 2003; Chartier-Harlin et al., 2004). In addition increases in copy number of the endogenous *SNCA* gene causing PD, certain mutations in *SNCA* can also cause PD (Sidach and Mintz, 2000). Furthermore, *SNCA* has been identified is a common risk factor for PD, and was the first PD related gene to be identified by GWAS studies (Simón-Sánchez et al., 2009).

Despite the physiological role of α-synuclein being poorly understood, it has been shown to function in a number of ways including regulating transcription, affecting ion channel function and modulating neurotransmission. Specifically related to DA function, α-synuclein has been found to reduce transcription of tyrosine hydroxylase (TH), which catalyses the rate limiting step of DA synthesis (Baptista et al., 2003). Secondly α-synuclein selectively controls DA release in the

PD sensitive CPu, while having no apparent role in the ventral striatum (Anwar et al., 2011). Anwar et al found that in triple synuclein knockout mice (TKO), DA release (measured by in vitro FCV) was facilitated compared to WT controls, whilst having a deficit in DA content (measured by HPLC) in CPu. However in NAc of TKO mice there is neither facilitation of DA release nor a deficit in DA content (Anwar et al., 2011). A complementary study has recently shown that the inverse is also true, where in mice overexpressing α-synuclein, DA release was inhibited, while DA content was increased in CPu but not NAc (Janezic et al., 2013).

In addition to the modulatory roles identified for α-synuclein on striatal DA function, α-synuclein has also been found to affect Ca^{2+} entry in a number of ways. It has been proposed that α-synuclein can form Ca^{2+} permeable pores in plasma membranes, which can damage cells (Schmidt et al., 2012). Furthermore α-synuclein can affect the function of VDCCs, including increasing the Ca^{2+} conductance of both N- and L-type calcium channels (Adamczyk and Strosznajder, 2006; Hettiarachchi et al., 2009).

The work described in this chapter aimed to explore the role of VDCCs in the control of DA release described in chapter 3 in a PD mouse model of PD. Using a PD mouse model recently developed and characterised (Janezic et al., 2013), this chapter investigates if the role of VDCCs in the control of DA release varies between mice that express different amounts of α-synuclein.

4.2 Methods

Unless otherwise described, methods are as detailed in chapter 2 and 3.

4.2.1 α-synuclein overexpression mice

In this chapter, the effect of VDCC blockade was compared between mice overexpressing α-synuclein (*SNCA* OVX) and α-synuclein null mice (*Snca*-/-). *SNCA* OVX mice were generated by the injection of a bacterial artificial chromosome (BAC) containing the entire human α-synuclein gene locus, into C57Bl6 pronuclei (Charles River). The resultant line was then backcrossed for nine generations onto *Snca*-/- C57Bl6 background. α-synuclein expression pattern in *SNCA* OVX mice is

equivalent to endogenous expression at levels which correspond to disease states (Janezic et al., *in press*). I was blind to the genotype of the animals throughout the experiments and analysis.

4.3 Results

4.3.1 Comparison of *SNCA OVX* and *Snca -/-* lines

It has been previously shown that 1p evoked $[DA]_O$ is reduced in *SNCA* OVX compared to *Snca -/-* in CPu, but not in NAc (Janezic et al., *in press*), and 1p evoked $[DA]_O$ in TKO is increased compared to WT in CPu but not NAc (Anwar et al., 2011). These two studies have shown that the role of α-synuclein is most prominent in CPu, therefore this chapter only explored the roles of VDCCs in the control of DA release in CPu regions of *SNCA* OVX and *Snca -/-* mice.

Previous studies have compared DA release between *SNCA* OVX and *Snca*-/- while nAChRs have been active. As has been previously stated, ChIs release ACh that can bind to nAChR on DA terminals, which can both modulate and drive DA release. In the work described in this chapter the nAChR were blocked throughout, allowing the modulation of DA release to be investigated in the absence of the potentially confounding effects of ACh. 1p evoked $[DA]_O$ was compared between genotypes in the presence of nAChR blockade (DHβE 1 μM). In agreement with previous studies, mean peak 1p $[DA]_O$ was ~30% lower in *SNCA* OVX compared to *Snca*-/- littermate controls (**figure 4.1a**. unpaired t-test *p<0.05)*. To investigate if α-synuclein affected the frequency dependence of DA release, DA was evoked by a range of physiologically relevant stimulation frequencies (1p, 5p at 5, 25, 40 and 100Hz). There was no significant difference between the frequency dependence of DA release between genotypes (**figure 4.1 b** 2-way ANOVA genotypeXfrequency interaction $F_{4,30}$=0.48 *p>0.05*)

4.3.2 Comparing the control of DA release by VDCCs between *SNCA* OVX and *Snca -/- mice*

In CPu of WT mice, 1p evoked $[DA]_O$ is inhibited by blockade of N>P/Q>T>L type channels (**Figure 4.2 a** {data from chapter 3.3.1}). To investigate if there were any gross differences in Ca^{2+}

dependence of striatal DA release between *SNCA* OVX and *Snca*-/- mice, the effect of N-type blockade with ω-conotoxin GVIA (100 nM) was compared between genotypes. There was no significant difference in effect of N-type channel blockade on evoked DA release at any frequency, between *SNCA* OVX and *Snca* -/- mice (**Figure 4.2 b** 2-way ANOVA effect of genotype $F_{1,30}$=1.22 *p=0.28*).

The multiple hit hypothesis of PD suggests that interactions between DA, Ca^{2+} entry via L-type VDCCs and α-synuclein promote a PD vulnerable environment, which makes SNc DA neurons especially vulnerable (Sulzer, 2007; Mosharov et al., 2009; Collier et al., 2011). Therefore the effect of L-type channels in the control of DA release was investigated in *SNCA* OVX mice and their *Snca-/-* littermate controls. Blockade of L-type channels with isradipine (5 μM) had no significant effect on DA release in *Snca* -/- mice (**Figure 4.2 c**: 2-way ANOVA effect of drug $F_{1,30}$=3.58 *p>0.05*), whereas L-type blockade reduced DA release by ~25% in *SNCA* OVX mice (**Figure 4.2 d**: 2-way ANOVA, effect of drug; $F_{1,20}$=16.19 *p=0.001*), in a frequency-independent manner (2-way ANOVA, genotypeXdrug interaction; $F_{4,20}$=0.54 *p>0.05*). It should be noted that the effect of L-type blockade on DA release in CPu of wild-type (WT) mice is equivalent to that seen in *SNCA* OVX mice (c.f. Chapter 3.3.4 for the effect of L-type block on DA release in WT mice). The effect of L-type block on DA release was significantly different between *SNCA* OVX and *Snca-/-* mice (2-way ANOVA effect of genotype, $F_{1,30}$=23.79 *p<0.001*). The reduction in CPu DA release following L-type channel block was not significantly different between *SNCA* OVX and WT mice (**Figure 4.2 e**: 2-way ANOVA effect of genotype $F_{1,30}$=2.8 *p=0.1*), therefore the effect of L-type blockade on DA release was not altered by increasing α-synuclein levels above levels in WT mice. However the decrease in DA release caused by L-type blockade seen in WT and OVX mice did not occur in the α-synuclein null mice.

To investigate if the roles of P/Q- and T-type channels in the control of DA release is altered when α-synuclein is not present compared to WT mice, pilot studies (n=1 animal) tested the effect of P/Q-type blockade (ω-agatoxin IVA (200 nM)) and T-type blockade (NNC 55-0396 (1 μM)) in CPu of *Snca* -/- mice. In CPu of *Snca-/-* mice, T-type channel blockade caused ~30% decrease in CPu that was uniform across stimulation frequencies (**figure 4.2 f**). The effect of T-type blockade in *Snca-/-* mice is consistent with the effect of T-type blockade in CPu of WT mice. P/Q-type channel blockade reduced DA release by ~50 % in a frequency independent manner (**Figure4.2 g**). In CPu of WT mice, P/Q-type blockade on average reduced 1p $[DA]_O$ to ~30% of control conditions, however the effects of P/Q-type blockade on 1p DA release was fairly variable between experiments ranging between ~85-40% reduction compared to controls. Therefore it may be true that P/Q-type channel blockade has reduced effect on DA release in the absence of α-synuclein, however this was not further explored, because following a power calculation with β value of 0.8, and assuming the effect of P/Q-blockade on DA release in *SNCA* OVX mice is the same as with WT mice, and that the true effect of P/Q-type blockade on 1p DA release in *Snca-/-* mice is 0.53 (1p DA release normalised to control conditions), then 19 pairs of animals would be necessary to reach significance level of $p<0.05$ using $\mu_{Snca-/-}0.53$, $\mu_{WT}0.33$ $\sigma_{WT}0.22$ http://www.stat.ubc.ca/~rollin/stats/ssize/n2.html).

4.4 Discussion

4.4.1 Overview

In this chapter I have shown that blockade of L-type VDCCs reduces DA release in WT and *SNCA* OVX mice but not in *Snca-/-* mice. From this one can infer that the control of DA release by L-type VDCCs is dependent on α-synuclein. The roles of N-, P/Q- and T-type channels on DA release do not appear to be affected by different levels of α-synuclein, as the effect of blocking N-, P/Q- or T-type channels did not seem to affect DA release differently between genotypes.

An unfortunate consequence of the in-bred nature of laboratory animals is the ability for spontaneous mutations to arise and rapidly spread through a population termed “wild-type” animals. One example of this is the spontaneous deletion of α-synuclein in a wild-type line of C57Bl mice (Specht and Schoepfer, 2001), therefore it may be important to consider interpretation of the role of L-type channels from experiments which use WT lines of mice that lack the α-synuclein gene.

The dependence of L-type channels on α-synuclein for controlling DA release offers insight into a possible functional role of α-synuclein in normal brain physiology that may inform our understanding of PD. It remains unresolved if the dependence of L-type channels in the control of DA release is by a direct interaction between α-synuclein and the channel or rather because of altered expression or trafficking of L-type channels into the dopamine terminals. Previous studies have shown that α-synuclein potentiates entry of Ca^{2+} through L-type channels (Hettiarachchi et al., 2009), which would support the first explanation. In chapter 3.4.2 it was briefly discussed that although blockade of L-type channels has no effect on DA release in NAc when extracellular Ca^{2+} was 2.4 mM, when it was raised to 3.6 mM, blockade of L-type channels did reduce DA release. As an extension of this, future experiments could investigate if a role for L-type channels in the control of DA release can also be exposed in CPu of *Snca-/-* mice when extracellular Ca^{2+} is raised from 2.4 mM used here, to 3.6 mM. Additionally it could be informative to establish if the role of L-type channels in somatodendritic regions of SNc DA neuron, which was proposed as a causal factor of SNc DA neurons heightened sensitivity in PD (Guzman et al., 2009), can also be altered by α-synuclein levels or by changing extracellular Ca^{2+} levels.

4.4.2 Implications for PD

Antagonism of the $Ca_V1.3$ with isradipine is being trialled in PD patients to reduce the Ca^{2+} oscillations and subsequent mitochondrial oxidative stress to prevent cell death (Simuni et al., 2010; Rees et al., 2011). The neuroprotective effect of isradipine may be also due to its action at DA terminals, because we have shown here that L-type calcium channels are also operating in the vast axonal arbors of DA neurons (Arbuthnott and Wickens, 2007). However it remains unclear whether the therapeutic reduction in Ca^{2+} load can offset the reduction in striatal DA release. If L-type antagonism reduces DA release in the already compromised terminals, it may cause more harm than good. It may be true that antagonism of the $Ca_V1.3$ needs to be restricted to PD patients at the early stages of the disease, or high risk non-symptomatic individuals.

The contribution of the huge axonal arbour to the metabolic state of the cell is especially important if PD progresses in a "dying back mechanism" (Hornykiewicz, 1998; Cheng et al., 2010). In contrast to neurons dying as a result of axonal degeneration, it is also possible that neurons die via classical apoptotic mechanisms, where amongst many other potential triggers, cellular stress caused by excess Ca^{2+} load, triggers the activation of a family of proteases known as caspases. Following caspase activation the architecture of the cells become dismantled including break down of nuclear membrane, DNA condensation and degradation and formation of apoptotic vesicles (Taylor et al., 2008). The idea that axonal degeneration occurs via different mechanisms to that of programmed cell death of the soma, is supported by evidence that suggests that the terminals are more sensitive to mitochondrial stress than the cell body (Pickrell et al., 2011). If the axons are more sensitive to oxidative stress than the cell body, and Ca^{2+} entry via VDCCs causes oxidative stress then, understanding the roles of VDCCs in axonal DA release should be a priority. However it is highly likely that axonal degeneration and programmed cell death, which would primarily occur in the soma, are two sides of the same coin, because excess Ca^{2+} load occurring in the axonal fields would likely be sensed in the soma, due to axonal Ca^{2+} being stored in the endoplasmic reticulum, which spans the length of the neuron (Orrenius et al., 2003;

Verkhratsky, 2005; Ramírez and Couve, 2011). Therefore, identifying different requirements for Ca^{2+} entry via VDCCs throughout the SNc and VTA dopaminergic neurons is necessary to determine if Ca^{2+} load causes SNc neurons to be especially sensitive to degeneration in PD, especially when considered in conjunction with other known risk factors such as α-synuclein.

The control that L and T-channels exhibit in DA terminals of the dorsal striatum (shown in chapter 3), may be small but the extra Ca^{2+} they supply over a lifetime could well contribute to the extra Ca^{2+} burden of the SNc DA neurons, thought to be key to their heightened sensitivity to PD. It has recently been shown that entry of Ca^{2+} via L-type channels results in more oxidative stress in dendrites than is seen in the soma (Dryanovski et al., 2013). It may be theorised from this work, that as the axons are even further from the soma than the dendrites, the oxidative stress arising from L-type Ca^{2+} entry may be even more marked than seen in the dendrites. Additionally the role of the L- and T-type channels in controlling DA release may be illustrating an interesting difference in the mechanism of controlling DA release in the two neuron types. The differing functional roles of L- and T-type channels in supplying the terminals with Ca^{2+} in the CPu but not NAc may provide insights into the increased sensitivity of SNc over VTA DA neurons to PD, especially as there are no reported differences in transcription levels of the different VDCC subtypes between SNc and VTA DA neurons (Grimm et al., 2004).

4.4.3 Summary

In summary, building on the finding in chapter 3 that PD sensitive and resistant areas of striatum have different requirements of VDCCs in the control of DA release, this chapter has investigated the roles of VDCCs in the control of DA release in a mouse model of PD, and its littermate controls. The mouse model of PD expresses α-synuclein at a level that is equivalent to pathological levels in humans. This chapter showed that blockade of L-type channels in α-synuclein null mice has no effect on DA release, whereas

in α-synuclein overexpressor and wild type mice L-type channel blockade decreases DA release in the striatum. Therefore it seems that L-type control of DA release is dependent on α-synuclein. None of the other VDCCs control of DA release appears to be affected by varying levels of α-synuclein.

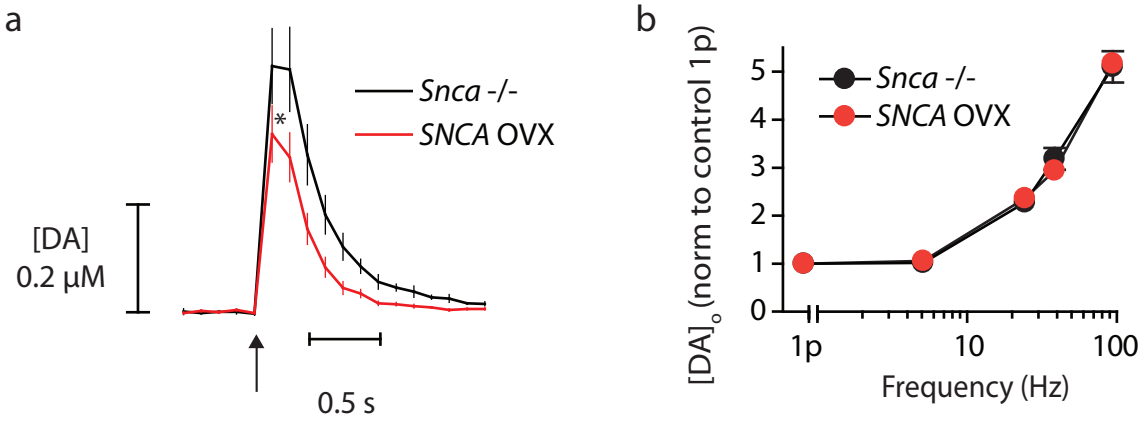

Figure 4.1. Evoked $[DA]_o$ is lower in CPu of *SNCA OVX* than *Snca-/-* mice
DHßE (1 µM) present in all experimental conditions. (a) Mean 1p evoked $[DA]_o$ (µM)± SEM vs time post stimulation for *Snca-/-* (black line) and *SNCA* OVX (red line). (b) Mean peak $[DA]_o$ ± SEM vs frequency (Hz) at 1p or 5p for *Snca-/-* (black cirlces) and *SNCA* OVX (red circles), data are normalised to mean peak 1p $[DA]_o$ of each genotype. *Snca-/-* n=4, *SNCA OVX*=3 animals

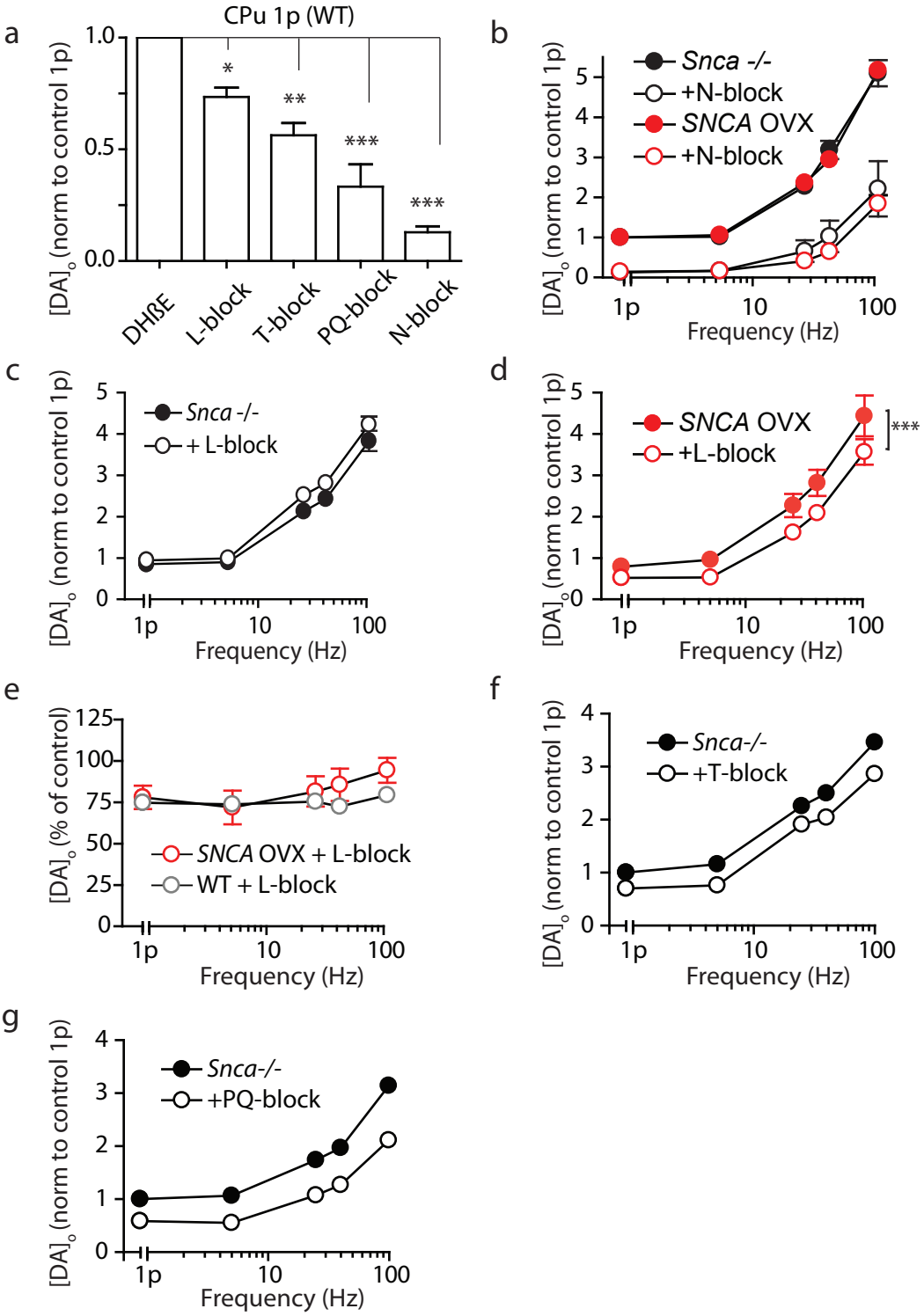

Figure 4.2. The control of DA release by L-type Ca^{2+} channels is dependent on α-synuclein. DHßE (1 μM) is present in all conditions. (a)Summary of the effects of VDCC blockade in WT CPu. Mean peak $[DA]_o$ normalised to control 1p. Data are from chapter 3. (b,c,d) Mean peak $[DA]_o$ ±SEM, data are normalised to peak control 1p $[DA]_o$, vs frequency at 1p or 5p. Control conditions are filled circles and in the presence of VDCC blocker are unfilled circles for *Snca-/-* (black) and *SNCA OVX* (red). (b) N-blockade with ω-conotoxin GVIA (100 nM) (c,d) L-blockade with isradipine (5 μM). (e) The effect of L-blockade in WT (grey unfilled circles)vs *SNCA OVX* mice (red unfilled circels). Mean peak $[DA]_o$ expressed as percentage of control ± SEM vs frequency at 1p or 5p. *Snca-/-* n=4, *SNCA OVX*=3 animals. (f,g) pilot studies of T-(f) and P/Q-(g) type channel blockade in *Snca-/-*. Mean peak $[DA]_o$ ±SEM, data are normalised to peak control 1p $[DA]_o$, vs frequency at 1p or 5p. Control conditions are filled circles and in the presence of VDCC blocker are unfilled circles. n=1 animal.

5. Investigating the modulatory role of Substance P in presynaptic dopamine release

5.1 Introduction

5.1.1 Substance P (SP)

Both DA and ACh are major neuromodulators of the striatum (Cragg, 2006; Arbuthnott and Wickens, 2007; Gerfen and Surmeier, 2010; Rice et al., 2011), where they regulate the flow of information from the input to the striatum (from the thalamus and cortex) to the striatal output neurons (the medium spiny neurons (MSNs)). In addition to DA and ACh there are many other neuromodulatory molecules within the striatum. These include peptides, cannabinoids and small molecules including ATP (Kalivas and Miller, 1984; Llona et al., 1994; Trendelenburg and Bültmann, 2000; Britt and McGehee, 2008; Sidló et al., 2008). Striatal neuromodulators may act on glutamatergic afferents to the striatum, on efferent MSNs, on striatal interneurons or on terminals of the DA neurons originating from the midbrain. As there are a large number of modulators and a large number of potential action sites the permutations for neuromodulation are vast. This high degree of complexity provides the striatum with a huge amount of computational power and could provide opportunities for pharmaceutical intervention for the many psychomotor disorders associated with the basal ganglia. However, in order to best tailor a medicinal intervention to a disease and we must first endeavour to understand each neuromodulatory system. In the striatum SP is not uniformly expressed, rather it is enriched in the striosome territories of the striatum. Here I aim to investigate the modulatory effect of SP on DA release, and whether any modulation varies between striosome and matrix territories.

SP is a small neuromodulatory peptide composed of 11 amino acid residues. It is the splice product of preprotachykinin A (PPT-A) gene, of which neurokinin A is also a product (Nawa et al., 1984). SP is associated with a wide range of physiological functions in the sensory system including pain perception, itch response and vomiting (Zubrzycka and Janecka, 2000; DeVane, 2001; Nakamura et al., 2013). SP also functions in the central nervous system (Petit and Glowinski, 1986; Bolam and Izzo, 1988; Anderson et al., 1993; Guevara Guzman et al., 1993). In

the striatum, SP is released from the collaterals of a population of MSNs. The MSNs which release SP also contain dynorphin and express the D1 receptor (Bolam and Izzo, 1988; Gerfen and Surmeier, 2010; Govindaiah et al., 2010; Durieux et al., 2011).

SP has highest affinity to the neurokinin (NK) receptor 1 (NK1R) but can also bind to NK2 and NK3 receptors with lower affinity (Quartara and Maggi, 1997; Govindaiah et al., 2010). In the striatum the NK1R is the most highly expressed type, but low levels of NK2 and 3 types are still detected. Originally it was thought that only the ChIs express NK1Rs, but this is now known not to be true, as MSNs, NOS positive interneurons and DA neurons also express NK1R (Bolam and Izzo, 1988; Gerfen, 1991; Tremblay et al., 1992). DA neurons are known to express all three NK receptor sub-types and it has been suggested that the majority of the expressed receptor is trafficked to the DA terminals because of the disparity between high expression levels but low binding levels in the midbrain (Jakab and Goldman-Rakic, 1996; Whitty et al., 1997), however there is limited evidence to support this: Low power microscopy show TH- and SP-immunoreactive terminals overlap and both NK1R and TH are highly expressed in the striatum (Ljungdahl et al., 1978; Mantyh et al., 1984).

In striatum SP and NK1R have been shown to modulate both the firing of striatal neurons and release of neurotransmitters, including modulating ChI firing and ACh release, MSN firing, and DA release (Table 1). SP is more often reported to have excitatory effects than inhibitory effects, despite it forming symmetrical type synapses, which are often thought to correspond to inhibitory synapses (Bolam and Izzo, 1988). However SP may activate its receptors via volume transmission rather than classical synapses, which may explain the lack of anatomical correlation (Liu et al., 1994). Table 1 shows a sample of studies which have investigated the role of SP in the striatum, and it is striking that SP modulates neurons and neurotransmitters, which are also capable of modulating one another, which may make interpreting these findings complicated. For example if SP decrease ACh release, ACh could increase DA release (depending on the

stimulation frequency), which will have differential effects on MSNs, depending on if they express D1 or D2 like receptors. To further complicate the story, SP is able to not only modulate DA, but also be modulated by DA. This reciprocity between these two neuromodulators could result in a flexible and dynamic system (Bannon et al., 1986; Young et al., 1986; Kovács et al., 2006; Sivam and Cox, 2006).

Table 1.

Region	**Effect of SP**	**Reference**
CPu	↑ spontaneous DA release	(Starr, 1982)
CPu	↓ K^+ evoked DA release	(Starr, 1982)
CPu	↑ spontaneous DA release	(Petit and Glowinski, 1986)
CPu	↑ spontaneous DA release	(Tremblay et al., 1992)
CPu	= (no effect) on DA release	(Boix et al., 1992)
NAc	↑ DA release	(Boix et al., 1992)
Striatum	↓ DA release (inferred from NK1 antagonist ↑ release)	(Gygi et al., 1993)
Medial striatum	= (no effect) on DA release	(Guevara Guzman et al., 1993)
neostriatum	↓ MSN firing in DA dependent manner	(Galarraga et al., 1999)
NAc	↓ cell (probably MSNs) firing rate (via ↑ in DA and adenosine release)	(Kombian et al., 2003)
CPu	↑ neuron firing rate (unspecified cell)	(Le Gal La Salle and Ben-Ari, 1977)
CPu	↓ IPSCs in ChIs	(Govindaiah et al., 2010)
neostriatum	↑ MSN firing in ACh dependent manner	(Galarraga et al., 1999)
CPu	↑ ACh release	(Anderson et al., 1993)
CPu and NAc	↓ ACh release	(Boix et al., 1994)
Medial striatum	↑ ACh release	(Guevara Guzman et al., 1993)

As is evident from Table 1 the effects of SP on DA release is highly variable, other neuromodulators including ACh have also have variable effects on DA release. The conflict surrounding the variable effects of ACh on DA release have now been resolved, as we now know that the effect of ACh on DA release is frequency dependent; where ACh clamps DA release across stimulation frequencies so that ACh increases 1p DA release but decreases burst release. It may be that the variable effects of SP on DA release can be explained by the studies using different stimulation paradigms, and SP modulatory effects of DA release may be frequency dependent. Therefore in this part of my thesis work I investigate the effect of SP on DA release across a range of stimulation frequencies.

Striatal ChIs release ACh, which powerfully modulates DA release, they also express high levels of NK1R, making it highly possible that SP could modulate DA release via the cholinergic system. As has been previously described ChIs release ACh, which binds to nAChR on DA terminals, which can gate how DA is released to different stimulation frequencies, and also drive DA release independently from activity in DA neurons. It is currently unknown if the modulatory effect of ACh on DA release varies with the amount of ACh released. It may be that there is a threshold level of ACh required to modulate DA, and increasing levels of ACh above this threshold has no additional effects. Alternatively the effects of ACh on DA release may be on a continuum, whereby low levels or un-synchronous release of ACh is responsible for the gating action of ACh, and high levels of synchronous ACh release is responsible for the driving action of ACh. If this is true, a neuromodulator (such as SP) acting upon the cholinergic system could also bring about a range of modulatory effects on DA release. However, as we are currently unable to measure ACh release with sufficient temporal resolution I have not investigated if modulation of DA by ACh is altered by SP, rather I have focused on direct effects of SP on DA release. In order to examine the effects of SP directly on DA terminals, nAChRs were blocked with DHβE (1 μM). The effect of SP on DA release may vary depending on whether recordings are done in the presence and absence of nAChR blockade, which may explain the conflicting effects of SP on DA release to date.

5.1.2 Biochemical classification of striosome-matrix axis

The striosome-matrix division of the striatum has been known about for over 30 years (Pert et al., 1976; Graybiel and Ragsdale, 1978; Gerfen, 1984). Since the identification of μ-opioid receptor (MOR)-rich regions in the striatum (Pert et al., 1976), other biochemical markers with uneven distribution throughout the striatum have been identified including D1 type of DA receptor (D_1R), SP, calretinin and Nr4a1 which have been found to be striosomally enriched in a number of species including mouse, rat, cat and primates including humans (Besson et al., 1988; Sakamoto et al., 1992; Crittenden and Graybiel, 2011; Davis and Puhl, 2011). The matrix, by contrast is enriched with calbindin and acetylcholineesterase (AChE) (Besson et al., 1988; Davis and Puhl, 2011). In addition to striosome and matrix territories, a third biochemically defined territory of the striatum has also been proposed known as the annulus. Annuli were described as rings of high SP and enkephalin immunoreactivity and low AChE immunoreactivity, and were sometimes found to have a low cell density (Faull et al., 1989; Holt et al., 1997). The somatostatin-positive interneurons and ChIs are also reported to cluster around the edges of striosomes in an annular pattern (Kawaguchi, 1993; Aosaki et al., 1995). It has not yet been characterised if the annular regions defined by SP, enkephalin, AChE and distribution of interneurons all correspond to the same structures, and the existence of annular regions has been questioned by some groups (Johnston et al., 1990).

5.1.3 Anatomical distinction between striosome and matrix

Striosomes and matrisomes also differ in terms of their development, circuitry and sensitivity to certain diseases, including PD. DA innervation of the striatum occurs in the striosomes first; during development there is formation or DA rich areas in the striatum, which are termed “DA islands”. These islands, later correspond to the striosomes, as DA innervation becomes uniform (Graybiel, 1984; Gerfen et al., 1987a). In addition to the early DA innervation of striosomes, in adult brains, only striosomal MSNs directly innervate the SNc and VTA (Gerfen, 1984; Crittenden and Graybiel, 2011; Watabe-Uchida et al., 2012). Additional anatomical segregation of

striosomes and matrisomes also exist: D2 DA receptors (D_2R)-expressing MSNs, which form the indirect pathway of the basal ganglia are preferentially located in the matrix and D_1R-expressing MSNs, which form the direct pathway are preferentially located in the striosomes (Gerfen et al., 1987a; Besson et al., 1988). There are also differential distribution of inputs to striosomes and matrisomes, which receive more limbic and sensorimotor inputs respectively (Gerfen, 1984, 1992; Crittenden and Graybiel, 2011).

Disruption of the striosome and matrix axis of the striatum may arise from a number of changes including altered expression of biochemical markers; changes in synaptic contacts or different sensitivities of striosome and matrix cells to diseases. All of these changes have been observed and associated with diseases including Parkinson's disease (PD) (up-regulation of Nurr77 in striosomes), dystonia, schizophrenia (increased asymmetrical synapses in the matrix), Huntington's disease (preferential loss of striosomal volume), and drug addiction (Crittenden and Graybiel, 2011). In PD it has been reported that there is reduced striosomal staining for MOR (Damier, 1999). Therefore fully understanding how SP, DA and the striosome-matrix compartments interact could provide key insights for both healthy and disease states of the striatum, and basal ganglia.

In this chapter I will test if SP can modulate DA release directly via NK1R on DA terminals, and if any modulation of DA release varies with stimulation frequency. I will also investigate if the effect of SP on striatal DA release is affected by the striosome-matrix axis of the striatum.

5.2 Methods

Unless otherwise described, methods are as detailed in previous chapters. In brief, 300 μm coronal sections containing both CPu and NAc were superfused in aCSF saturated with 95% O_2 5% CO_2, and maintained at 30-32^{O}C. Extracellular DA ($[DA]_O$) was monitored using fast-scan cyclic voltammetry (FCV) at carbon fibre microelectrodes ((CFM) 7μm in diameter, tip length 50-100

µm), the scanning voltage was a triangular waveform -700 to 1300 mV vs. Ag/AgCl electrode at a sampling rate of 8 Hz (Julian Millar, Barts and the London School of Medicine and Dentistry).

5.2.1 Experimental design

Recordings were mostly performed in the dorsolateral quadrant of the CPu. This region was selected because the MOR-rich striosomes have more defined boundaries in the CPu compared to the striosomes of the NAc. As the source of striatal SP is the collaterals of striatal MSNs, stimulation paradigms were chosen that were in keeping with *in vivo* MSN activity (Bolam and Izzo, 1988; Anderson et al., 1993; Yung et al., 1996). The stimulation paradigms 1p, 5p 5Hz, 20p 5Hz and 20p 20Hz were chosen for both their frequency and duration: 5 and 20Hz span both tonic and phasic frequencies at which DA neurons are known to fire. Striatal MSNs exhibit up-states and down-states, the MSNs are only thought to fire in the up-state. To allow MSNs to reach up-state and subsequently fire, long stimulation paradigms were chosen (Vergara et al., 2003). Additional support for using long stimulation paradigms is that SP acts upon metabotropic receptors meaning any activity of SP may require sufficient time to be released from MSNs, act upon its receptor and exert its downstream effects to potentially modulate DA release. These stimulation paradigms allow comparisons of pulse number, frequency and stimulation duration.

5.2.2 Drugs

Dihydro-β-erythroidine (DHβE) was purchased from Tocris or Ascent scientific, Substance P and L-732,138 were purchased from AbCam. DHβE and substance P were dissolved in dH_2O to 1000-2000x final concentrations and stored at -20^{o}C. L-732,138 was dissolved in ethanol at 1000x final concentration and stored at -20^{O}C. Drugs were diluted in oxygenated aCSF immediately prior to use to final concentrations required. Drug concentrations were chosen in accordance with previous studies (Anderson et al., 1993; Kombian et al., 2003; Blomeley et al., 2009). GABA receptor blockers bicuculline (10 µM), saclofen (50 µM) and glutamate receptor blockers MCPG (200 µM), D-AP5 (50 µM) and GYKI (10 µM) were used in pilot studies.

5.2.4 Data analysis

Data were acquired and analysed as described in previous chapters. In brief data are expressed as mean ± standard error of the mean (SEM), where n = number of recording site, for single recording sites per striatal slices. Data from each site were calculated by averaging at least 3 recordings at each stimulation frequency and normalised to control conditions for each site. Means were compared using one- or two-way ANOVA with post-hoc Bonferroni's t-test where appropriate, using GraphPad Prism. Parametric tests were appropriate as raw control data passed Shapiro-Wilk normality test (*p=0.11)*.

5.2.3 Immunohistochemistry

Recordings made in CPu in the presence of nAChR blockade were further analysed to determine if a recording site was in a striosome or matrix region of the striatum. Only recordings in CPu were processed for immunohistochemistry as the distinction between striosomes and the surrounding matrix is much more definite in CPu compared to in NAc, where there is a more gradual distinction between MOR-rich striosomes and MOR-poor matrix (**Figure 5.1**). After recording DA at CFM, electrode placement sites were marked using yellow-green FluoSpheres (1 µm diameter Invitrogen product number F-13081) and tissue was processed for MOR immunoreactivity to allow their location in terms of striosome-matrix regions to be determined. To mark recording sites and co-label for MOR immunoreactivity the protocol described in chapter 2.4.2 was developed.

5.2.4 Method for classification of recording site as "striosome", "matrix" or "boundary" regions.

FluoSphere marking was used to indicate CFM recording sites. However, there is likely to be some error introduced through this method, which makes the sites marked an approximation to those recorded. Therefore, when characterising the recording sites in terms of striosome or matrix locations, these caveats should be borne in mind, and a cautious approach was used to

categorise each site. I used both qualitative and qualitative methods to classify recording sites: Ternary classification, divides markings as having matrix, striosome or boundary locations. I also use a quantitative system to determine the distance between the recording site and the nearest striosome.

5.2.4a Ternary classification of recording site

Outlines of MOR-rich striosomes were drawn to define the boundaries of the striosomes (S) nearest to a marked site (**Figure 5.2**). The outlines were drawn using "free-draw tool" in q-capture pro7. The size and positioning of outline S was initially drawn by eye, and then refined by increasing contrast of the image so there was a much steeper contrast between "coloured and black pixels". The outline was then further refined by focusing through the *z*-axis, which sometimes helped clarify the overall shape and maximum dimensions of the striosome. A high density of MOR staining was only considered a striosome if it was at least 100 µm across (in any single direction). The identity of the recording site was made using two different approaches, approach 1 and 2.

Approach 1: The FluoSpheres used to mark the recording site were drawn around using the "oval tool" in q-capture pro7, so that it incorporated all of the beads. The area was then doubled by increasing the circumference by $\sqrt{2}$ (**Figure 5.2** oval A). The identity of the recording site as matrix, striosome or boundary was decided using the following criteria: As matrix when oval A was completely distinct from outline S; as Striosome when oval A is completely contained within outline S; and as boundary when oval A intersects outline S.

This method allowed the error of a recording site to be incorporated into the definition of the site whilst allowing a simple ternary outcome. A yet more cautious approach in which the circumference of the initial oval was doubled, so the area of this more cautious oval is the area of oval A squared. However, as it did not alter the classification of any of the marked sites it was not illustrated or used.

Approach 2: It can be argued that the region from which DA is being recorded from has a fixed volume. Therefore a recording site was defined as being a circle of 25 µm radius, centred on the brightest point of the FluoSpheres, regardless of the area labelled by the FluoSpheres (**Figure 5.2** circle B). A 25 µm radius circle was chosen, as it is estimated that in the time taken for DA to peak following 1p DA can diffuse ~20 µm (Cragg and Rice, 2004) using computational modelling or ~6 µm using modelled experimental data (Venton et al., 2003). The identity of the recording site was decided using analogous criteria as approach 1: As matrix when circle B is completely distinct from outline S; as striosome when circle B is completely contained within outline S; and as boundary when circle B intersects outline S.

5.2.4b Quantitative classification of recording sites

The distance between the FluoSpheres-marked site and nearest striosome was measured to quantitatively examine the effect of SP on evoked $[DA]_O$ along the striosome-matrix axis of the striatum. In addition to corroborating the ternary classification method, measuring the distance between marked sites and striosomes may illustrate a "SP effect gradient" that would not be apparent with a simple ternary classification. Two distances were measured, b1 and b2. b1 is the shortest distance from the centre of circle B (B*) to the striosome boundary (S). Secondly b2 was measured, which is the distance from B* to the centre of the nearest striosome (S*) (**Figure 5.2**). S* was defined by selecting a "region of interest" (ROI) on the central area of the striosome by eye, and then choosing the point with the brightest pixels within ROI as S*. The relationship between the effect of SP on DA release, and the marked site to striosome distance could be compared between when the distance was defined by either b1 or b2. This was especially important when the boundary of a striosome was not very well defined and there was a more gradual decrease in MOR staining from the centre of a striosome to the low levels of staining seen in the matrix, as b2 is independent from S, whereas both b1 and the ternary classifications are dependent on S. The distance was measured using the "ruler tool" in q-capture pro7.

Both the ternary and quantitative classification systems were performed blind with respect to the FCV data: Fixed slices of tissue were labelled with the date of experiment only. In some instances the FCV data were analysed prior to the striosome-matrix classification, however they were not consulted during this process.

5.3 Results

5.3.1 SP modulates DA release via NK1 receptors (NK1R) on DA terminals

SP has previously been shown to modulate both ACh and DA release (see table 1), however the published effects are inconsistent. Possible reasons for this inconsistency are that the modulatory effects of SP are frequency dependent; alternatively SP may be changing the levels of additional neuromodulators, which then go on to differentially modulate DA release. For example (Anderson et al., 1994) show that SP modulates D1R dependent ACh release, and SP has been shown to directly modulate ACh, which is well known to powerfully modulate DA release (Rice and Cragg, 2004; Exley and Cragg, 2008; Threlfell et al., 2012). Many of the studies which have investigated the effect of SP on DA release have used microdialysis, which allows the normal neurological contacts to be maintained, ensuring DA is released in a physiological manner. The preservation of neuronal contacts is generally considered a strength of microdialysis, but as SP can modulate so many of the neuronal populations present in the striatum, which also modulate each other, interpreting the data as a whole becomes very complicated. Because of the potential for SP to affect ACh release, and the powerful modulatory effects of ACh on DA release, I have investigated the effect of SP in the absence of the potentially confounding effects of ACh. Microdialysis has been used to investigate the effect of SP on DA release over a long time course, where it has been found to have a stable effect for up to 30 minutes (Petit and Glowinski, 1986; Tremblay et al., 1992). As a point of comparison with these studies I will be investigating how SP affects DA release during different frequency stimulations and if it changes during long train stimulations.

Experiments were conducted in the presence of nAChR blockade (DHβE 1μM). Under these control conditions, bath applied SP (1 μM) was found to have highly variable effects on 1p $[DA]_O$. In CPu, SP could decrease n=8/22 (**Figure 5.3 a,b**), increase n=4/22 (**Figure 5.3 c,d**) or have no effect n=10/22 (**Figure 5.3 e**) on 1p $[DA]_O$. Both the decrease in evoked DA (referred to here as a type 1 response) and increase in evoked DA (referred to here as a type 2 response) could be reversed by washing off with aCSF (**Figure 5.3 a,c**) or by blocking NK1R with L-732,138 (at 10 μM to reverse a type 1 effect) (**Figure 5.3b**) (and 1 μM to reverse a type 2 effect)(**Figure 5.3d**). A decrease or increase in 1p evoked $[DA]_O$ release of at least 15% was required to class a response as type 1 or 2 response respectively. The variable effects of SP on DA release were seen in both CPu and NAc in the presence of nicotinic blockade, and also in CPu in the absence of nicotinic block (**Figure 5.4**). The means and variances of the effect of SP was not significantly different between CPu or NAc in the presence of DHβE or CPu without DHβE (**Figure 5.4**: 1-way ANOVA $F_{2,42}$=1.1 *p>0.05*; Bartlett's test of variances X^2 (2)=0.33 *p>0.05*)

A wide range of stimulation protocols were chosen to probe the type 1 and type2 modulatory effects of SP on DA release: 1p, 5p 5Hz, 20p 5Hz and 20p 20Hz. This was to allow for SP acting at metabotropic receptors, which may need time to exert their downstream effects. For 5p 5Hz, 20p 5Hz and 20p 20Hz, the DA transients have a distinct shape with an initial peak followed by a lower level plateau. The effect of SP (1 μM) on DA release was relatively constant across stimulation paradigms. The effect of SP was present at the peak max of 1p stimulations, and on the initial peaks of trains as well as during the long-train stimulations, in the sites where SP caused a type 1 response (**Figure 5.5a**) or type 2 response (**Figure 5.5b**). The effect of SP was consistent across stimulation paradigms; there was an approximate 1:1 relationship between the effect of SP (% of control) for 1p $[DA]_O$ and 20p 20 Hz $[DA]_O$ (**Figure 5.5c** linear regression: slope= 1.194 R^2=0.86).

These data suggest that SP can modulate DA release directly by binding to NK1R on DA terminals, which can both decrease or increase evoked DA release. If SP was modulating DA

release via another neurotransmitter system you would not expect to see the effects at 1p DA release, and as the effect of SP on DA release is stable throughout train stimulations lasting almost 4 seconds, it would appear that SP is only affecting DA release directly. To confirm that SP is acting directly on DA terminals and not via other inputs (GABA and glutamate), which do not normally modify DA release by 1p, pilot studies were conducted in the presence of GABA and glutamate blockade {bicuculline (10 μM), saclofen (50 μM) MCPG (200 μM), D-AP5 (50 μM) and GYKI (10 μM)}. The modulatory effect of SP remained in the presence of GABA and glutamate blockade, supporting the premise that SP is modulating DA directly at the DA terminals (data not shown).

In CPu when nAChRs are not blocked, the effect of SP on the peak max of 1p evoked $[DA]_O$ was often less than on 20p 20Hz evoked $[DA]_O$ (**Figure 5.5d** linear regression: slope=1.48 R^2=0.78). Additionally the effect of SP 20p 5Hz evoked $[DA]_O$ is only seen for the peak of the transient and not during the plateau phase of the transients (**Figure 5.5e**). These data suggest additional effects of SP, including changing ACh release, however these effects are not investigated further in this thesis work.

5.3.2 The effect of SP on DA release varies along the striosome-matrix axis

In order to understand the variable effect of SP on DA transmission at different electrode placements, recording sites were marked with FluoSpheres (Invitrogen) and slices were immunostained with MOR to determine a recording sites' location with respect to the striosome-matrix axis of the striatum. Investigations were focused on the dorsal-lateral quadrant of the CPu, where the striosomal boundaries of the CPu are more definite; in the NAc there is more of a gradual gradient of MOR expression compared to the high contrast between striosome and matrix as is seen in CPu (**Figure 5.1**).

As described in methods, the marked site boundary was defined by two means: Oval A (oval that is twice the area required to contain all of the FluoSpheres), which is shown by the

dashed green line; and Circle B (25 µm radius, centred upon the brightest point of the marked site), which is shown by the solid green line (**Figure 5.6 left panel a,b,c**). A marked site was considered as "matrix" when the striosome boundary (S) was completely non-overlapping with oval A or circle B; as "striosome" when A or B were contained within S; and a boundary site when S was intersected by A or B. In no single case did changing the boundary of the marked site from oval A to circle B affect the classification of any site.

When the data were grouped with respect to their striosomal-matrix location it was found that the effect of SP on mean evoked $[DA]_O$ varied between striosome, matrix and boundary locations. In the matrix DA release was unaffected by SP (**Figure 5.6 a**). The left panel shows an example matrix recording site and its 1p transient in control and SP condition (middle panel), the right panel shows the peak max $[DA]_O$ in control and SP for each individual recording sites defined as being in the matrix. When recording sites were within a striosome, SP caused an increase in DA release (**Figure 5.6 b**). The left panel shows an example striosome recording site and its 1p transient in control and SP condition (middle panel), the right panel shows the peak max $[DA]_O$ in control and SP conditions for each of the recording sites defined as being in the striosome. When recording sites were on a boundary region between the striosome and matrix, SP caused a decrease in DA release (**Figure 5.6 c**). The left panel shows an example boundary recording site and its 1p transient in control and SP condition (middle panel), the right panel shows the peak max $[DA]_O$ in control and SP conditions for each of the recording sites defined as being on the boundary. The effect of SP is significantly different between recordings in the matrix, striosome or boundary regions (**Figure 5.6 d** One-way ANOVA $F_{2,21}=15.2$ *$p<0.001$* with bonferroni posttests)

To investigate if the effect of SP was on a continuum that correlated further with the striosomal-matrix positioning of the recording site rather than simply ternary responses depending on matrix, striosome or boundary positioning, the distance from a marked site to the

nearest striosome was measured. This distance was calculated in 2 ways: b1 measured the shortest distance from the centre of a marked site (B*) to the edge of the nearest striosome. b2 measured the distance between B*and the centre of the nearest striosome (S*). b1 (**Figure 5.7 a**) and b2 (**Figure 5.7 b**) were plotted against the effect of SP on 1p DA release. Both plots show a similar trend, whereby points furthest from a striosome had the smallest percentage effect on 1p $[DA]_O$ release, and as you approach the striosome there is a decrease in release until you reach a threshold which results in an increase in DA release. B2 (**figure 5.7 b**) can also be used to corroborate the relationship between ternary classification of marked site and effect of SP on DA, as measuring the distance between the A* and S* requires no assignment of boundaries, so may be considered independent from boundaries drawn earlier (**Figure 5.6**).

5.4 Discussion

In this chapter I have shown that SP can modulate DA release. The effect of SP on DA release varied between recording sites, capable of reducing 1p evoked $[DA]_O$ (referred to as type 1 response) down to 50% of control levels and increasing 1p evoked $[DA]_O$ (type 2 response) up to 170% of control levels. In almost half of cases, SP did not alter evoked DA release by more than 15%, and in these cases SP was classed as having no effect on DA release. Both type 1 and type 2 effects were reversible by washing out with aCSF and by blocking NK1R with L-732,138. SP could modulate DA directly, appearing to act at NK1R on DA terminals, and not via other neuron types such as ChIs, as SP could modulate DA release when nAChR were blocked with DHβE (1 μM), and the modulatory effect of SP was unaffected by GABA and glutamate block in pilot studies. SP had the same percentage effect on the peak $[DA]_O$ for all stimulation paradigms (1p, 5p 5Hz, 20p 5Hz and 20p 20Hz), and the effect of SP during long train stimulations was consistent throughout the transient. SP does not change the frequency dependency of DA release, and the effect of SP remains constant throughout stimulation trains, suggesting that SP is not dynamically changing the release probability (P_R) of DA terminals depending on stimulation frequency. Changing the

DA content of vesicles may be a possible mechanism for increasing the amount of DA released across all frequencies, however I have found no examples in the literature of NK1 receptors altering vesicle content from any neuron type; alternatively it may be increasing the number of vesicle fusion events, which is the putative mechanism for how nitric oxide (NO) enhances transmitter (including DA) release in a frequency independent manner (Hartung et al., 2011).

When nAChR are active SP still has the same range of effects on the peak of 1p evoked $[DA]_O$. However, the effect of SP on the peak max of 1p evoked $[DA]_O$ is often less than on 20p 20Hz evoked $[DA]_O$. Additionally the effect of SP on long train stimulations is only seen for the peak of the transient and not during the plateau phase of the transients. This indicates that when nAChR are not blocked, the effect of SP on DA release is due a combined effect of SP acting on ChIs as well as on DA terminals, emphasising the importance of considering the confounding effects of the cholinergic system when investigating how DA release is modulated.

5.4.1 The variable effect of SP on DA release is dependent upon its striosomal-matrix location

In this chapter I have aimed to investigate if SP modulation of DA release varies along striosome-matrix axis of the striatum. In order to achieve this I marked my recording sites with yellow-green FluoSpheres, and processed the tissue for MOR immunoreactivity to allow the marked site to be classified by its striosome-matrix location. This technique is subject to certain limitations including: Possible inaccuracies in the marking of the recording site with the FluoSpheres. I.e. marked site may not be equivalent to recording site; the location of the marked site with respect to MOR staining was only examined in two-dimensions; and the area of tissue labelled by the FluoSpheres varies, and may not accurately reflect the volume of tissue from which DA release is being detected. I have tried to overcome these limitations during the analysis of the data by: Being blind to the effect of SP on DA release during the classification of recording sites; and although I could not find a way of measuring the accuracy of my site marking, it can be assumed that this error is the same for all data points, and therefore is incorporated in the general

experimental error. The boundaries of marked sites were determined two ways: Oval A (**Figure 5.2**) assumed that the more diffuse the FluoSpheres were spread, the less accurate the marking was, and therefore the area of the marked site needed to be larger. Whereas circle B assumed that the volume from which DA is recorded will be constant and therefore the area used to define the marked site should also. Circle B is 25 μm radius, as from modelling studies the time taken for DA transients to peak DA can diffuse between 10-20 μm, and the amount of DA diffusing more than 20 μm is negligible (<100 pM). However these assumptions may be introducing errors of their own: A site with a small area of beads may be due to too few beads being unloaded into the tissue therefore a small oval A is less likely to contain the true recording site. Oval A may be skewing sites to be classified as boundary sites because of marked sites having too large a boundary. However, none of the marked sites classifications changed between using oval A or circle B to define the marked site area. Striosomes are 3-dimentional irregular structures, therefore it would have been ideal to reconstruct the striosomes surrounding the marked sites in 3-dimentions. However I would not have been able to retain sufficient data throughout the experimental procedure, as even with 2-dimentional analysis of the post-hoc marked tissue, a significant proportion of the data was lost.

Using the technique described in the methods, and critiqued above, I found that the different effects of SP on DA release did correspond to their striosomal locations. When DA was recorded in the matrix, striosome or on a boundary, SP had no effect, type 2 effect and type 1 effect on DA release respectively. To determine if the differential effects were on a continuum or separate categories, the distances between the marked sites and the nearest striosome were measured. When the effect of SP on 1p $[DA]_O$ was plotted against the shortest distance from B* to S (b1) (**Figure 5.7a**) it showed the same trend as was seen with the ternary classification: Sites furthest outside the striosome are unresponsive to SP, as the sites approach the edge of the striosome SP reduces DA, then as sites move inside the striosome SP increases DA release. The effect of SP on DA release does appear to be on a continuum; however it does not seem to be

modelled by a simple equation. One drawback of plotting the effect of SP against b1 is that it is dependent on my subjective definition of a striosome boundary. Often the boundaries of striosomes are very clear, yet sometimes there is more of a gradual gradient from high MOR immunoreactivity in the centre of a striosome, which fades to low levels seen in the matrix. Therefore I also plotted the effect of SP against b2, which measures the distance between B* and S*(**Figure 5.7b**), which is a less subjective measure, and also is less affected by the size of the striosome. This plot showed the same trend as both the ternary classification and SP effect vs. b1. However instead of suggesting a single continuum, it appears to be a mixture of two functions, inverse to one another. If the relationship between effect of SP on DA release and the distance from the striosome centre is described by two separate curves, it may indicate that two separate mechanisms govern type 1 and type 2 effects. The lack of DA modulation seen in the matrix may be because type 1 and type2 effects cancel each other out, or because SP simply has no effect on DA modulation in this region.

If the hypothesis of SP having differential effects of DA release depending on striosomal location is correct, and striatal recording sites are randomly selected, the striosomal effects of SP on DA release (Type 2) should occur much less often than a lack of effect. This is indeed the case, where SP has no effect on DA release 10/22 times, has a type 1 effect 8/22 times and a type 2 effect 4/22 times. The approximate correlation between ratio of effects and ratio of volume of striosome and matrix territories supports our hypothesis

5.4.2 Possible mechanisms for the variable effects of SP on DA release

All of the effects of SP (increases and decreases) were found to be dependent on NK_1R, however it has yet to be determined if the modulatory effect of SP on DA release is exerted directly via the NK_1R. Because the effects of SP vary along the striosome-matrix axis, which is widely characterised by MOR expression it may be true that the modulation of DA release by SP occurs via the opioid system. There are several lines of evidence which would support further

investigation into this hypothesis: Firstly, absence of NK_1R prevents opioid addiction, which, is presumably a DA dependent process. Secondly, the NK_1R and MOR receptors are known to functionally associate and affect one another's rate of turnover (Pfeiffer et al., 2003; Yu et al., 2009). And thirdly the δ-opioid receptor (DOR) is also known to have high striosomal expression: DOR expression was found to overlap with MOR staining, but only occupying the centre of the MOR rich striosomes (Koizumi et al., 2013). DOR activation has previously been shown to increase DA release, whereas MOR activation either decreased or had no effect on DA release (Pentney and Gratton, 1991). It may be true that the range of effects of SP on DA release occur due to differential coupling of receptors e.g. MOR vs. DOR. This would mean that the facilitatory and inhibitory effects of SP on DA release are governed by separate pathways rather than the effects of SP being on a single continuum.

An alternate mechanism could be that NK_1R may be differentially coupled to downstream signalling cascades in different regions leading to variable effects on DA release. The NK_1R is predominantly G_q-coupled, which leads to the activation of phospholipase C (PLC) and production of inositol triphosphate (IP3). However by altering the lipid content of the plasma membrane NK_1R have been also shown to associate with $G_{\alpha s}$ (Monastyrskaya et al., 2005). This may tally with the observation that SP has a biphasic concentration profile, where low and high concentrations of SP (or analogues) can cause an increase or decrease in neurotransmission respectively (Kalivas and Miller, 1984; Reid et al., 1988).

5.4.3 Tools for further study

The striosome-matrix axis is not visible in rodent striatum without immunochemical labelling, therefore fully characterising the effects of SP on DA release is slightly problematic as high number of animals are required to generate sufficient data from all striatal territories, as the striosome core only represents ~13% of the striatum. Ideally, follow up experiments and further characterisation would occur in a mouse line that would allow live imaging of striosomes. A

genetic mouse line currently exists that uses eGFP fused to Nr4a1 gene, which results in striosomal expression of eGFP (Davis and Puhl, 2011). The eGFP expression correlates well with MOR and calretinin staining and is the inverse to calbindin staining. Unfortunately the mouse line is on a Swiss-webster background, which has been reported to differ greatly to other mice lines (including C57Bl6) (Sunstro¨m et al., 1987; Chan et al., 2012). The differences may well affect DA transmission, as one of the main differences between C57Bl6 and Swiss-webster mice is D_2R distribution, and sensitivity to PD inducing toxins (information from conversations with Dr Valjent and Dr Davis). Therefore it was decided to wait until the development of the eGFP-Nr4a1 C57Bl6 mice.

5.4.4 Physiological implications of differential modulation of DA release along the striosome-matrix axis

As both input and outputs of the striatum to some degree respect striosome-matrix boundaries, the ability of a neuromodulator to differentially modulate DA in the striosomes and matrisomes may allow input-output pathways to remain separate, and possibly amplify differences between striatal inputs.

The contrasting effects of SP on DA release: causing an increase, decrease or no effect depending upon its location is highly reminiscent of centre surround inhibition. Centre surround inhibition is most commonly associated with photoreceptors in the eye, where strongly stimulated cells inhibit the surrounding ,less strongly stimulated cells, resulting in a high-contrast image (Priebe and Ferster, 2008).

DA has different effects on its downstream neurons depending upon which DA receptors they express; D_1R are excitatory and D_2R are inhibitory. The pattern of D1 and D2 receptors expression varies between striosome and matrix, so if neuromodulators also alter the amount of DA released in these regions it may allow the contrast between outputs to be fine-tuned. There are many inputs to the striatum from numerous parts of the cortex. The striatum needs to be

able to integrate inputs whilst keeping unrelated outputs separated to allow the information flow to be preserved. The series of cortical loops may allow the integration of information from large areas of the cortex, so that excitatory signals of the desired movement are integrated with inhibitory signals of undesired movements by directing information from the striatum through either the "go" (direct) or "no-go" (indirect) pathways (Beck and Hallett, 2011) . This is an example of how centre-surround inhibition can occur at the network level as well as the inhibition of individual neighbouring neurons. Network wide inhibition in the basal ganglia may combine with the neuromodulator driven centre-surround inhibition to allow selected pathways to be enhanced and extraneous signals to be inhibited.

5.4.5 Implications for treatments of diseases

SP and NK_1R have been regarded as a targets for pharmaceutical intervention in a range of neurological disorders including anxiety and depression, neuropathic pain, ischemic damage, addiction and PD (DeVane, 2001; Griebel and Holsboer, 2012). Many of these disorders are associated with aberrant DA transmission, so it may be true that the therapeutic effects of SP for disorders such as PD and addiction may be achieved by modulating DA release. Fully understanding the complex modulatory action of SP on DA release will be important for both increasing the efficacy of SP for DA related disorders, and also limiting the side effects of SP application in non-DA associated disorders.

Despite there being much evidence that SP and NK_1R are involved in neurogenesis and neurodegeneration, there is conflicting evidence about if SP is neuroprotective or promotes cell death (Salthun-Lassalle et al., 2005; Wang and Angulo, 2011; Thornton and Vink, 2012). These conflicting data may relate to the data shown here, that the effect of SP on DA varies with striosome-matrix location. This highly variable effect of SP on DA release may affect its suitability as a pharmaceutical target, because the net effect may be unpredictable and inconsistent. However, understanding the mechanism by which NK_1R activation results in opposite effects on

DA release in neighbouring regions may allow drugs to be precisely targeted to specific pathways, allowing increased efficacy and limiting side-effects.

5.4.6 Summary

In summary, SP was found to be able to modulate DA release via NK1 receptors acting directly on DA terminals in a frequency independent manner. The effect of SP on DA release was dependent of striosome-matrix locations, where SP caused had no effect on DA release when recording in the matrix, but increased or decreased DA release when recording in a striosome or boundary region respectively. The finding that SP differentially modulates DA depending on striosome-matrix location illustrates a functional role of the striosome-matrix axis of the striatum.

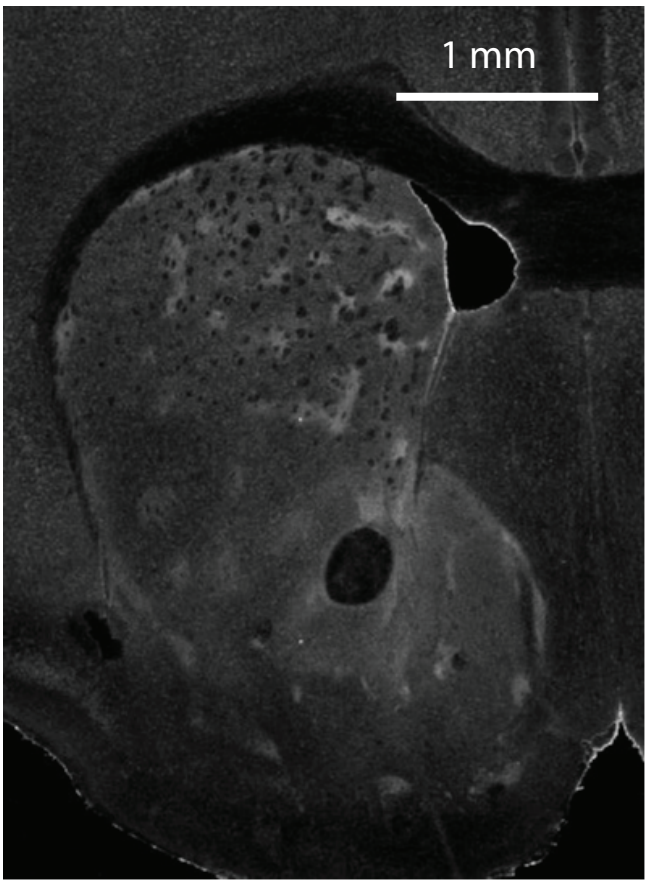

Figure 5.1. A striatal section showing variable μ-opioid receptor (MOR) expression

MOR are enriched in the striosomes throughout the striatum. Boundaries between striosomes and the surrounding matrix are more defined in CPu than NAc.

Scale bar is 1 mm.

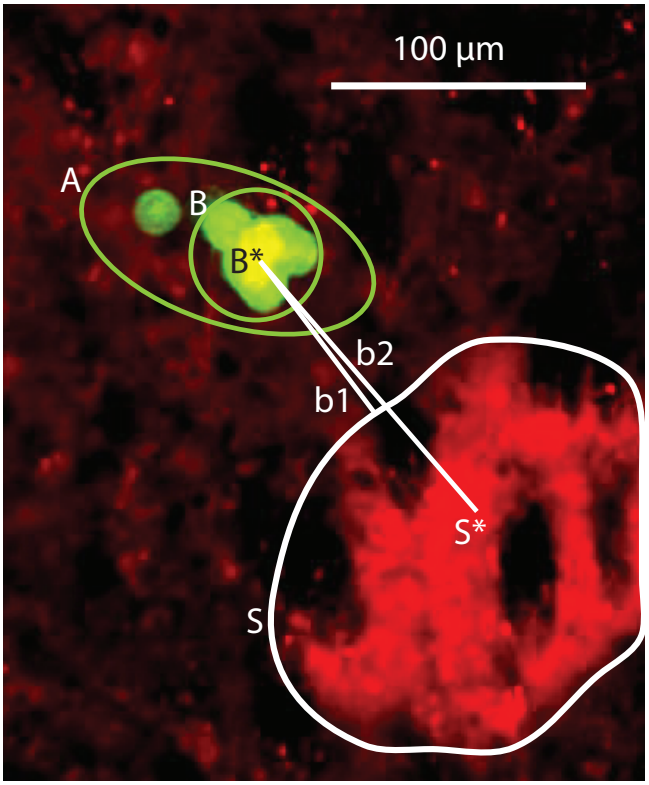

Figure 5.2. recording sites were marked with FluoSpheres, and tissue was processed for MOR immunoreactivity

MOR staining is enriched in striosomes (red; DyLight 594), boundaries are drawn by eye. Oval A is the oval twice the area required to incorporate all FluoSpheres. Circle B radius=25 μm, the centre (B*) is centred on the brightest point of the FluoSpheres. S is the outline of the nearest striosome, with S* being the brightest point in the middle of the striosome. b1 is the shortest distance from B* to S. b2 is the distance from B* to S*. Scale bar is 100 μm.

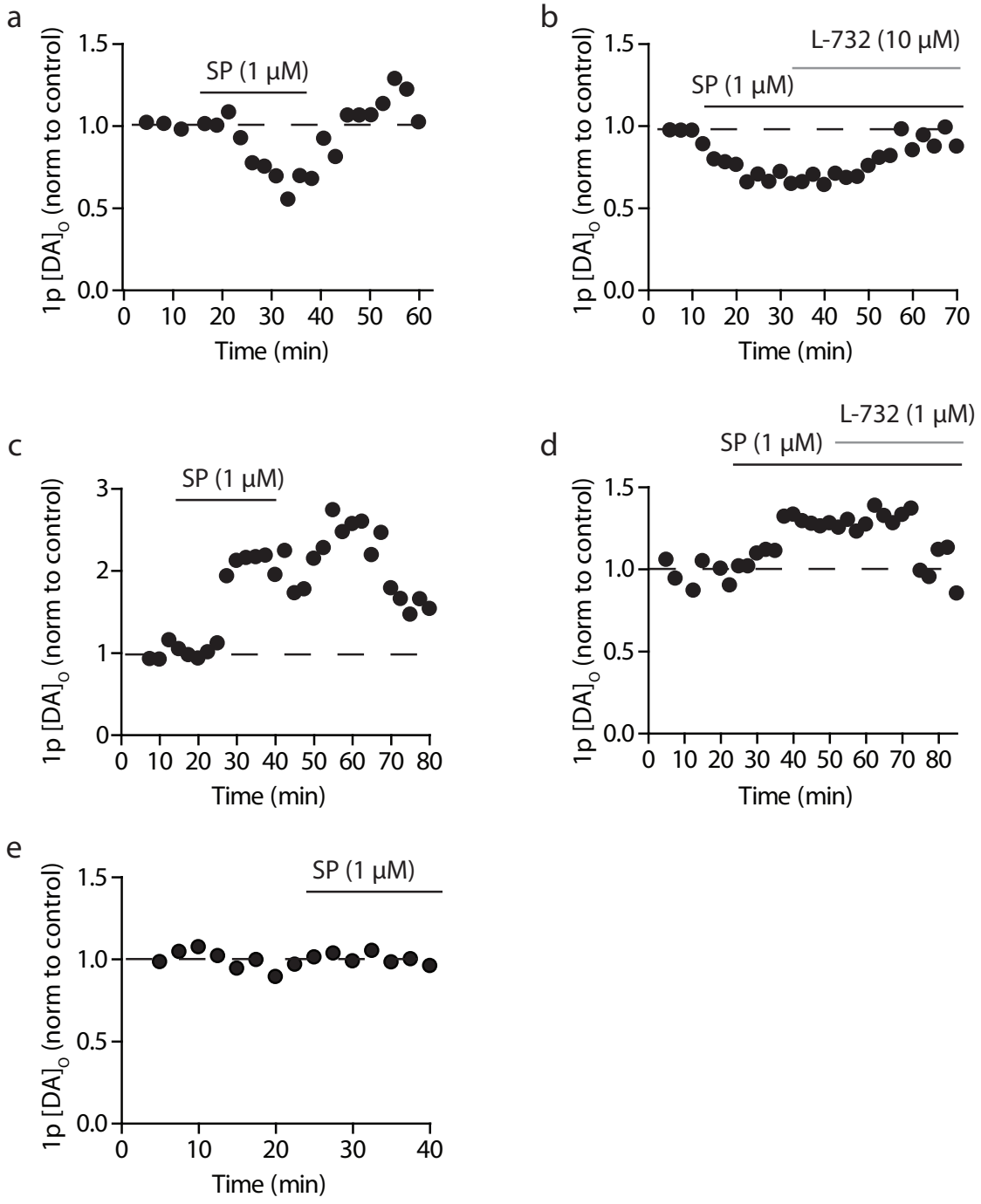

FIgure 5.3. The modulatory effect of SP on DA release is reversible and NK1R dependent. DHßE (1 µM) is present throughout. SP has a variable effect on DA release, representitive examples of the variable effects of SP on DA release are shown: It can decrease 1p $[DA]_O$ (Type 1 response) (a,b); increase 1p $[DA]_O$ (type 2 response) (c,d) or have no effect on 1p $[DA]_O$ (e). Data 1p evoked mean peak $[DA]_O$ normalised to mean peak 1p $[DA]_O$ in control conditions. The duration of SP application is shown by the black bar. In (b,d) the effect of SP on 1p $[DA]_O$ release is reversed by NK1R blockade with L-732,138 at 10 µM (b) or 1 µM (d), the duration of L-732,138 is shown by the grey bar. $[DA]_O$ was recorded every 2.5 minutes.

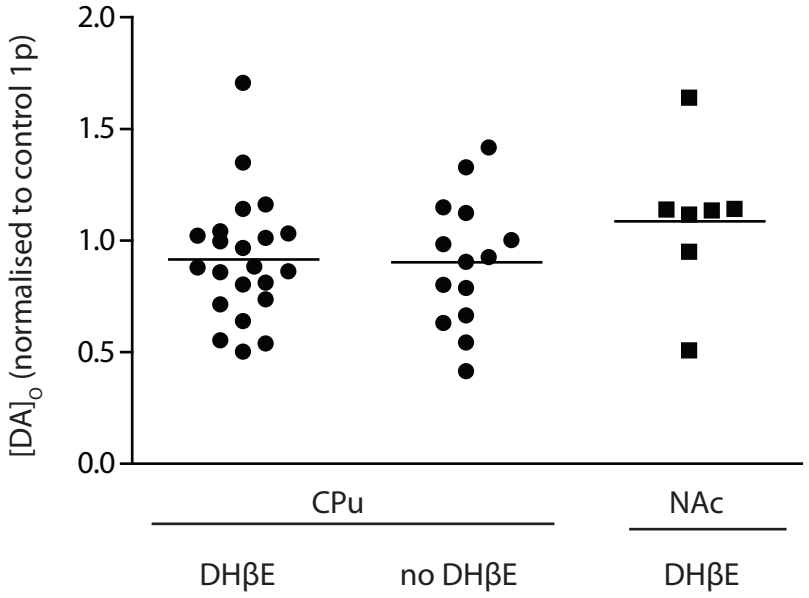

Figure 5.4. SP has a variable effect on DA release in CPu, NAc and CPu when nAChR are active (i.e. no DHβE)

The effect of SP on DA release was highly variable. Data are 1p evoked mean $[DA]_O$ in the presence of SP normalised to mean peak $[DA]_O$ in control conditions. Data are overlayed on a colour gradient, with the red background indicating an increase, green no effect and blue a decrease. Each data point shows the effect of SP (1 μM) in a single striatal slice

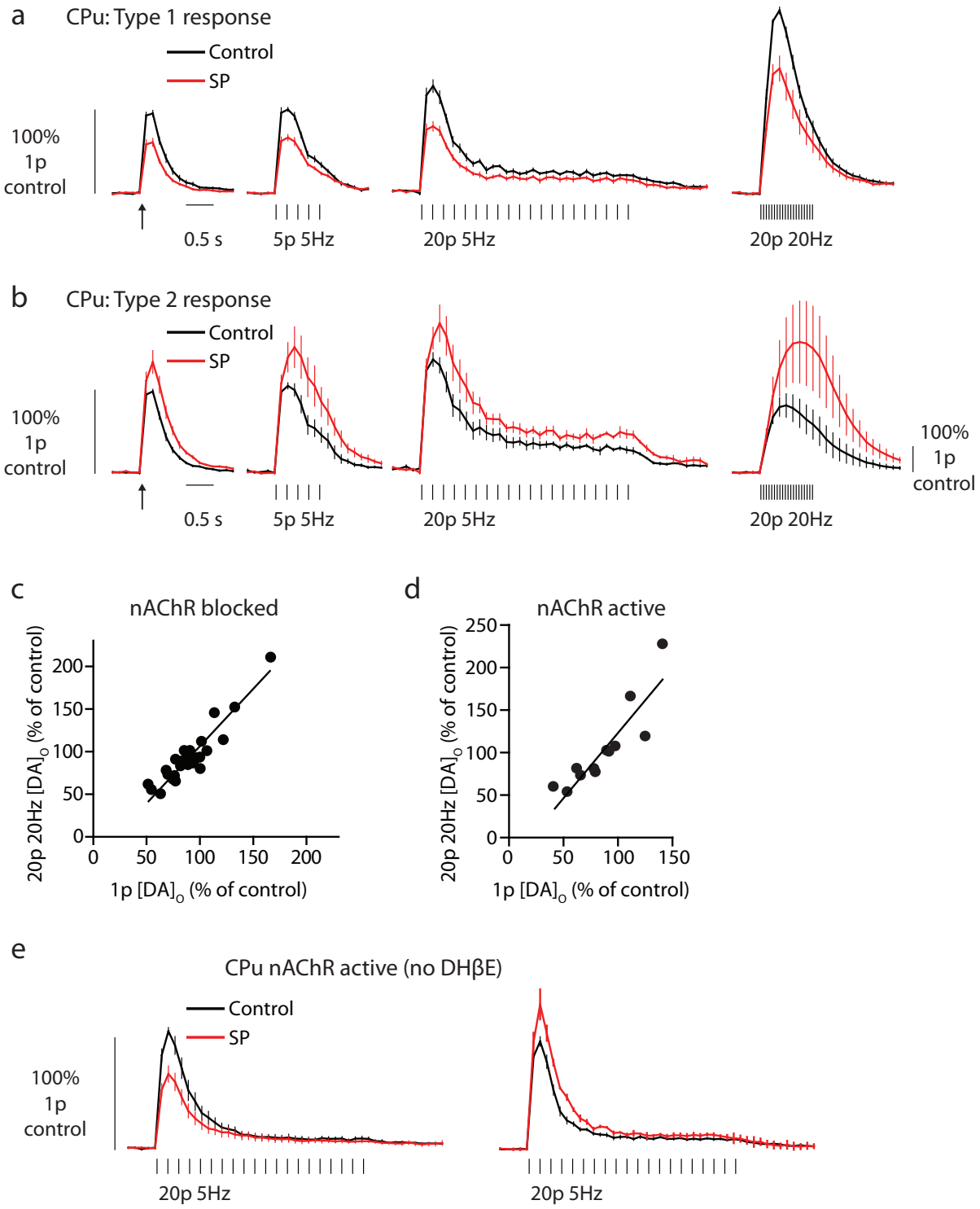

Figure 5.5. The modulation of DA release by SP is consistent across stimulation protocols when nAChRs are blocked with DHßE (1 µM).

During nAChR blockade: (a,b) Mean $[DA]_o$ ± SEM vs time post stimulation, data are normalised to peak 1p-evoked $[DA]_o$ in control conditions, for type 1 response (a) and type 2 response (b). n=4 for type 1 and n=5 for type 2. (c) % change in 20p 20Hz evoked $[DA]_o$ vs %change in 1p evoked $[DA]_o$, each data point is from a recording site. The linear regression line for the data is also shown. When nAChR are active: (d) % change in 20p 20Hz evoked $[DA\}_o$ vs %change in 1p evoked $[DA]_o$, each data point is from a single animal. The linear regression line for the data is also shown. (e) Mean $[DA]_o$ ± SEM vs time post stimulation, data are normalised to peak 1p-evoked $[DA]_o$ in control conditions, for type 1 response (left panel) and type 2 response (right panel). n=3 for type 1 and n=5 for type 2

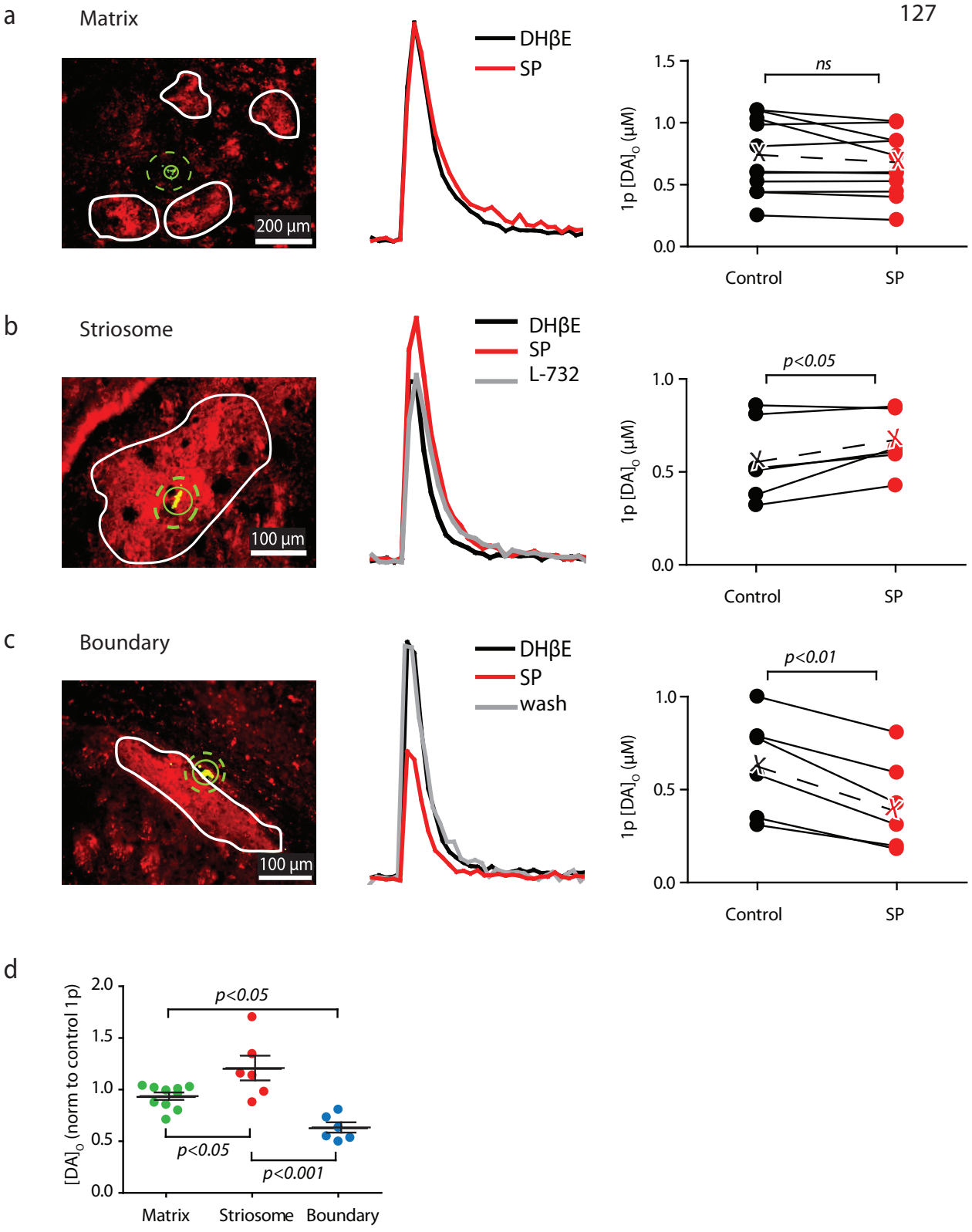

Figure 5.6. SP differentially modulates DA release depending upon striosome-matrix location
(a,b,c) Left panel: Example recording site of a matrix (a), striosome (b) and boundary (c) site. Recording sites are marked with green FluoSpheres. Green dashed lines shows oval A. Solid green line shows circle B. MOR staining is enriched in striosomes (red; DyLight 594), S are freedrawn and shown by white lines. Scale bar is 200 µm (a) and 100 µM (b,c). Middle panel: Transients of 1p evoked [DA]o vs time post stimulation for the recording site shown in left panel. Data are normalised to peak 1p evoked $[DA]_o$ in control conditions, control condtions (presence of DHβE) (black line), SP (red line), wash off or NK1R antagonist (grey line). Right panel: peak max of 1p evoked $[DA]_o$ (1 µM) in control and SP conditions for each of the recording sites defined as being in matrix (a), striosome (b) and boundary (c). (d) The effect of SP separated by region. Data are normalised to mean peak 1p evoked $[DA]_o$ in control conditions.

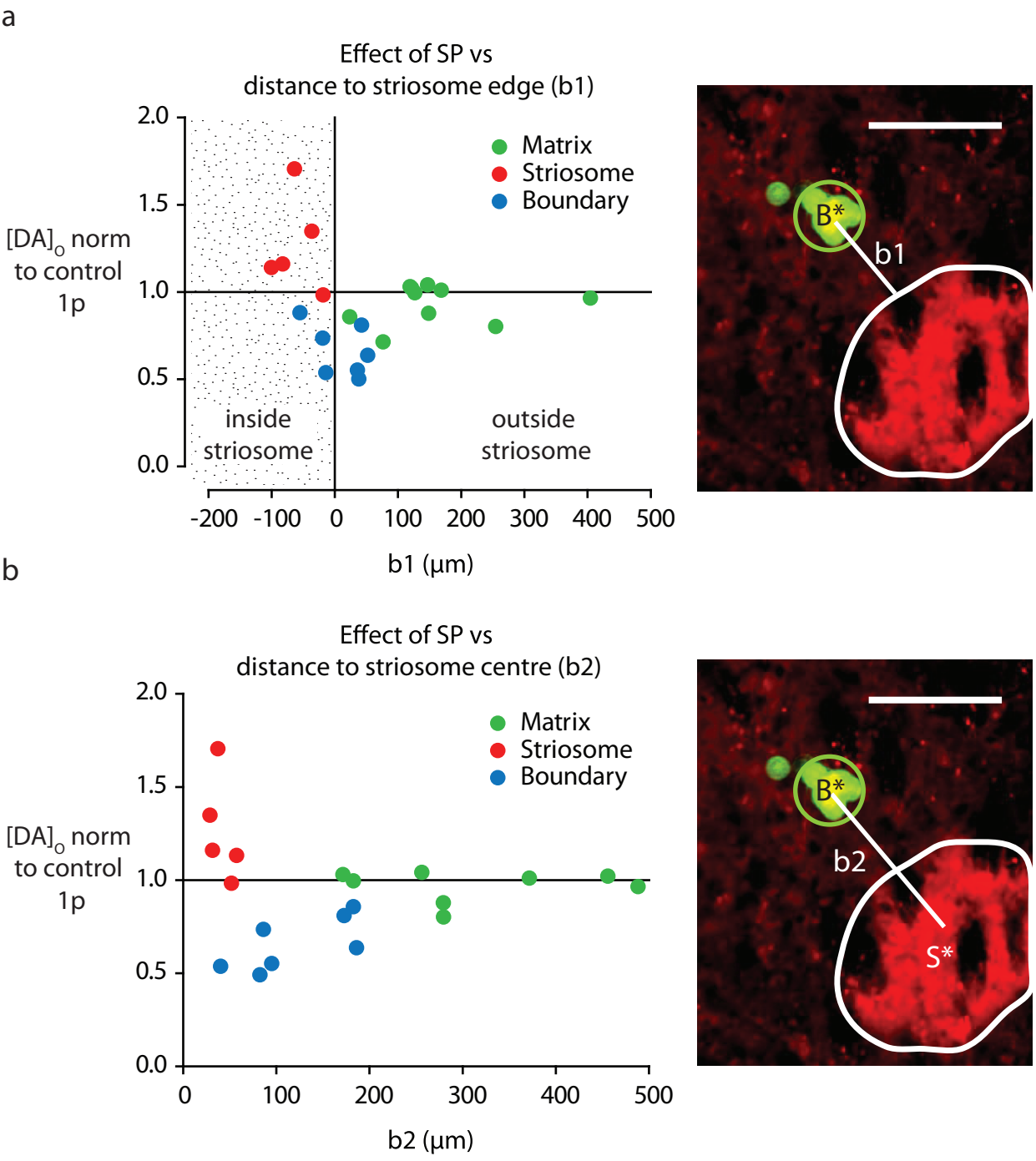

Figure 5.7 Effect of SP varies with distance from nearest striosome
(a,b) Left panel: effect of SP vs b1 (a) and b2 (b) (µm). Data are normalised to mean peak [DA]O in control conditions. Matrix sites defined by the ternary classification are green, striosome sites are red and boundary sites are blue. Right panel: an example recording site showing how the distance is determined. Recording sites are marked with green FluoSpheres.. Solid green line shows circle B. b1 and b2 are shown by labelled white straight lines. S shown by labelled free drawn line. MOR staining is enriched in striosomes (red; DyLight 594), Scale bar is 100 µm

6. Discussion

6.1 VDCC role in controlling DA release

6.1.1 ACh has confounded our understanding of which VDCC control DA release

In chapter 3 I investigated which VDCC types modulated the release of DA in the presence of nAChR blockade. The ability of VDCCs to control striatal DA release was determined by measuring the effect of specific pharmacological blockers of VDCCs on electrically and light evoked DA release, measured using FCV. Previous studies have investigated which VDCC control DA release in CPu (Phillips and Stamford, 2000b; Chen et al., 2006), however in light of recent findings that ACh can bind to nAChR on DA terminals and drive DA release independently from activity in DA neurons, it was deemed necessary to re-address this question in the absence of the potentially confounding effects of ACh. Therefore in this thesis I determined which VDCCs could modulate DA release without the influence of nAChR by pharmacological blockade of nAChR, or when DA terminals are exclusively activated using optogenetic technologies coupled to FCV.

In agreement with Phillips et al (2000) and Chen et al (2006), I found a dominant role for N and P/Q type channels in the control of DA release, where in CPu N- and P/Q-type inhibition decreased 1p DA release by ~85 and 70% respectively; and in NAc N- and P/Q-type inhibition decreased 1p DA release by ~75 and 35% respectively. However in contrast to these two studies I also identified roles for T- and L-type channels in the control of DA release in CPu: When T- and L-type channels were blocked, DA release at all frequencies in CPu was reduced by ~30% and 25% respectively. The role of T- and L-type channels in the control of DA release was regionally specific, because in NAc neither T- or L-type channels appeared to control DA release at any frequency.

T and L-type channels are not classically thought of as routes of Ca^{2+} entry to trigger synaptic vesicle release because of their physiological characteristics: T-type channels have been characterised as having low single channel conductance, and are only transiently active, making them suited to establishing Ca^{2+} oscillations and shaping action potentials at the axon initiation

segment, they are also activated at low membrane potentials (Chevalier et al., 2006; Bender et al., 2012). L-type channels are characterised as requiring strong membrane depolarisations; showing calcium-induced inhibition and no voltage-induced inhibition; and predominant post-synaptic location, they are generally thought of as controlling somatodendritic calcium oscillations, modulating transcription and controlling developmental processes such as axon guidance (Brandt et al., 2003; Catterall et al., 2005; Chan et al., 2007; Vacher et al., 2008). However, there is also mounting evidence for presynaptic roles for both T- and L-type calcium channels, where they have been shown to control exocytotic events (Bergquist et al., 1998; Bonci et al., 1998; Carbone et al., 2006; Fourcaudot et al., 2009), and despite their lack of synprint, they have also been shown to be presynaptically located and associate with exocytotic machinery (Wiser et al., 1999; Tippens et al., 2008; Weiss et al., 2012).

There is a significant body of literature that shows L-type channels have presynaptic roles, which supports the finding reported here that L-type channels control of DA release. However we deemed it necessary to confirm the reduction in DA release following L-type channel blockade was due to the inhibition of L-type channels on DA terminals and not via a neuromodulator. Striatal DA terminals of ChR2-injected DAT-cre mice, were exclusively activated using 1 or 5p (5, 25 Hz) of blue light. Light-evoked DA release is Ca^{2+}- is action potential-dependent, and DA transients are equivalent to electrically evoked transients with respect to magnitude and time course to that of electrically evoke DA in the presence of nAChR blockade (Threlfell et al., 2012). Under these conditions, 1p DA release is reversibly reduced by ~25% by isradipine (L-type channel antagonist, 5 µM), which is equivalent to the effect of isradipine seen when DA is electrically evoked, in the presence of nAChR blockade. I chose to use light evoked DA release only to corroborate the findings seen in electrically evoked DA release in the presence of nAChR blockade because ChR2 is a non-specific cation channel, and is highly permeable to Ca^{2+} (Nagel et al., 2003). A large Ca^{2+} conductance by ChR2 has been demonstrated at 80 mM extracellular Ca^{2+}, but is lower when extracellular Ca^{2+} is reduced to more physiological levels of 2 mM (Lin et al., 2009).

New light-activated channels are being developed, with the aim that they may be engineered to be selective for specific ions, allowing cells to be depolarised or hyperpolarised, and to allow channels to be either highly permeable or impermeable to Ca^{2+}, which would avoid the potentially confounding effects of non-physiological routes of Ca^{2+} entry occurring following activation (Kleinlogel et al., 2011; Lin, 2011).

As it is possible that isradipine might be having off-target effects, and for example, antagonising non-L-type channels, I repeated the experiment with an alternative L-type channel blocker nifedipine (10 μM). When DA was light-evoked, nifedipine was found to be photoreactive, generating an electroactive product, which interacted with the CFM, therefore nifedipine is not suitable for use in this experimental set up. The potential for a drug to be photoactive illustrates an important point with the advent of optogenetic technologies. Some drugs are large reactive molecules, which may be photoactive, and it is possible for the products to have off-target effects, FCV fortunately flagged up this issue, but many other techniques would not, therefore it may be wise to avoid photoactive drugs, and companies manufacturing the drugs could aid this by reporting if a drug is photoactive, and potential targets of the products. Although the ability to selectively activate a population of cells is clearly highly informative, it should not be viewed as infallible, as there is potential for the introduction of foreign channels to affect the normal physiology of the cells, which should be borne in mind if this is the aspect of interest and findings should be compared to wild-type tissue. Despite nifedipine not being appropriate for use with light-activated DA release, when DA was electrically evoked, nifedipine had analogous effects on 1p DA release as isradipine, further supporting the finding that DA release is controlled by L-type channels acting on DA terminals.

An additional difference between Chen et al (2006)and the data presented here is the paradoxical increase in DA release reported here following R-type channel blockade with SNX-482: In both regions in the presence of nAChR blockade, DA release increased following R-type

channel blockade. When nAChRs were not blocked, SNX 482 no longer increased DA release in CPu, and the increase seen in NAc was much reduced. Chen et al (2006) found that SNX-482 reduced striatal DA by ~30%. The conflict between these data could be due to a number of reasons, which are discussed in full below. The increase in DA release caused by SNX-482 was not due to disinhibition via GABA or glutamate receptors. A working hypothesis for the increase in DA release following R-type blockade is that R-type channels are coupling to small conductance Ca^{2+} activated potassium (SK) channels, so that a reduction in Ca^{2+} entry through R-type channels reduces the efflux of K^{+} through SK channels, which has the net result of broadening the action potential and increasing DA release. To investigate this possible mechanism, future experiments could attempt to reproduce the increase in DA release by broadening the width of the electrically delivered stimulation pulse, or block SK channels with apamin (Cui et al., 2004; Zampini et al., 2010). This hypothesis is supported by the finding that in C*av2.3* (R-type channel) null mice, hippocampal neurons have broader action potentials and increased glutamate release (Giessel and Sabatini, 2011). Complexities which may surround experiments probing the roles of R-type channel in the control of DA release, are that SK channels have been shown to couple to N, P/Q, T and L-type channels, and it has been shown that inhibiting SK channels alters Ca^{2+} conductance (Wikström and El Manira, 1998; Shepard and Stump, 1999; Wolfart and Roeper, 2002; Malinina et al., 2010; Nanou et al., 2013). Large conductance Ca^{2+}-activated potassium (BK) channels have not been found to control DA release (Martire et al., 2010), however they are known to couple to VDCCs (N- and L-types), so it may be necessary to block both SK and BK channels to cause an increase in DA release (Lee and Cui, 2010). Blocking SK or BK channels has not been found to affect DA release (unpublished observations), but this was in the presence of ACh, which may drive DA release in such a way that is unaffected by SK- and BK-channel activity. Additionally it may be true that due to the interactive nature between SK-channels and VDCC, the roles of SK-channels are only apparent if Ca^{2+} entry is changed. In contrast to data shown here, Chen et al (2006) found that R-type blockade inhibited striatal DA release, our differing findings may be

explained by a number of differences between our experimental paradigms: The nAChR were active in Chen et al(2006) study, and it is currently unknown if ACh depolarises DA terminal membrane, mirroring action potential-dependent release, or if it directly triggers release without depolarising the whole membrane. If it is the latter mechanism, ACh driven DA release may be unaffected by SK or BK channels. Secondly, Chen et al (2006) used a stimulation pulse of 1 ms duration, in comparison to 200 μs used in this thesis, this longer stimulation duration may be insensitive to broadening of action potentials by inhibition of Ca^{2+} activated K^{+} channels, revealing an inhibitory effect of R-type blockade on DA release. Moreover, Chen et al used GBR-12909 to block DAT to amplify DA signals, however the DAT is now known to modulate DA release probability and synaptic plasticity (Platt unpublished data), which may affect how VDCC control DA release. Chen et al used guinea pig striatum, as opposed to mouse striatum used here, it is possible that putative R-type coupling to SK channels in DA terminals may be species-specific.

The inability to verify the effect of SNX 482 as R-type specific has impeded our investigation into the mechanism by which R-type blockade increases DA release, as there are no alternative R-type specific blockers, and SNX 482 does not completely block R-type channels. Many studies have used Ni^{2+} to block both T- and R-type channels, but in this thesis work I showed that Ni^{2+} is an unsuitable VDCC blocker due to putative interactions with the DAT.

6.1.2CPu and NAc have differing dependencies on VDCC for controlling DA release

In Chapter 3 I compared the effect of blocking VDCC on DA release in CPu and NAc regions of the striatum, allowing their relative contributions to controlling DA release to be inferred. DA release was consistently less inhibited by blockade of VDCCs in NAc than in CPu: In CPu, N-, P/Q-, L- and T-type channels control DA release whereas in NAc only N- and P/Q-types had roles. In addition to L- and T-type channels having minor roles in controlling DA release in CPu but not NAc, the percentage effects of N- and P/Q-type blockade was greater in CPu than NAc. In both regions N- and P/Q-type channels are the dominant channels in controlling DA release. In CPu N-

and P/Q-type channels have roughly equivalent roles, especially at higher frequencies, whereas in NAc N-type channels control DA release to a greater extent than P/Q-type channels.

For 1p DA release, the total percentage effect of VDCC block obtained by summing the effects of each individual VDCC is ~100% in NAc, but exceeds 100% in CPu. The difference in summated effects of VDCCs in CPu and NAc, may indicate that the coupling of Ca^{2+} entry and DA release is fundamentally different between the two regions. One possible explanation for the difference in the summated effects of VDCCs, could be that in NAc there are two separate "pools" of DA, one that is triggered by Ca^{2+} entry either through N-type channels, and another that is triggered by entry through P/Q-type channels, which is why summated percentage effect of P/Q-type and N-type blockade on DA release equals ~100%. In contrast, In CPu, the percentage reduction for 1p evoked DA release by each of the VDCC blockers exceeds 100%, which may indicate that cooperativity between the VDCC subtypes is necessary to reach a threshold level of Ca^{2+} required to trigger DA release. However, it seems probable that the effect of VDCC-blockade on DA release, will be a function of how much VDCC blockade reduces Ca^{2+} level below threshold, rather than a reflection of the size of DA pool controlled by a particular channel type. Therefore, depending on how much blockade of a certain VDCC reduces Ca^{2+} available to trigger exocytosis below a threshold, will determine the degree to which DA release is decreased. If the amount each channel contributes to reaching this threshold is independent of one another, there is no reason why this should equal 100%. Furthermore, the fact that in NAc the percentage reduction in 1p evoked DA by N- and P/Q-type block equals ~100% may be a coincidence, and liable to change depending on conditions such as extracellular Ca^{2+} concentration (**Figure 6.1**). It is improbable that the relationship between 1p $[DA]_O$ and $[Ca^{2+}]_O$ is linear, as there will be a minimal concentration of extracellular Ca^{2+} required to evoke measurable amounts of DA, and there will be a point where extracellular Ca^{2+} concentration is no longer a limiting factor for DA release, so increasing extracellular Ca^{2+} will not lead to an increase in evoked DA, meaning the relationship is more likely to be sigmoidal. Therefore the perceived contribution of certain VDCC subtypes may

change with extracellular Ca^{2+} concentration. This is supported by the finding, briefly described in Chapter 3 (Section 3.4.2), that L- and T-type VDCC blockade reduces DA release in NAc when extracellular calcium concentration is 3.6 mM (opposed to 2.4 mM used in this thesis).

In order to test this hypothesis in future experiments, it will be investigated if the percentage effect of each VDCC blocker changes when extracellular calcium is either increased or decreased. Presently, it seems that the Ca^{2+} threshold for maximum 1p DA release is relatively lower at 3.6 mM than 2.4 mM Ca^{2+}, allowing more VDCC subtypes to contribute to surpassing it in NAc. In NAc, increasing extracellular calcium to 3.6 mM may place DA release into the linear section of the calcium response curve of DA release, which may not be true in CPu. If the calcium response curve of DA release for CPu is more leftward shifted then raising extracellular calcium to 3.6 mM may place DA release towards the plateau phase of the curve, so that fewer VDCC subtype contribute to surpassing a calcium threshold necessary to trigger exocytosis. In this thesis I investigated the effect of increasing $[Ca^{2+}]_O$ to 3.6 mM, which was not sufficient to show the upper plateau of the Ca^{2+} response curve for either CPu or NAc, but the curve did show that increasing $[Ca^{2+}]_O$ from 2.4 to 3.6 mM resulted in a larger increase in 1p $[DA]_O$ in NAc than CPu, which would support the calcium response curve of DA release in CPu being leftward shifted to that of NAc. Because 2.4 mM $[Ca^{2+}]_O$ is already a supraphysiological concentration, it may be considered unnecessary to investigate the control of DA release at higher concentrations, however it might produce interesting mechanistic insights for differences in the control of DA release between CPu and NAc, that could inform our understanding of how DA release is controlled in both healthy and disease states of the brain.

6.1.3 There is a dynamic relationship between DA initial and re-release, which can be modulated by Ca^{2+} availability

Phillips and Stamford (2000) showed that N-type channel blockade reduced DA release for low frequency stimulations more than high frequency stimulation when nAChR were active, and inferred that N-type channels controlled low frequency DA release and that other, including

unidentified VDCCs, were responsible for controlling high frequency DA release. When the nAChR were blocked, I also found that N-type channel blockade reduced DA release to low frequency stimulation more than to high frequency stimulations, resulting in an increase in the ratio between 5p 100Hz:1p $[DA]_O$ (burst ratio). However, the activity-dependent effects of N-type block could also be a function of the extent of loss of Ca^{2+} entry, i.e. N-type block causes a large enough decrease in Ca^{2+} entry to reveal a dynamic relationship between initial release and re-release. To test this, I attempted to increase the burst ratio by reducing extracellular calcium levels to 0.8 mM, which results in 1p $[DA]_O$ equivalent to levels of 1p $[DA]_O$ in the presence of N-type blockade. Under these conditions, high frequency DA release is also equivalent to levels seen in N-type channel blockade, meaning that 5p:1p DA release ratio was increased both when N-type channels were blocked and when extracellular calcium was sufficiently reduced. To further investigate this relationship 5p:1p ratio of DA release was plotted against 1p $[DA]_O$, which showed that there was a dynamic relationship between the burst ratio and initial DA release, so that when initial release (1p $[DA]_O$) was low burst ratio (5p:1p) was high. L-type channel blockade only increases burst ratio when N-type channels are also blocked, which illustrates that the burst ratio is dependent on initial release and not a specific property of a channel.

The dependency of the relationship between burst ratio and initial release on Ca^{2+} is consistent with our understanding of classical synapses, which has not been previously shown for DA release. It is noteworthy that the curves that describe the relationships between burst release and initial release for both CPu and NAc are relatively flat until initial DA release becomes sufficiently low, and then the relationship between 5p:1p and 1p $[DA]_O$ becomes very steep (**Figure 3.9e**). This may indicate a mechanism by which differences in DA release between tonic and phasic patterns of activity can be accentuated, as Ca^{2+} concentrations could conceivably be dynamically controlled by calcium buffering proteins; modifying VDCC conductance by association with either accessory subunits or interactions with modulatory proteins, for example Gβγ; or by

controlling calcium release from intracellular stores (Catterall, 2000; Colecraft et al., 2001; Verkhratsky, 2005; Dolphin, 2006; Matveev et al., 2011).

6.1.4 Alpha synuclein

In chapter 4 I explored how the control of striatal DA release by VDCC is affected by expression levels of α-synuclein. Mice overexpressing human α-synuclein (OVX) were compared with α-synuclein null (*Snca* -/-) littermate controls. The OVX line is generated using BAC transgenic technology, allowing the whole human *SNCA* gene locus to be expressed in mice with a physiological pattern of expression at levels thought to be analogous to *SNCA* duplication in humans, which is known to cause Parkinson's disease (PD) (Janezic et al; Chartier-Harlin et al., 2004). Previous studies have shown that in α-, β- and γ-synuclein null mice (TKO) DA release is increased while content is decreased, which is complimented by the finding that in OVX mice, DA release is decreased while content is increased (Anwar et al., 2011; Janezic et al).

The multiple hit hypothesis of PD posits that a number of factors including α-synuclein, Ca^{2+} load, dopamine and aging all contribute to SNc DA neuron specific cell death in PD (Mosharov et al., 2009; Dryanovski et al., 2013; Surmeier and Sulzer, 2013). Much of the emphasis on Ca^{2+} contribution to SNc DA neuron cell death is from the finding that L-type calcium channels, specifically Cav1.3, support the pacemaker firing of SNc but not VTA DA neurons, which are established instead by Na^{+} channels (Chan et al., 2007; Guzman et al., 2009). Cav1.3 activity in SNc neurons has been shown to generate oxidative stress in the neurons, which is greater in distal dendrites than proximal dendrites and the soma (Guzman et al., 2010; Dryanovski et al., 2013), however the role of VDCC in the enormous axonal arbors has been largely overlooked. α-synuclein has been shown to modulate the Ca^{2+} conductance of VDCCs including Cav1.3 (Adamczyk and Strosznajder, 2006; Hettiarachchi et al., 2009), therefore in the work described in Chapter 4, I aimed to build on the initial characterisation of the VDCCs that control DA release in CPu (in the work described in Chapter 3), to explore how the control of DA release by L-type

VDCCs changes in the presence and absence of α-synuclein. The work described in Chapter 4 therefore tested the hypothesis an interaction between Ca^{2+} entry through L-type channels and α-synuclein could affect striatal DA transmission, which could lead to conditions that are toxic for the neurons and may contribute to the selective cell death of SNc DA neurons in PD.

As has already been discussed, ACh has powerful modulatory effects on DA release, therefore all data discussed here is obtained in the presence of nAChR blockade (DHβE 1 μM). Experiments in chapter 4 were all performed in dorsolateral CPu, since previous studies of the synuclein-dependence of DA release indicated DA was only regulated by synucleins in dorsal striatum (Anwar et al., 2011; Janezic et al). Additionally dorsolateral CPu is innervated by ventral tier SNc DA neurons, which are most vulnerable in PD. In agreement with a study from our laboratory now in press (Janezic et al *in press*), I found that in dorsolateral CPu, 1p DA release in α-synuclein-overexpressing (SNCA-OVX) mice is reduced by approximately one third to that of *Snca*-/- mice. The effect of N-type blockade on DA release was no different in OVX and *Snca* -/- mice, and was consistent with the effect in wild type mice shown in chapter 3. However blockade of L-type channels with isradipine (5 μM) differed between genotypes, where DA release in OVX mice was reduced by isradipine by ~25% but DA release in *Snca* -/- was unaffected. The ~ 25% reduction in DA release by L-type channel blockade seen in OVX mice is equivalent to the reduction seen in wild type mice (chapter 3). From these data it seems that the control of DA release by L-type channels is dependent on α-synuclein expression, however it is currently unclear why this is the case. α-synuclein may regulate the expression of L-type channels, however this seems unlikely due to α-synuclein being predominantly presynaptically located (Clayton and George, 1998; Kahle et al., 2000), but there have been reports of α-synuclein having a nuclear location and some reports of α-synuclein regulating transcription (Baptista et al., 2003; Goers et al., 2003; Yu et al., 2007). Even if α-synuclein does not increase transcription levels of L-type channels, it may facilitate L-type channels being functionally inserted into the membrane of DA terminals; α-synuclein binds to membranes and may be associated with vesicle trafficking

(Goedert, 2001; Marques and Outeiro, 2012). A-synuclein has been shown to increase L-type calcium channels conductance (Hettiarachchi et al., 2009), so it may be that without α-synuclein L-type channels do not contribute sufficiently during DA release events for L-type blockade to affect the amount of DA released. Another possible explanation is that α-synuclein affects the relationship between Ca^{2+} and DA vesicle release generally and not in an L-type specific manner, as α-synuclein has been found to inhibit late endosomes and associate with synaptic vesicles, which may increase Ca^{2+} levels required to trigger exocytosis; however as I found that the roles of other VDCC types in the control of DA release appear to be unaffected by α-synuclein levels, this seems unlikely. Further experiments are required to investigate if α-synuclein affects the presence of L-type channels in DA terminals, which will require dual gold electron microscopy to visualise L-type channels on tyrosine hydroxylase (TH) positive terminals. A simpler approach, may be to see if a role of L-type calcium channels in DA release can be found in *Snca* -/- by increasing extracellular Ca^{2+} concentration, which as discussed earlier (and in chapter 3 discussion) occurs for L-type channels in NAc.

6.1.5 Summary and implications

Calcium is a ubiquitous signalling ion, which is central to neuronal physiology in both health and disease states of the brain, where it is necessary for controlling exocytosis, activation of enzymes and modulating conductivity of ion channels in addition to many other signalling functions. In this thesis work I have explored the role of VDCC in the control of striatal DA release, in the absence of the potentially confounding effects of ACh (chapter 3). I have excluded these potentially confounding effects by blocking nAChRs with DHβE, which revealed roles for L- and T-type channels in the control of DA release. The finding that L- and T-type channels control DA release in the CPu but not NAc illustrates heterogeneity in how DA release is controlled between striatal regions, which are known to have differing susceptibility to PD. Activity of L-type calcium channels in the cell bodies of SNc DA neurons has already been proposed as a reason for these neurons having heightened sensitivity in PD, and now I have shown that there is also differential

VDCC recruitment in the vast axonal arbours of DA neurons in addition to in the cell bodies. It has been shown that the mitochondrial oxidative stress caused by calcium entry via L-type channels is greater in distal dendrites than proximal dendrites and cell bodies (Dryanovski et al., 2013); therefore it is possible that the oxidative stress caused by axonal calcium entry through L-type channels is even greater than in somatodendritic regions by virtue of their great distance from the cell bodies. Therefore even though the reduction of DA release by L-type channel blockade is modest, it may have a significant impact on the oxidative stress of axonal regions and therefore the cell as a whole. The modest contribution of L-type channel activity in DA release may also be highly cumulative over a life time and therefore have implications for the aetiology and progression of PD, especially if DA cell death in PD occurs in a "dying back" mechanism opposed to classic apoptotic mechanisms (Hornykiewicz, 1998; Cheng et al., 2010). Blockade of L-type channels with isradipine, which is currently approved for the treatment of hypertension, has been proposed as a treatment for PD. The therapeutic effects of isradipine, may be due to its action at the terminals of DA neurons, in addition to their original targets of somatodendric L-type channels (Simuni et al., 2010). However because L-type channels control striatal DA release, there is potential for isradipine to reduce striatal DA release in the already compromised dorsal striatum of PD patients, which may limit use of isradipine to patients in the early stages of the disease or high risk non-symptomatic individuals to avoid exacerbation of PD symptoms by further reducing DA release in people whose DA release is already highly compromised. In support of the potential for L-type channel activity to be a contributing factor in PD, I have also shown that the control of DA release by L-type channels requires α-synuclein, which is known to be both a causal and risk factor in inherited and idiopathic forms of PD respectively (Singleton et al., 2003; Simón-Sánchez et al., 2009). The finding that L-type channel control of DA release is dependent on α-synuclein may provide insights into the normal functional role of α-synuclein, which is at present still uncharacterised; further investigation into the mechanism of how α-synuclein "recruits" L-type channels during DA release may elucidate the normal function of α-

synuclein. It would be of great interest to investigate if the selective role of L-type channel in the somatodendritic region of SNc DA neurons is also dependent on α-synuclein.

Previous studies investigating the role of VDCCs in DA release have indicated that different VDCC subtypes are functional depending on if the DA neuron is firing at high or low frequencies (Phillips and Stamford, 2000a). However data shown here illustrates that there is a dynamic relationship between initial release and re-release, where low levels of initial release results in increased re-release, and therefore the ability of a channel subtype to control high frequency release will be a function of how it affects initial release. This inverse relationship between initial release and burst release has been characterised in synapses (Katz and Miledi, 1968; Sakaba and Neher, 2001; Wang et al., 2009), but has not been fully explored for DA release, which also signals extrasynaptically by volume transmission. Illustrating the relationship between initial and re-release of DA, and how it can be affected by Ca^{2+} availability is non-trivial as despite the relationship between residual calcium and paired-pulse facilitation being conserved between vertebrate and mammalian central synapses (Katz and Miledi, 1968; Wu and Saggau, 1994), the relationship between calcium influx and release is known to vary: Invertebrate synapses require fewer Ca^{2+} channels to be activated by an action potential to facilitate release than vertebrate central synapses and in invertebrate synapses broadening of action potentials leads to increased activation of VDCCs, whereas in vertebrate central synapses broadening of action potentials has complex effects on VDCC activation including modulation of their gating properties (Wang et al., 2009).

6.2 The effect of Substance P (SP) on DA release

6.2.1 SP can modulate DA release directly on DA terminals

There have been conflicting reports of the effect of SP on DA release, where SP has been found to increase, decrease or have no effect on DA release (see chapter 5 table 1). A possible reason for the discrepancies could be that the effect of SP on DA release is frequency-dependent, as was

seen with ACh. Until the gating action of ACh on DA release was understood the reports of ACh both increasing and decreasing DA release were seen as conflicting, but have now been reconciled with the finding that ACh alters the frequency dependence of DA release: ACh maintains high release probability (Pr) so that there is little difference in release between DA release to tonic and phasic patterns of DA neuron activity. When the action of ACh is blocked low frequency release is depressed, and high frequency release is facilitated (Cragg, 2003; Rice and Cragg, 2004). To investigate the hypothesis that the variable effects of SP on DA release are due to SP modulating DA release in a frequency-dependent manner, the effect of SP on DA was measured across a range of stimulation frequencies (chapter 5).

An alternative hypothesis is that SP has modulatory targets other than, or in addition to DA terminals, which are indirectly affecting DA release. An example of how this may occur is by SP modulating ACh release that in turn affects DA release. This is plausible as cholinergic interneurons (ChIs) express high levels of NK1 receptors (NK1R), which have been considered the predominant target of SP in the striatum (Bolam et al., 1986; Tsuchida et al., 1990). Therefore in chapter 5, the effect of SP on DA release was investigated without nAChR activation, in order to exclude the possibility of SP affecting DA release indirectly via the cholinergic system. In the presence of nAChR blockade, SP was capable of modulating DA release in a frequency-independent manner. Furthermore the modulatory effect of SP was apparent for a single pulse and constantly throughout longer train stimulations without obvious enhancement or diminution. The lack of additional modulator effects of SP on DA release during long train stimulations is pertinent, since some striatal neuromodulators such as hydrogen peroxide (H_2O_2) or others acting at slow metabotropic receptors may require initial activation of local circuits and have effects that only become apparent during trains of activity (Avshalumov and Rice, 2003). This suggests that SP is not acting on a local circuit driven by the electrical stimulus that regulates DA via metabotropic receptors, or via other mechanisms such as H_2O_2. Therefore the variable effects of SP on DA release are not due to SP modulating DA release in a frequency-dependent manner and do not

seem to be mediated by local modulatory circuits activated by local electrical stimulation. Using optogenetics coupled to FCV to exclusively drive dopaminergic terminals could be used to confirm that SP is acting directly at DA terminals. However, the viral vector used to induce ChR2 expression exclusively in DA neurons is fused to the eYFP transcript, therefore it would make post-hoc analysis of striosome-matrix location more difficult. Therefore in this thesis I have focused on charactering how SP modulation of DA release is affected by striosome-matrix location, rather than focusing on whether SP is acting at NK1R directly on DA terminals, although this would be an informative line of enquiry in the future.

6.2.2 The effect of SP on DA release depends on striosome-matrix location

Even in the absence of active nAChR, the effects of SP on DA release were still highly variable, being able to decrease (type 1 effect), increase (type 2 effect) or not effect DA release (chapter 5). Both type 1 and type 2 effects were reversible and NK1R-dependent. In order to investigate the variable effects of SP on DA release, recording sites were marked with yellow-green FluoSpheres, and then the tissue was processed for MOR immunoreactivity to visualise the striosome-matrix axis of the striatum, where high and low levels of immunoreactivity indicates striosome and matrix regions respectively, allowing the effect of SP on DA release to be compared to its striosomal location. The effect of SP on DA release was dependent on striosome-matrix location, where SP exerted a type 1, 2 or no effect when DA was recorded from a boundary region between the matrix and a striosome, within a striosome or in the matrix respectively.

Recording sites were classified using a number of criteria and measurements to limit the potential for a recording site to be incorrectly characterised. Firstly a qualitative, ternary classification system was used, and the location of the recording site was estimated by determining a “marked site” either by oval A or circle B (see chapter 5 methods). Importantly none of the recording site classifications were changed when either oval A or circle B were used. In addition to the ternary classification system, the distance between the recording site and the

nearest striosome was also measured, and then was compared to the effect of SP on 1p DA release. Using both the ternary classification system and this quantitative measurement to compare the effect of SP on DA release and striosomal positioning corroborated the relationship identified by the ternary system; but also showed that the effects of SP on DA release are on a continuum rather than discrete increase, decrease or no effect of SP on DA release.

Both b1 and b2 plots illustrated the same trend of SP having no effect when furthest from a striosome, type 1 effect when recording on an boundary and type 2 effect when recording within a striosome. The fact that the trends of b1 and b2 plots are consistent is very reassuring as b2 is not dependent on an accurate definition of the striosome border, which may have introduced error into both the ternary classification and b1 distance.

The matrix occupies the majority of the striatum (~80% depending upon rostral-caudal axis) (Johnston et al., 1990; Desban et al., 1993; Tajima and Fukuda, 2013), therefore if the hypothesis of SP having differential effects of DA release depending on striosomal location is correct, and striatal recording sites are randomly selected, the striosomal effects of SP on DA release (Type 2) should occur much less often than a lack of effect. This is indeed the case, where SP has no effect on DA release 10/22 times, has a type 1 effect 8/22 times and a type 2 effect 4/22 times. The approximate correlation between ratio of effects and ratio of volume of striosome and matrix territories supports our hypothesis that the effect of SP on DA release depends on striosomal location, and helps to explain the discrepancies in the effects of SP on DA release, published in the literature to date.

Both type 1 and 2 effects of SP on DA release seem to be via NK1R, so it remains to be determined how activation of the same receptors elicits diametric effects on DA release. This could be explained by NK1R coupling to $G_{\alpha s}$ and $G_{\alpha i}$ in the centre and boundaries of striosomes respectively, which could therefore result in SP increasing and decreasing DA release in the centre and boundaries of striosome respectively. Alternatively NK1R activation may be upstream of a

pathway which affects DA release, and intermediate signalling may facilitate divergent effects of SP on DA release. The opioid receptors are possible intermediary candidates: MOR are enriched in striosomal compartments of the striatum, and δ-opioid receptor (DOR) are enriched particularly in the central regions of the striosomes (Koizumi et al., 2013). NK1R and MOR have been shown to affect the function of one another, including affecting the rate of turnover of the receptors in the membrane, and furthermore, the addictive properties of morphine (MOR agonist) are not present in NK1R-null mice, suggesting their interactions have physiological significance (Murtra et al., 2000). SP can inhibit the facilitation of GIRK conductance by DOR activation, indicating that they too functionally interact (Velimirovic et al., 1995). In support of the hypothesis that SP has opposing actions on DA release by differentially coupling to either MOR or DOR, it has been shown that DOR activation in the striatum can enhance DA release, whereas MOR activation has mixed effects, either inhibiting DA release, or having no effect (Pentney and Gratton, 1991). However it should be noted that despite DOR being reported to be enhanced in the centre of striosomes there are many studies that report DOR as having a diffuse pattern of expression in the striatum, and that the modulatory effects of MOR and DOR activation on DA release are also quite variable (Tempel and Zukin, 1987).

An alternative intermediate neuromodulator is nitric oxide (NO), which in the absence of ACh effects increases DA release in a frequency-independent manner (Hartung et al., 2011). Although no effect of endogenous NO was identified by Hartung et al, SP may be able to facilitate NO production. However if SP is facilitating NO production in NO synthase- (NOS-) positive interneurons, NO levels would need to be present between stimulations (at 2.5 min intervals) for there to be an effect of NO on 1p DA release. Like SP, the reported effects of NO on DA release in CPu are highly variable (Black et al., 1994; Iravani et al., 1998), but as NO is a freely permeable molecule, how its modulatory effects could be constrained anatomically to have distinct outcomes in striosome vs. matrix regions would be a necessary question to address. One possibility is that because blood vessels are concentrate along striosomal boundaries (Breuer et

al., 2005), the haem groups in blood may provide a barrier against the free diffusion of NO throughout the striatum. This is highly speculative, but could be an interesting avenue to explore.

Despite not knowing how SP can elicit such a range of effects on DA release, the effect of SP on DA release can be mapped onto an "ideal striosome" (**Figure 6.2**), which indicates that SP increases DA release in the core of a striosome, then towards the outer edge of the striosome and into the surrounding matrix SP decreases DA release, and in the outer matrix SP has no effect on DA release. This model of an ideal striosome and the modulatory effects of SP on DA release is highly reminiscent of centre surround inhibition. Centre surround inhibition is most commonly associated with sensory systems, where strongly activated neurons inhibit surrounding, less strongly activated neurons, giving rise to a high spatial contrast between activated and non-activated neurons. The modulatory effect of SP on DA release may be giving rise to a form of centre surround inhibition, but rather than an individual neuron inhibiting its adjacent similar neighbour, DA release is modulated in spatially distinct manner by an independent neuromodulator (SP), resulting in a dense patch of high DA release surrounded by an area of low DA release. How the pattern of high DA release surrounded by an area of low DA release affects downstream neurons, is still very much to be determined, but may provide key insights into the physiological role of the striosome-matrix division of the striatum.

In support of annuli being a true sub-compartment of the striatum, using data from chapter 5 I have created a model of the regions surrounding an ideal striosome which is analogous to a model of striosome core, annuli and matrix created by an independent study (Goto et al., 2013). I created a two-dimensional model of a striosome core, surrounded by a boundary ring and outer matrix: I assumed that an average striosome in the mouse striatum is 100 µm in radius (based on my observations from MOR-stained tissue and the literature), and that striosomes account for 20% of striatal area. A circle of radius 100 µm has an area of 31400 μm^2. Therefore a circle with an area five times 31400 μm^2 has a radius of 224 µm. Subtracting

the striosome radius, a model of a striosome imbedded in the surrounding matrix can be drawn:

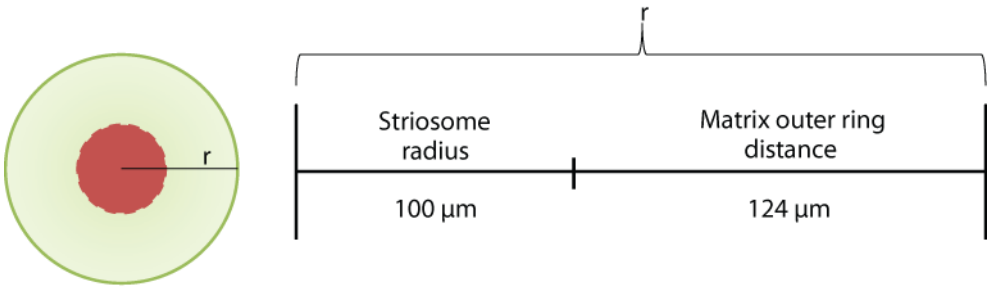

Using **figure 5.6a** it can be estimated that the boundary region spans from 20 µm within the striosome to 40 µm out into the matrix, as between these distance SP causes a decrease in DA. Therefore a model of a striosome core, surrounding boundary region (annulus) and matrix can be estimated to have the following dimensions:

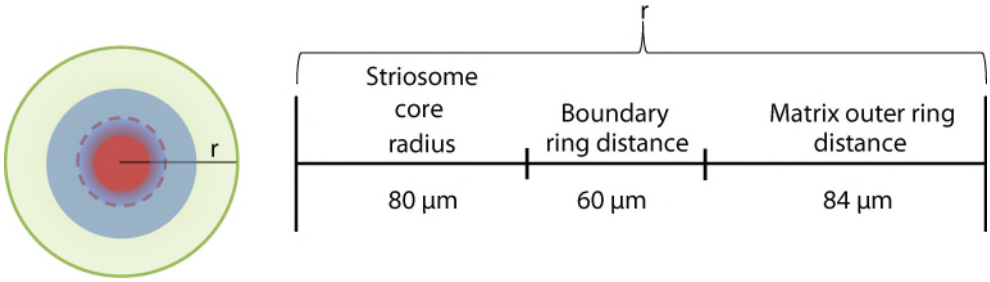

Where the red circle with dotted boundary is the striosome, the blue zone is the boundary region and the green zone is the matrix. These dimensions based on SP effects are very similar to those found anatomically using met-enkephalin staining by Goto et al (2013). Therefore data shown in this thesis would support a functional role of an annular region of the striosome.

6.2.3 Utilising emerging technologies

Transgenic mouse lines are currently being developed to allow the striosome-matrix axis of the striatum to be viewed live, circumventing the need for post-hoc classification of sites as being striosome/matrix/boundary. A particularly promising line has fused the striosomally enriched protein Nr4a1 to eGFP, however it is currently only available on a Swiss Webster background, which are known to differ from other strains of wild-type mice (Davis and Puhl, 2011). Once the

Nr4a1-eGFP line is established on a C57bl6 line, we will be able to dissect the effect of a number of neuromodulators along striosome-matrix axis without the need for post-hoc marking of recording sites. Being able to choose a site based on its striosomal location will also enable the number of animals required to carry out experiments to be kept to a minimum, and could allow for differences between striosomes in different anatomical locations to be investigated, amongst many other lines of inquiry.

6.2.4 Implications for disease: PD and addiction

In both animal models of PD and in post-mortem brains of PD patients SP levels have been found to be reduced (Sakamoto et al., 1992; Hornykiewicz, 1998), and the expression of other striosomal-matrix markers disrupted (Crittenden and Graybiel, 2011; Koizumi et al., 2013). DA content in striosomes is reduced and the SNc DA neurons that innervate the striosomes are especially vulnerable (Fukui et al., 1986; Bannon et al., 1987; Gerfen et al., 1987b). Striosomal markers, most notable of which is MOR, tend to be reduced in PD models. There is conflicting evidence of the effect of NK1R activation in PD and other neurotoxic models, with instances of both SP, and NK1R antagonists being neuroprotective (Salthun-Lassalle et al., 2005; Thornton et al., 2010; Wang and Angulo, 2011; Thornton and Vink, 2012).

It is unclear if the non-dopaminergic neurons in striosomes also are particularly sensitive in PD, or if they are preferentially affected because DA can modulate expression levels of striosomally enriched proteins such as MOR, NK1R and SP. As DA release is especially impaired in striosome regions, and SP facilitates release in striosomes, SP and other NK1R agonists may be good targets for PD treatments, as they will have a focused effect on the areas of the brain most affected by PD, while not modulating DA release in the less affected matrix region. SP may well have more limited side effects because of this compared to other drugs such as the anti-cholinergics, which modulate DA release throughout the striatum. A problem with using SP in the treatment of PD, is that NK1R are expressed throughout the nervous system and other parts of

the body, so although DA related side effects may be limited, systemic NK1R activation could result in side effects including pain, vomiting and itching. However as drug technologies are continually being advanced there may be a way of creating a SP analogue whose bioavailability is such to target it to the brain.

As has been mentioned above, NK1R and MOR interact to affect the addictive properties of morphine (Murtra et al., 2000), and because of the potential for NK1R antagonists to alleviate withdrawal symptoms of opiates, NK1R are attractive pharmacological targets. Drugs which target both opioid receptors and NK1R are currently being developed for the treatment of substance abuse. Therefore increasing our understand how NK1R activation affects DA release, which is known to have a central role in the addictive properties of drugs of abuse including opiates, will only improve the efficacy of treatments.

6.3 Concluding remarks

The striatum is heterogeneous

In parallel to the basal ganglia being a series of cortical loops, the striatum is a microcosm of this, as the plethora of striatal neuromodulators can interact and modulate one another. In order to understand the net effects of increasing or decreasing a neuromodulator within the whole circuit we need to be able to understand the rules of each modulator's release. Here I have investigated how DA release is modulated, and illustrated that multiple factors including anatomical location, striosome-matrix location, stimulation paradigm and presence of other neuromodulators especially ACh, can interact and affect how DA is released.

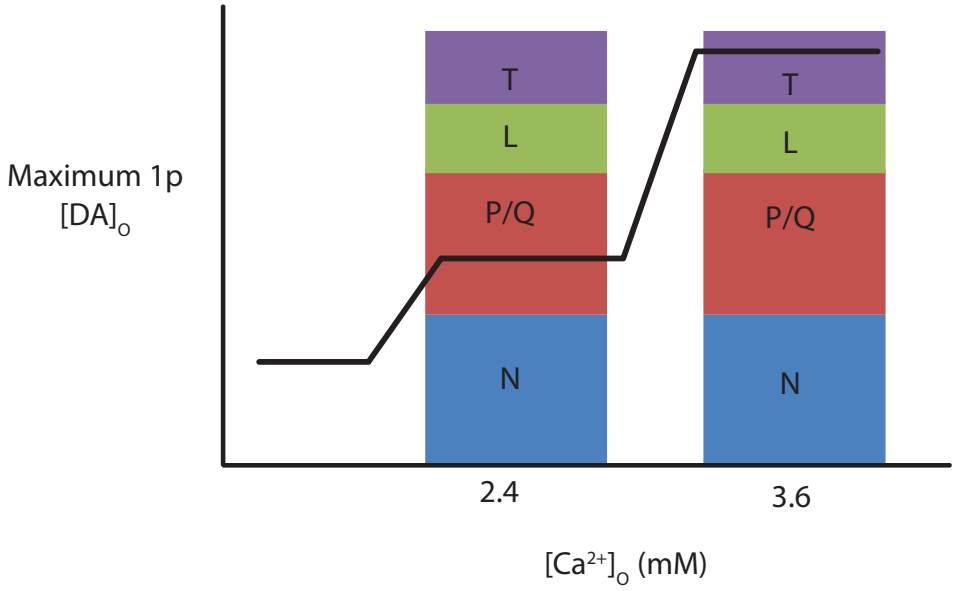

Figure 6.1: Cartoon of the contribution of different VDCCs during 1p evoked DA release in CPu at varying extracellular Ca^{2+} concentrations.
Hypothetical roles of VDCCs during 1p DA release at 2.4 mM and 3.6 mM extracellular Ca^{2+} concentrations in NAc. Black line shows a putitive Ca^{2+} response curve of 1p DA release. This illustrates how the contribution of VDCCs to DA release may vary at different extracellular Ca^{2+} concentrations. When Ca^{2+} entry is limited, 1p DA release is lower, so fewer VDCC subtypes contribute to the Ca^{2+} entry required to achieve maximal DA release. When 1p DA release is increased by increasing extracellular Ca^{2+} levels, more VDCC subtypes are contributing to Ca^{2+} entry required for maximal DA release.

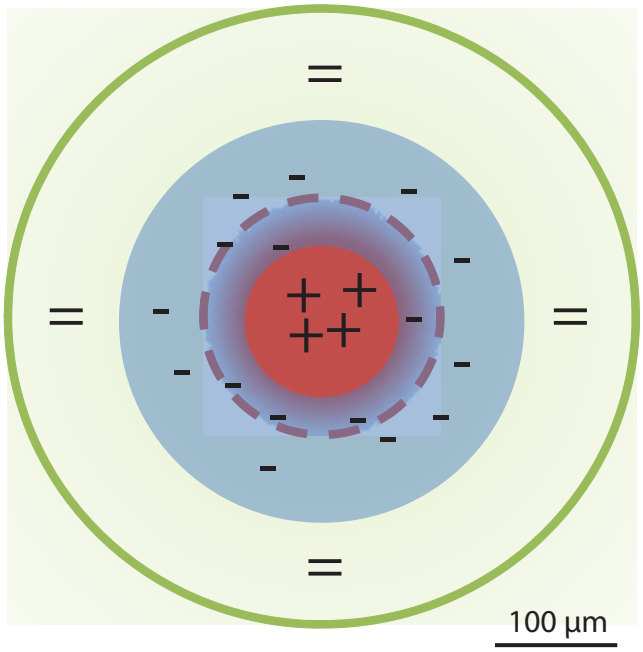

Figure 6.2: An ideal striosome: SP causes centre surround inhibition of DA release
The strisoome (red circle, up to the dashed red line) has a radius of 100 µm. The boundary region (blue area) is a ring which starting from 20 µm into the striosome and spanning 40 µm into the surrounding matrix. Not including the boundary region, the matrix (green area) accounts for 80% of the area, and the striosome (red circle up to dashed line) occupies 20% of the total area. Including the boundary region, the matrix, boundary and striosome core account for 55%, 32% and 13% of the total area respectively. SP increases DA release in the striosome core (red circle); SP decreases DA release in the boundary region (blue area); SP has no effect on DA release in the matrix

Bibliography

Adamantidis AR, Tsai H-C, Boutrel B, Zhang F, Stuber GD, Budygin EA, Touriño C, Bonci A, Deisseroth K, De Lecea L (2011) Optogenetic interrogation of dopaminergic modulation of the multiple phases of reward-seeking behavior. J Neurosci 31:10829–10835.

Adamczyk A, Strosznajder JB (2006) Alpha-synuclein potentiates Ca2+ influx through voltage-dependent Ca2+ channels. Neuroreport 17:1883–1886.

Airaksinen MS, Thoenen H, Meyer M (1997) Vulnerability of Midbrain Dopaminergic Neurons in Calbindin-D 28k -deficient Mice: Lack of Evidence for a Neuroprotective Role of Endogenous Calbindin in MPTPtreated and Weaver Mice. Eur J Neurosci 9:120–127.

Alfaro-Rodriguez A, Alonso-Spilsbury M, Arch-Tirado E, Gonzalez-Pina R, Arias-Montaño J-A, Bueno-Nava A (2013) Histamine H3 receptor activation prevents dopamine D1 receptor-mediated inhibition of dopamine release in the rat striatum: A microdialysis study. Neurosci Lett.

Anderson JJ, Chase TN, Engber TM (1993) Substance P increases release of acetylcholine in the dorsal striatum of freely moving rats. Brain Res 623:189–194.

Anderson JJ, Kuo S, Chase TN, Engber TM (1994) Dopamine D1 receptor-stimulated release of acetylcholine in rat striatum is mediated indirectly by activation of striatal neurokinin1 receptors. J Pharmacol Exp Ther 269:1144–1151.

Anwar S, Peters O, Millership S, Ninkina N, Doig N, Connor-Robson N, Threlfell S, Kooner G, Deacon RM, Bannerman DM, Bolam JP, Chandra SS, Cragg SJ, Wade-Martins R, Buchman VL (2011) Functional alterations to the nigrostriatal system in mice lacking all three members of the synuclein family. J Neurosci 31:7264–7274.

Aosaki T, Kimura M, Graybiel AM (1995) Temporal and spatial characteristics of tonically active neurons of the primate's striatum. J Neurophysiol 73:1234–1252.

Aosaki T, Tsubokawa H, Ishida A, Watanabe K, Graybiel AM, Kimura M (1994) Responses of tonically active neurons in the primate's striatum undergo systematic changes during behavioral sensorimotor conditioning. J Neurosci 14:3969–3984.

Arbuthnott GW, Wickens J (2007) Space, time and dopamine. Trends Neurosci 30:62–69.

Arikkath J, Campbell KP (2003) Auxiliary subunits: essential components of the voltage-gated calcium channel complex. Curr Opin Neurobiol 13:298–307.

Avshalumov M V, Rice ME (2003) Activation of ATP-sensitive K+ (K(ATP)) channels by H2O2 underlies glutamate-dependent inhibition of striatal dopamine release. Proc Natl Acad Sci U S A 100:11729–11734.

Balleine BW, Delgado MR, Hikosaka O (2007) The role of the dorsal striatum in reward and decision-making. J Neurosci 27:8161–8165.

Bamford NS, Robinson S, Palmiter RD, Joyce JA, Moore C, Meshul CK (2004) Dopamine modulates release from corticostriatal terminals. J Neurosci 24:9541–9552.

Bannon MJ, Elliott PJ, Bunney EB (1987) Striatal tachykinin biosynthesis: regulation of mRNA and peptide levels by dopamine agonists and antagonists. Mol Brain Res 3:31–37.

Bannon MJ, Lee JM, Giraud P, Young A, Affolter HU, Bonner TI (1986) Dopamine antagonist haloperidol decreases substance P, substance K, and preprotachykinin mRNAs in rat striatonigral neurons. J Biol Chem 261:6640–6642.

Baptista MJ, O'Farrell C, Daya S, Ahmad R, Miller DW, Hardy J, Farrer MJ, Cookson MR (2003) Co-ordinate transcriptional regulation of dopamine synthesis genes by α-synuclein in human neuroblastoma cell lines. J Neurochem 85:957–968.

Bean BP (2007) The action potential in mammalian central neurons. Nat Rev Neurosci 8:451–465.

Beaulieu J-M, Gainetdinov RR (2011) The physiology, signaling, and pharmacology of dopamine receptors. Pharmacol Rev 63:182–217.

Beck S, Hallett M (2011) Surround inhibition in the motor system. Exp Brain Res 210:165–172.

Beckstead MJ, Grandy DK, Wickman K, Williams JT (2004) Vesicular dopamine release elicits an inhibitory postsynaptic current in midbrain dopamine neurons. Neuron 42:939–946.

Bekris LM, Mata IF, Zabetian CP (2010) The genetics of Parkinson disease. J Geriatr Psychiatry Neurol 23:228–242.

Bender KJ, Uebele VN, Renger JJ, Trussell LO (2012) Control of firing patterns through modulation of axon initial segment T-type calcium channels. J Physiol 590:109–118.

Bennett BD, Wilson CJ (1999) Spontaneous activity of neostriatal cholinergic interneurons in vitro. J Neurosci 19:5586–5596.

Bergquist F, Jonason J, Pileblad E, Nissbrandt H (1998) Effects of Local Administration of L-, N-, and P/Q-Type Calcium Channel Blockers on Spontaneous Dopamine Release in the Striatum and the Substantia Nigra: A Microdialysis Study in Rat. J Neurochem 70:1532–1540.

Bergquist F, Nissbrandt H (2003) Influence of R-type (Cav2.3) and t-type (Cav3.1-3.3) antagonists on nigral somatodendritic dopamine release measured by microdialysis. Neuroscience 120:757–764.

Bertrand D, Gopalakrishnan M, Donnelly-Roberts D, Gotti C, Clementi F, Fornari A, Gaimarri A, Guiducci S, Manfredi I, Moretti M, Pedrazzi P, Pucci L, Zoli M (2009) Structural and functional diversity of native brain neuronal nicotinic receptors. Biochem Pharmacol 78:703–711.

Besson MJ, Graybiel AM, Nastuk MA (1988) [3H]SCH 23390 binding to D1 dopamine receptors in the basal ganglia of the cat and primate: delineation of striosomal compartments and pallidal and nigral subdivisions. Neuroscience 26:101–119.

Björklund A, Dunnett SB (2007) Dopamine neuron systems in the brain: an update. Trends Neurosci 30:194–202.

Björklund A, Lindvall O (1975) Dopamine in dendrites of substantia nigra neurons: suggestions for a role in dendritic terminals. Brain Res 83:531–537.

Black MD, Matthews EK, Humphrey PP (1994) The effects of a photosensitive nitric oxide donor on basal and electrically-stimulated dopamine efflux from the rat striatum in vitro. Neuropharmacology 33:1357–1365.

Blandini F, Armentero M-T (2012) Animal models of Parkinson's disease. FEBS J 279:1156–1166.

Blomeley CP, Bracci E (2009) Serotonin excites fast-spiking interneurons in the striatum. Eur J Neurosci 29:1604–1614.

Blomeley CP, Kehoe LA, Bracci E (2009) Substance P mediates excitatory interactions between striatal projection neurons. J Neurosci 29:4953–4963.

Boix F, Huston JP, Schwarting RK (1992) The C-terminal fragment of substance P enhances dopamine release in nucleus accumbens but not in neostriatum in freely moving rats. Brain Res 592:181–186.

Boix F, Pfister M, Huston JP, Schwarting RKW (1994) Substance P decreases extracellular concentrations of acetylcholine in neostriatum and nucleus accumbens in vivo: Possible relevance for the central processing of reward and aversion. Behav Brain Res 63:213–219.

Bolam JP, Hanley JJ, Booth PAC, Bevan MD (2000) Synaptic organisation of the basal ganglia. J Anat 196:527–542.

Bolam JP, Ingham CA, Izzo PN, Levey AI, Rye DB, Smith AD, Wainer BH (1986) Substance P-containing terminals in synaptic contact with cholinergic neurons in the neostriatum and basal forebrain: a double immunocytochemical study in the rat. Brain Res 397:279–289.

Bolam JP, Izzo PN (1988) The postsynaptic targets of substance P-immunoreactive terminals in the rat neostriatum with particular reference to identified spiny striatonigral neurons. Exp Brain Res 70:361–377.

Bolam JP, Izzo PN, Graybiel AM (1988) Cellular substrate of the histochemically defined striosome/matrix system of the caudate nucleus: A combined golgi and immunocytochemical study in cat and ferret. Neuroscience 24:853–875.

Bolam JP, Pissadaki EK (2012) Living on the edge with too many mouths to feed: why dopamine neurons die. Mov Disord 27:1478–1483.

Bonci A, Grillner P, Mercuri NB, Bernardi G (1998) L-Type Calcium Channels Mediate a Slow Excitatory Synaptic Transmission in Rat Midbrain Dopaminergic Neurons. J Neurosci 18:6693–6703.

Bourinet E, Soong TW, Sutton K, Slaymaker S, Mathews E, Monteil A, Zamponi GW, Nargeot J, Snutch TP (1999) Splicing of alpha 1A subunit gene generates phenotypic variants of P- and Q-type calcium channels. Nat Neurosci 2:407–415.

Braak H, Ghebremedhin E, Rüb U, Bratzke H, Del Tredici K (2004) Stages in the development of Parkinson's disease-related pathology. Cell Tissue Res 318:121–134.

Bracci E, Centonze D, Bernardi G, Calabresi P (2002) Dopamine excites fast-spiking interneurons in the striatum. J Neurophysiol 87:2190–2194.

Brandt A, Khimich D, Moser T (2005) Few CaV1.3 channels regulate the exocytosis of a synaptic vesicle at the hair cell ribbon synapse. J Neurosci 25:11577–11585.

Brandt A, Striessnig J, Moser T (2003) CaV1.3 channels are essential for development and presynaptic activity of cochlear inner hair cells. J Neurosci 23:10832–10840.

Breuer O, Lawhorn C, Miller T, Smith DM, Brown LL (2005) Functional architecture of the mammalian striatum: mouse vascular and striosome organization and their anatomic relationships. Neurosci Lett 385:198–203.

Brice NL, Berrow NS, Campbell V, Page KM, Brickley K, Tedder I, Dolphin AC (1997) Importance of the Different |β Subunits in the Membrane Expression of the α1A and α2 Calcium Channel Subunits: Studies Using a Depolarization-sensitive α1A Antibody. Eur J Neurosci 9:749–759.

Britt JP, McGehee DS (2008) Presynaptic opioid and nicotinic receptor modulation of dopamine overflow in the nucleus accumbens. J Neurosci 28:1672–1681.

Brown DA (2010) Muscarinic acetylcholine receptors (mAChRs) in the nervous system: some functions and mechanisms. J Mol Neurosci 41:340–346.

Brown MTC, Henny P, Bolam JP, Magill PJ (2009) Activity of neurochemically heterogeneous dopaminergic neurons in the substantia nigra during spontaneous and driven changes in brain state. J Neurosci 29:2915–2925.

Brown P (2003) Oscillatory nature of human basal ganglia activity: relationship to the pathophysiology of Parkinson's disease. Mov Disord 18:357–363.

Bull DR, Palij P, Sheehan MJ, Millar J, Stamford JA, Kruk ZL, Humphrey PP (1990) Application of fast cyclic voltammetry to measurement of electrically evoked dopamine overflow from brain slices in vitro. J Neurosci Methods 32:37–44.

Bungay PM, Newton-Vinson P, Isele W, Garris PA, Justice JB (2003) Microdialysis of dopamine interpreted with quantitative model incorporating probe implantation trauma. J Neurochem 86:932–946.

Cachope R, Mateo Y, Mathur BN, Irving J, Wang H-L, Morales M, Lovinger DM, Cheer JF (2012) Selective activation of cholinergic interneurons enhances accumbal phasic dopamine release: setting the tone for reward processing. Cell Rep 2:33–41.

Capecchi MR (1989) Altering the genome by homologous recombination. Science 244:1288–1292.

Carbone E, Giancippoli A, Marcantoni A, Guido D, Carabelli V (2006) A new role for T-type channels in fast "low-threshold" exocytosis. Cell Calcium 40:147–154.

Cardozo DL, Bean BP (1995) Voltage-dependent calcium channels in rat midbrain dopamine neurons: modulation by dopamine and GABAB receptors. J Neurophysiol 74:1137–1148.

Carvalho CM, Ferreira IL, Duarte CB, Malva JO, Tretter L, Adam-Vizi V, Carvalho AP (1995) Relation of [Ca2+]i to dopamine release in striatal synaptosomes: role of Ca2+ channels. Brain Res 669:234–244.

Catterall WA (2000) Structure and regulation of voltage-gated Ca2+ channels. Annu Rev Cell Dev Biol 16:521–555.

Catterall WA (2011) Voltage-gated calcium channels. Cold Spring Harb Perspect Biol 3:a003947.

Catterall WA, Perez-Reyes E, Snutch TP, Striessnig J (2005) International Union of Pharmacology. XLVIII. Nomenclature and structure-function relationships of voltage-gated calcium channels. Pharmacol Rev 57:411–425.

Centonze D, Grande C, Usiello A, Gubellini P, Erbs E, Martin AB, Pisani A, Tognazzi N, Bernardi G, Moratalla R, Borrelli E, Calabresi P (2003) Receptor subtypes involved in the presynaptic and postsynaptic actions of dopamine on striatal interneurons. J Neurosci 23:6245–6254.

Chan CS, Guzman JN, Ilijic E, Mercer JN, Rick C, Tkatch T, Meredith GE, Surmeier DJ (2007) "Rejuvenation" protects neurons in mouse models of Parkinson's disease. Nature 447:1081–1086.

Chan CS, Peterson JD, Gertler TS, Glajch KE, Quintana RE, Cui Q, Sebel LE, Plotkin JL, Shen W, Heiman M, Heintz N, Greengard P, Surmeier DJ (2012) Strain-specific regulation of striatal phenotype in Drd2-eGFP BAC transgenic mice. J Neurosci 32:9124–9132.

Chapman ER (2002) Synaptotagmin: a Ca(2+) sensor that triggers exocytosis? Nat Rev Mol Cell Biol 3:498–508.

Charlety PJ, Grenhoff J, Chergui K, De La Chapelle B, Buda M, Svensson TH, Chouvet G (1991) Burst firing of mesencephalic dopamine neurons is inhibited by somatodendritic application of kynurenate. Acta Physiol Scand 142:105–112.

Chartier-Harlin M-C, Kachergus J, Roumier C, Mouroux V, Douay X, Lincoln S, Levecque C, Larvor L, Andrieux J, Hulihan M, Waucquier N, Defebvre L, Amouyel P, Farrer M, Destée A (2004) Alpha-synuclein locus duplication as a cause of familial Parkinson's disease. Lancet 364:1167–1169.

Chen BT, Moran KA, Avshalumov M V, Rice ME (2006) Limited regulation of somatodendritic dopamine release by voltage-sensitive Ca channels contrasted with strong regulation of axonal dopamine release. J Neurochem 96:645–655.

Chen BT, Rice ME (2001) Novel Ca2+ dependence and time course of somatodendritic dopamine release: substantia nigra versus striatum. J Neurosci 21:7841–7847.

Cheng H-C, Ulane CM, Burke RE (2010) Clinical progression in Parkinson disease and the neurobiology of axons. Ann Neurol 67:715–725.

Chevalier M, Lory P, Mironneau C, Macrez N, Quignard J-F (2006) T-type CaV3.3 calcium channels produce spontaneous low-threshold action potentials and intracellular calcium oscillations. Eur J Neurosci 23:2321–2329.

Chun LS, Free RB, Doyle TB, Huang X-P, Rankin ML, Sibley DR (2013) D1-D2 dopamine receptor synergy promotes calcium signaling via multiple mechanisms. Mol Pharmacol 84:190–200.

Chung CY, Seo H, Sonntag KC, Brooks A, Lin L, Isacson O (2005) Cell type-specific gene expression of midbrain dopaminergic neurons reveals molecules involved in their vulnerability and protection. Hum Mol Genet 14:1709–1725.

Clayton DF, George JM (1998) The synucleins: a family of proteins involved in synaptic function, plasticity, neurodegeneration and disease. Trends Neurosci 21:249–254.

Colecraft HM, Brody DL, Yue DT (2001) G-Protein Inhibition of N- and P/Q-Type Calcium Channels: Distinctive Elementary Mechanisms and Their Functional Impact. J Neurosci 21:1137–1147.

Collier TJ, Kanaan NM, Kordower JH (2011) Ageing as a primary risk factor for Parkinson's disease: evidence from studies of non-human primates. Nat Rev Neurosci 12:359–366.

Comoli E, Coizet V, Boyes J, Bolam JP, Canteras NS, Quirk RH, Overton PG, Redgrave P (2003) A direct projection from superior colliculus to substantia nigra for detecting salient visual events. Nat Neurosci 6:974–980.

Condliffe SB, Corradini I, Pozzi D, Verderio C, Matteoli M (2010) Endogenous SNAP-25 regulates native voltage-gated calcium channels in glutamatergic neurons. J Biol Chem 285:24968–24976.

Consolo S, Girotti P, Russi G, Di Chiara G (1992) Endogenous dopamine facilitates striatal in vivo acetylcholine release by acting on D1 receptors localized in the striatum. J Neurochem 59:1555–1557.

Cragg S, Rice ME, Greenfield SA (1997) Heterogeneity of electrically evoked dopamine release and reuptake in substantia nigra, ventral tegmental area, and striatum. J Neurophysiol 77:863–873.

Cragg SJ (2003) Variable Dopamine Release Probability and Short-Term Plasticity between Functional Domains of the Primate Striatum. J Neurosci 23:4378–4385.

Cragg SJ (2006) Meaningful silences: how dopamine listens to the ACh pause. Trends Neurosci 29:125–131.

Cragg SJ, Rice ME (2004) DAncing past the DAT at a DA synapse. Trends Neurosci 27:270–277.

Crittenden JR, Graybiel AM (2011) Basal Ganglia disorders associated with imbalances in the striatal striosome and matrix compartments. Front Neuroanat 5:59.

Cui G, Okamoto T, Morikawa H (2004) Spontaneous opening of T-type Ca2+ channels contributes to the irregular firing of dopamine neurons in neonatal rats. J Neurosci 24:11079–11087.

Damier P (1999) The substantia nigra of the human brain: I. Nigrosomes and the nigral matrix, a compartmental organization based on calbindin D28K immunohistochemistry. Brain 122:1421–1436.

Davis MI, Puhl HL (2011) Nr4a1-eGFP is a marker of striosome-matrix architecture, development and activity in the extended striatum. PLoS One 6:e16619.

Dean B (2012) Neurochemistry of schizophrenia: the contribution of neuroimaging postmortem pathology and neurochemistry in schizophrenia. Curr Top Med Chem 12:2375–2392.

DeBoer P, Abercrombie ED (1996) Physiological release of striatal acetylcholine in vivo: modulation by D1 and D2 dopamine receptor subtypes. J Pharmacol Exp Ther 277:775–783.

Desban M, Kemel ML, Glowinski J, Gauchy C (1993) Spatial organization of patch and matrix compartments in the rat striatum. Neuroscience 57:661–671.

Descarries L, Mechawar N (2000) Ultrastructural evidence for diffuse transmission by monoamine and acetylcholine neurons of the central nervous system. Prog Brain Res 125:27–47.

DeVane CL (2001) Substance P: a new era, a new role. Pharmacotherapy 21:1061–1069.

Di Matteo V, Pierucci M, Esposito E, Crescimanno G, Benigno A, Di Giovanni G (2008) Serotonin modulation of the basal ganglia circuitry: therapeutic implication for Parkinson's disease and other motor disorders. Prog Brain Res 172:423–463.

Di Virgilio F, Milani D, Leon A, Meldolesi J, Pozzan T (1987) Voltage-dependent activation and inactivation of calcium channels in PC12 cells. Correlation with neurotransmitter release. J Biol Chem 262:9189–9195.

Doig NM, Moss J, Bolam JP (2010) Cortical and thalamic innervation of direct and indirect pathway medium-sized spiny neurons in mouse striatum. J Neurosci 30:14610–14618.

Dolphin AC (2006) A short history of voltage-gated calcium channels. Br J Pharmacol 147 Suppl :S56–62.

Donoghue JP, Herkenham M (1986) Neostriatal projections from individual cortical fields conform to histochemically distinct striatal compartments in the rat. Brain Res 365:397–403.

Dryanovski DI, Guzman JN, Xie Z, Galteri DJ, Volpicelli-Daley LA, Lee VM-Y, Miller RJ, Schumacker PT, Surmeier DJ (2013) Calcium Entry and -Synuclein Inclusions Elevate Dendritic Mitochondrial Oxidant Stress in Dopaminergic Neurons. J Neurosci 33:10154–10164.

Durieux PF, Schiffmann SN, de Kerchove d'Exaerde A (2011) Targeting neuronal populations of the striatum. Front Neuroanat 5:40.

Emptage NJ, Reid CA, Fine A (2001) Calcium stores in hippocampal synaptic boutons mediate short-term plasticity, store-operated Ca2+ entry, and spontaneous transmitter release. Neuron 29:197–208.

Ermak G, Davies KJA (2002) Calcium and oxidative stress: from cell signaling to cell death. Mol Immunol 38:713–721.

Exley R, Cragg SJ (2008) Presynaptic nicotinic receptors: a dynamic and diverse cholinergic filter of striatal dopamine neurotransmission. Br J Pharmacol 153 Suppl:S283–97.

Exley R, McIntosh JM, Marks MJ, Maskos U, Cragg SJ (2012) Striatal α5 nicotinic receptor subunit regulates dopamine transmission in dorsal striatum. J Neurosci 32:2352–2356.

Falkenburger BH, Barstow KL, Mintz IM (2001) Dendrodendritic inhibition through reversal of dopamine transport. Science 293:2465–2470.

Faull RLM, Dragunow M, Villiger JW (1989) The distribution of neurotensin receptors and acetylcholinesterase in the human caudate nucleus: evidence for the existence of a third neurochemical compartment. Brain Res 488:381–386.

Flaherty AW, Graybiel AM (1994) Input-output organization of the sensorimotor striatum in the squirrel monkey. J Neurosci 14:599–610.

Ford CP, Beckstead MJ, Williams JT (2007) Kappa opioid inhibition of somatodendritic dopamine inhibitory postsynaptic currents. J Neurophysiol 97:883–891.

Ford CP, Gantz SC, Phillips PEM, Williams JT (2010) Control of extracellular dopamine at dendrite and axon terminals. J Neurosci 30:6975–6983.

Fortin GD, Desrosiers CC, Yamaguchi N, Trudeau L-E (2006) Basal somatodendritic dopamine release requires snare proteins. J Neurochem 96:1740–1749.

Fourcaudot E, Gambino F, Casassus G, Poulain B, Humeau Y, Lüthi A (2009) L-type voltage-dependent Ca(2+) channels mediate expression of presynaptic LTP in amygdala. Nat Neurosci 12:1093–1095.

Fox AP, Nowycky MC, Tsien RW (1987) Single-channel recordings of three types of calcium channels in chick sensory neurones. J Physiol 394:173–200.

Franco R, Ferré S, Prezeau L, Rives M-L, Comps-Agrar L, Maurel D, Kniazeff J, Pin J-P (2010) Functional crosstalk between GPCRs: with or without oligomerization. Curr Opin Pharmacol 10:6–13.

Fujiyama F, Sohn J, Nakano T, Furuta T, Nakamura KC, Matsuda W, Kaneko T (2011) Exclusive and common targets of neostriatofugal projections of rat striosome

neurons: a single neuron-tracing study using a viral vector. Eur J Neurosci 33:668–677.

Fukui K, Kariyama H, Kashiba A, Kato N, Kimura H (1986) Further confirmation of heterogeneity of the rat striatum: Different mosaic patterns of dopamine fibers after administration of methamphetamine or reserpine. Brain Res 382:81–86.

Galarraga E, Hernández-López S, Tapia D, Reyes A, Bargas J (1999) Action of substance P (neurokinin-1) receptor activation on rat neostriatal projection neurons. Synapse 33:26–35.

Geffen LB, Jessell TM, Cuello AC, Iversen LL (1976) Release of dopamine from dendrites in rat substantia nigra. Nature 260:258–260.

Gerfen CR (1984) The neostriatal mosaic: compartmentalization of corticostriatal input and striatonigral output systems. Nature 311:461–464.

Gerfen CR (1985) The neostriatal mosaic. I. Compartmental organization of projections from the striatum to the substantia nigra in the rat. J Comp Neurol 236:454–476.

Gerfen CR (1989) The neostriatal mosaic: striatal patch-matrix organization is related to cortical lamination. Science 246:385–388.

Gerfen CR (1991) Substance P (neurokinin-1) receptor mRNA is selectively expressed in cholinergic neurons in the striatum and basal forebrain. Brain Res 556:165–170.

Gerfen CR (1992) The neostriatal mosaic: multiple levels of compartmental organization in the basal ganglia. Annu Rev Neurosci 15:285–320.

Gerfen CR, Baimbridge KG, Miller JJ (1985) The neostriatal mosaic: compartmental distribution of calcium-binding protein and parvalbumin in the basal ganglia of the rat and monkey. Proc Natl Acad Sci U S A 82:8780–8784.

Gerfen CR, Baimbridge KG, Thibault J (1987a) The neostriatal mosaic: III. Biochemical and developmental dissociation of patch-matrix mesostriatal systems. J Neurosci 7:3935–3944.

Gerfen CR, Herkenham M, Thibault J (1987b) The neostriatal mosaic: II. Patch- and matrix-directed mesostriatal dopaminergic and non-dopaminergic systems. J Neurosci 7:3915–3934.

Gerfen CR, McGinty J, Young W (1991) Dopamine differentially regulates dynorphin, substance P, and enkephalin expression in striatal neurons: in situ hybridization histochemical analysis. J Neurosci 11:1016–1031.

Gerfen CR, Surmeier DJ (2010) Modulation of Striatal Projection Systems by Dopamine. Annu Rev Neurosci 34:441–466.

Giessel AJ, Sabatini BL (2011) Boosting of Synaptic Potentials and Spine Ca Transients by the Peptide Toxin SNX-482 Requires Alpha-1E-Encoded Voltage-Gated Ca Channels. PLoS One 6:e20939.

Giraudo CG, Eng WS, Melia TJ, Rothman JE (2006) A clamping mechanism involved in SNARE-dependent exocytosis. Science 313:676–680.

Goedert M (2001) Alpha-synuclein and neurodegenerative diseases. Nat Rev Neurosci 2:492–501.

Goers J, Manning-Bog AB, McCormack AL, Millett IS, Doniach S, Di Monte DA, Uversky VN, Fink AL (2003) Nuclear localization of alpha-synuclein and its interaction with histones. Biochemistry 42:8465–8471.

Goldberg JA, Reynolds JNJ (2011) Spontaneous firing and evoked pauses in the tonically active cholinergic interneurons of the striatum. Neuroscience 198:27–43.

Goto S, Kawarai T, Morigaki R, Okita S, Koizumi H, Nagahiro S, Munoz EL, Lee L V, Kaji R (2013) Defects in the striatal neuropeptide Y system in X-linked dystonia-parkinsonism. Brain 136:1555–1567.

Govindaiah G, Wang Y, Cox CL (2010) Substance P selectively modulates GABA(A) receptor-mediated synaptic transmission in striatal cholinergic interneurons. Neuropharmacology 58:413–422.

Grace AA, Bunney BS (1984a) The control of firing pattern in nigral dopamine neurons: single spike firing. J Neurosci 4:2866–2876.

Grace AA, Bunney BS (1984b) The control of firing pattern in nigral dopamine neurons: burst firing. J Neurosci 4:2877–2890.

Graveland GA, DiFiglia M (1985) The frequency and distribution of medium-sized neurons with indented nuclei in the primate and rodent neostriatum. Brain Res 327:307–311.

Graybiel AM (1984) Correspondence between the dopamine islands and striosomes of the mammalian striatum. Neuroscience 13:1157–1187.

Graybiel AM (2008) Habits, rituals, and the evaluative brain. Annu Rev Neurosci 31:359–387.

Graybiel AM, Aosaki T, Flaherty AW, Kimura M (1994) The basal ganglia and adaptive motor control. Science 265:1826–1831.

Graybiel AM, Pickel VM, Joh TH, Reis DJ, Ragsdale CW (1981) Direct demonstration of a correspondence between the dopamine islands and acetylcholinesterase patches in the developing striatum. Proc Natl Acad Sci U S A 78:5871–5875.

Graybiel AM, Ragsdale CW (1978) Histochemically distinct compartments in the striatum of human, monkeys, and cat demonstrated by acetylthiocholinesterase staining. Proc Natl Acad Sci U S A 75:5723–5726.

Greene JG (2006) Gene expression profiles of brain dopamine neurons and relevance to neuropsychiatric disease. J Physiol 575:411–416.

Greene JG, Dingledine R, Greenamyre JT (2005) Gene expression profiling of rat midbrain dopamine neurons: implications for selective vulnerability in parkinsonism. Neurobiol Dis 18:19–31.

Griebel G, Holsboer F (2012) Neuropeptide receptor ligands as drugs for psychiatric diseases: the end of the beginning? Nat Rev Drug Discov 11:462–478.

Grimm J, Mueller A, Hefti F, Rosenthal A (2004) Molecular basis for catecholaminergic neuron diversity. Proc Natl Acad Sci U S A 101:13891–13896.

Guevara Guzman R, Kendrick KM, Emson PC (1993) Effect of substance P on acetylcholine and dopamine release in the rat striatum: a microdialysis study. Brain Res 622:147–154.

Guzman JN, Sánchez-Padilla J, Chan CS, Surmeier DJ (2009) Robust pacemaking in substantia nigra dopaminergic neurons. J Neurosci 29:11011–11019.

Guzman JN, Sanchez-Padilla J, Wokosin D, Kondapalli J, Ilijic E, Schumacker PT, Surmeier DJ (2010) Oxidant stress evoked by pacemaking in dopaminergic neurons is attenuated by DJ-1. Nature 468:696–700.

Gygi SP, Gibb JW, Johnson M, Hanson GR (1993) Blockade of tachykinin NK1 receptors by CP-96345 enhances dopamine release and the striatal dopamine effects of methamphetamine in rats. Eur J Pharmacol 250:177–180.

Harris JJ, Jolivet R, Attwell D (2012) Synaptic Energy Use and Supply. Neuron 75:762–777.

Hartung H, Threlfell S, Cragg SJ (2011) Nitric oxide donors enhance the frequency dependence of dopamine release in nucleus accumbens. Neuropsychopharmacology 36:1811–1822.

Helton TD, Xu W, Lipscombe D (2005) Neuronal L-type calcium channels open quickly and are inhibited slowly. J Neurosci 25:10247–10251.

Henny P, Brown MTC, Northrop A, Faunes M, Ungless MA, Magill PJ, Bolam JP (2012) Structural correlates of heterogeneous in vivo activity of midbrain dopaminergic neurons. Nat Neurosci 15:613–619.

Hersch SM, Gutekunst CA, Rees HD, Heilman CJ, Levey AI (1994) Distribution of m1-m4 muscarinic receptor proteins in the rat striatum: light and electron

microscopic immunocytochemistry using subtype-specific antibodies. J Neurosci 14:3351–3363.

Hervé D, Pickel VM, Joh TH, Beaudet A (1987) Serotonin axon terminals in the ventral tegmental area of the rat: fine structure and synaptic input to dopaminergic neurons. Brain Res 435:71–83.

Hettiarachchi NT, Parker A, Dallas ML, Pennington K, Hung C-C, Pearson HA, Boyle JP, Robinson P, Peers C (2009) alpha-Synuclein modulation of Ca2+ signaling in human neuroblastoma (SH-SY5Y) cells. J Neurochem 111:1192–1201.

Holmgaard K, Jensen K, Lambert JDC (2009) Imaging of Ca2+ responses mediated by presynaptic L-type channels on GABAergic boutons of cultured hippocampal neurons. Brain Res 1249:79–90.

Holt DJ, Graybiel AM, Saper CB (1997) Neurochemical architecture of the human striatum. J Comp Neurol 384:1–25.

Hoover DB, Muth EA, Jacobowitz DM (1978) A mapping of the distribution of acetycholine, choline acetyltransferase and acetylcholinesterase in discrete areas of rat brain. Brain Res 153:295–306.

Hornykiewicz O (1998) Biochemical aspects of Parkinson's disease. Neurology 51:S2–9.

Hyland BI, Reynolds JNJ, Hay J, Perk CG, Miller R (2002) Firing modes of midbrain dopamine cells in the freely moving rat. Neuroscience 114:475–492.

Iacopino A, Christakos S, German D, Sonsalla PK, Altar CA (1992) Calbindin-D28K-containing neurons in animal models of neurodegeneration: possible protection from excitotoxicity. Mol Brain Res 13:251–261.

Iravani MM, Millar J, Kruk ZL (1998) Differential release of dopamine by nitric oxide in subregions of rat caudate putamen slices. J Neurochem 71:1969–1977.

Izzo PN, Bolam JP (1988) Cholinergic synaptic input to different parts of spiny striatonigral neurons in the rat. J Comp Neurol 269:219–234.

Jakab RL, Goldman-Rakic P (1996) Presynaptic and postsynaptic subcellular localization of substance P receptor immunoreactivity in the neostriatum of the rat and rhesus monkey (Macaca mulatta). J Comp Neurol 369:125–136.

Jan LY, Siegelbaum SA, Pietrobon D (2005) Function and dysfunction of synaptic calcium channels: insights from mouse models. Curr Opin Neurobiol 15:257–265.

Janezic S, Threlfell S, Dodson PD, Dowie MJ, Taylor TN, Potgieter D, Parkkinen L, Senior SL, Anwar S, Kosillo P, Cioroch M, Wagner K, Ansorge O, Bolam JP, Cragg SJ, Wade-Martins R (2013) Deficits in dopaminergic transmission precede

neuron loss and dysfunction in a new Parkinson's model. Proc Natl Acad Sci In press.

Jeong J, Shi W-X, Hoffman R, Oh J, Gore JC, Bunney BS, Peterson BS (2012) Bursting as a source of non-linear determinism in the firing patterns of nigral dopamine neurons. Eur J Neurosci 36:3214–3223.

John CE, Jones SR (2006) Exocytotic release of dopamine in ventral tegmental area slices from C57BL/6 and dopamine transporter knockout mice. Neurochem Int 49:737–745.

Johnston JG, Gerfen CR, Haber SN, van der Kooy D (1990) Mechanisms of striatal pattern formation: conservation of mammalian compartmentalization. Brain Res Dev Brain Res 57:93–102.

Kahle PJ, Neumann M, Ozmen L, Muller V, Jacobsen H, Schindzielorz A, Okochi M, Leimer U, van Der Putten H, Probst A, Kremmer E, Kretzschmar HA, Haass C (2000) Subcellular localization of wild-type and Parkinson's disease-associated mutant alpha -synuclein in human and transgenic mouse brain. J Neurosci 20:6365–6373.

Kalivas PW, Miller JS (1984) Substance P modulation of dopamine in the nucleus accumbens. Neurosci Lett 48:55–59.

Kamp MA, Krieger A, Henry M, Hescheler J, Weiergräber M, Schneider T (2005) Presynaptic "Ca2.3-containing" E-type Ca channels share dual roles during neurotransmitter release. Eur J Neurosci 21:1617–1625.

Kato T, Otsu Y, Furune Y, Yamamoto T (1992) Different effects of L-, N- and T-type calcium channel blockers on striatal dopamine release measured by microdialysis in freely moving rats. Neurochem Int 21:99–107.

Katz B, Miledi R (1968) The role of calcium in neuromuscular facilitation. J Physiol 195:481–492.

Kawaguchi Y (1993) Physiological, morphological, and histochemical characterization of three classes of interneurons in rat neostriatum. J Neurosci 13:4908–4923.

Kawaguchi Y, Wilson CJ, Augood SJ, Emson PC (1995) Striatal interneurones: chemical, physiological and morphological characterization. Trends Neurosci 18:527–535.

Kawamoto EM, Vivar C, Camandola S (2012) Physiology and patholoy of calcium signalling in the brain. Front Pharmacol 3:61.

Kelly RS, Wightman RM (1987) Detection of dopamine overflow and diffusion with voltammetry in slices of rat brain. Brain Res 423:79–87.

Kim Y, Park MK, Chung S (2008) Voltage-operated Ca2+ channels regulate dopamine release from somata of dopamine neurons in the substantia nigra pars compacta. Biochem Biophys Res Commun 373:665–669.

King JD, Meriney SD (2005) Proportion of N-type calcium current activated by action potential stimuli. J Neurophysiol 94:3762–3770.

Kleinlogel S, Feldbauer K, Dempski RE, Fotis H, Wood PG, Bamann C, Bamberg E (2011) Ultra light-sensitive and fast neuronal activation with the Ca^2+-permeable channelrhodopsin CatCh. Nat Neurosci 14:513–518.

Koizumi H, Morigaki R, Okita S, Nagahiro S, Kaji R, Nakagawa M, Goto S (2013) Response of striosomal opioid signaling to dopamine depletion in 6-hydroxydopamine-lesioned rat model of Parkinson's disease: a potential compensatory role. Front Cell Neurosci 7:74.

Kombian SB, Ananthalakshmi KV V, Parvathy SS, Matowe WC (2003) Substance P depresses excitatory synaptic transmission in the nucleus accumbens through dopaminergic and purinergic mechanisms. J Neurophysiol 89:728–737.

Koós T, Tepper JM (1999) Inhibitory control of neostriatal projection neurons by GABAergic interneurons. Nat Neurosci 2:467–472.

Kovács KA, Steinmann M, Magistretti PJ, Halfon O, Cardinaux J-R (2006) C/EBPbeta couples dopamine signalling to substance P precursor gene expression in striatal neurones. J Neurochem 98:1390–1399.

Kreitzer AC (2009) Physiology and pharmacology of striatal neurons. Annu Rev Neurosci 32:127–147.

Kume-Kick J, Rice ME (1998) Dependence of dopamine calibration factors on media Ca2+ and Mg2+ at carbon-fiber microelectrodes used with fast-scan cyclic voltammetry. J Neurosci Methods 84:55–62.

Lavoie B, Parent A (1991) Dopaminergic neurons expressing calbindin in normal and parkinsonian monkeys. Neuroreport 2:601–604.

Le Gal La Salle G, Ben-Ari Y (1977) Microiontophoretic effects of substance P on neurons of the medial amygdala and putamen of the rat. Brain Res 135:174–179.

Le Moine C, Normand E, Bloch B (1991) Phenotypical characterization of the rat striatal neurons expressing the D1 dopamine receptor gene. Proc Natl Acad Sci U S A 88:4205–4209.

Le Moine C, Tison F, Bloch B (1990) D2 dopamine receptor gene expression by cholinergic neurons in the rat striatum. Neurosci Lett 117:248–252.

Leach K, Simms J, Sexton PM, Christopoulos A (2012) Structure-function studies of muscarinic acetylcholine receptors. Handb Exp Pharmacol:29–48.

Lee US, Cui J (2010) BK channel activation: structural and functional insights. Trends Neurosci 33:415–423.

Levey AI, Hersch SM, Rye DB, Sunahara RK, Niznik HB, Kitt CA, Price DL, Maggio R, Brann MR, Ciliax BJ (1993) Localization of D1 and D2 dopamine receptors in brain with subtype-specific antibodies. Proc Natl Acad Sci U S A 90:8861–8865.

Li M, Hansen JB, Huang L, Keyser BM, Taylor JT (2005) Towards selective antagonists of T-type calcium channels: design, characterization and potential applications of NNC 55-0396. Cardiovasc Drug Rev 23:173–196.

Li M, Wang Y, Pinon VI, Weck M (2011) nifedipine photoactive. Chem Commun 47:2802–2804.

Lin JY (2011) A user's guide to channelrhodopsin variants: features, limitations and future developments. Exp Physiol 96:19–25.

Lin JY, Lin MZ, Steinbach P, Tsien RY (2009) Characterization of engineered channelrhodopsin variants with improved properties and kinetics. Biophys J 96:1803–1814.

Lindgren N, Xu ZQ, Herrera-Marschitz M, Haycock J, Hökfelt T, Fisone G (2001) Dopamine D(2) receptors regulate tyrosine hydroxylase activity and phosphorylation at Ser40 in rat striatum. Eur J Neurosci 13:773–780.

Lipscombe D, Helton TD, Xu W (2004) L-type calcium channels: the low down. J Neurophysiol 92:2633–2641.

Liu H, Brown JL, Jasmin L, Maggio JE, Vigna SR, Mantyh PW, Basbaum AI (1994) Synaptic relationship between substance P and the substance P receptor: light and electron microscopic characterization of the mismatch between neuropeptides and their receptors. Proc Natl Acad Sci 91:1009–1013.

Ljungdahl Å, Hökfelt T, Nilsson G, Goldstein M (1978) Distribution of substance P-like immunoreactivity in the central nervous system of the rat—II. Light microscopic localization in relation to catecholamine-containing neurons. Neuroscience 3:945–976.

Llona I, Annaert WG, Jacob W, De Potter WP (1994) Co-storage in large "dense-core" vesicles of dopamine and cholecystokinin in rat striatum. Neurochem Int 25:573–581.

Lüscher C, Slesinger PA (2010) Emerging roles for G protein-gated inwardly rectifying potassium (GIRK) channels in health and disease. Nat Rev Neurosci 11:301–315.

Malach R, Graybiel AM (1986) Mosaic architecture of the somatic sensory-recipient sector of the cat's striatum. J Neurosci 6:3436–3458.

Malinina E, Druzin M, Johansson S (2010) Differential control of spontaneous and evoked GABA release by presynaptic L-type Ca(2+) channels in the rat medial preoptic nucleus. J Neurophysiol 104:200–209.

Mantyh PW, Hunt SP, Maggio JE (1984) Substance P receptors: localization by light microscopic autoradiography in rat brain using [3H]SP as the radioligand. Brain Res 307:147–165.

Marques O, Outeiro TF (2012) Alpha-synuclein: from secretion to dysfunction and death. Cell Death Dis 3:e350.

Martin RL, Lee J-H, Cribbs LL, Perez-Reyes E, Hanck DA (2000) Mibefradil Block of Cloned T-Type Calcium Channels. J Pharmacol Exp Ther 295:302–308.

Martire M, Barrese V, D'Amico M, Iannotti FA, Pizzarelli R, Samengo I, Viggiano D, Ruth P, Cherubini E, Taglialatela M (2010) Pre-synaptic BK channels selectively control glutamate versus GABA release from cortical and hippocampal nerve terminals. J Neurochem 115:411–422.

Matsuda W, Furuta T, Nakamura KC, Hioki H, Fujiyama F, Arai R, Kaneko T (2009) Single nigrostriatal dopaminergic neurons form widely spread and highly dense axonal arborizations in the neostriatum. J Neurosci 29:444–453.

Matsumoto M, Hikosaka O (2009) Two types of dopamine neuron distinctly convey positive and negative motivational signals. Nature 459:837–841.

Matveev V, Bertram R, Sherman A (2011) Calcium cooperativity of exocytosis as a measure of Ca^2+ channel domain overlap. Brain Res 1398:126–138.

McDonough SI, Mintz IM, Bean BP (1997) Alteration of P-type calcium channel gating by the spider toxin omega-Aga-IVA. Biophys J 72:2117–2128.

McFarlane C, Warner DS, Dexter F (1995) Interactions between NMDA and AMPA glutamate receptor antagonists during halothane anesthesia in the rat. Neuropharmacology 34:659–663.

Michael DJ, Wightman RM (1999) Electrochemical monitoring of biogenic amine neurotransmission in real time. J Pharm Biomed Anal 19:33–46.

Mintz IM, Bean BP (1993) Block of calcium channels in rat neurons by synthetic omega-Aga-IVA. Neuropharmacology 32:1161–1169.

Mirenowicz J, Schultz W (1996) Preferential activation of midbrain dopamine neurons by appetitive rather than aversive stimuli. Nature 379:449–451.

Miyawaki A, Schnitzer MJ (2007) New technologies for neuroscience. Curr Opin Neurobiol 17:565–566.

Miyazaki I, Asanuma M (2008) Dopaminergic neuron-specific oxidative stress caused by dopamine itself. Acta Med Okayama 62:141–150.

Monastyrskaya K, Hostettler A, Buergi S, Draeger A (2005) The NK1 receptor localizes to the plasma membrane microdomains, and its activation is dependent on lipid raft integrity. J Biol Chem 280:7135–7146.

Moosmang S, Lenhardt P, Haider N, Hofmann F, Wegener JW (2005) Mouse models to study L-type calcium channel function. Pharmacol Ther 106:347–355.

Moran RJ, Mallet N, Litvak V, Dolan RJ, Magill PJ, Friston KJ, Brown P (2011) Alterations in brain connectivity underlying beta oscillations in Parkinsonism. PLoS Comput Biol 7:e1002124.

Morris G, Arkadir D, Nevet A, Vaadia E, Bergman H (2004) Coincident but distinct messages of midbrain dopamine and striatal tonically active neurons. Neuron 43:133–143.

Mosharov E V, Larsen KE, Kanter E, Phillips KA, Wilson K, Schmitz Y, Krantz DE, Kobayashi K, Edwards RH, Sulzer D (2009) Interplay between cytosolic dopamine, calcium, and alpha-synuclein causes selective death of substantia nigra neurons. Neuron 62:218–229.

Moss J, Bolam JP (2010) The Relationship between Dopaminergic Axons and Glutamatergic Synapses in the Striatum: Structural Considerations : Dopamine Handbook Oxford Scholarship Online (Iversen L., D. IS, S.B. D, Björklund A, eds). Oxford: Oxford University Press.

Murtra P, Sheasby AM, Hunt SP, De Felipe C (2000) Rewarding effects of opiates are absent in mice lacking the receptor for substance P. Nature 405:180–183.

Myoga MH, Regehr WG (2011) Calcium microdomains near R-type calcium channels control the induction of presynaptic long-term potentiation at parallel fiber to purkinje cell synapses. J Neurosci 31:5235–5243.

Nagel G, Szellas T, Huhn W, Kateriya S, Adeishvili N, Berthold P, Ollig D, Hegemann P, Bamberg E (2003) Channelrhodopsin-2, a directly light-gated cation-selective membrane channel. Proc Natl Acad Sci U S A 100:13940–13945.

Nakai J (1998) Two Regions of the Ryanodine Receptor Involved in Coupling with L-Type Ca2+ Channels. J Biol Chem 273:13403–13406.

Nakamura Y, Izumi H, Shimizu T, Hisaoka-Nakashima K, Morioka N, Nakata Y (2013) Volume transmission of substance P in striatum induced by intraplantar formalin injection attenuates nociceptive responses via activation of the neurokinin 1 receptor. J Pharmacol Sci 121:257–271.

Nanou E, Alpert MH, Alford S, El Manira A (2013) Differential regulation of synaptic transmission by pre- and postsynaptic SK channels in the spinal locomotor network. J Neurophysiol 109:3051–3059.

Nawa H, Kotani H, Nakanishi S (1984) Tissue-specific generation of two preprotachykinin mRNAs from one gene by alternative RNA splicing. Nature 312:729–734.

Nedergaard M, Verkhratsky A, Szydlowska K, Tymianski M (2010) Calcium, ischemia and excitotoxicity. Cell Calcium 47:122–129.

Nelson EL, Liang CL, Sinton CM, German DC (1996) Midbrain dopaminergic neurons in the mouse: computer-assisted mapping. J Comp Neurol 369:361–371.

Newcomb R, Szoke B, Palma A, Wang G, Chen X h, Hopkins W, Cong R, Miller J, Urge L, Tarczy-Hornoch K, Loo JA, Dooley DJ, Nadasdi L, Tsien RW, Lemos J, Miljanich G (1998) Selective peptide antagonist of the class E calcium channel from the venom of the tarantula Hysterocrates gigas. Biochemistry 37:15353–15362.

Nirenberg MJ, Chan J, Liu Y, Edwards RH, Pickel VM (1997) Vesicular monoamine transporter-2: immunogold localization in striatal axons and terminals. Synapse 26:194–198.

Niznik HB, Van Tol HH (1992) Dopamine receptor genes: new tools for molecular psychiatry. J Psychiatry Neurosci 17:158–180.

Orrenius S, Zhivotovsky B, Nicotera P (2003) Regulation of cell death: the calcium-apoptosis link. Nat Rev Mol Cell Biol 4:552–565.

Overton P, Clark D (1992) Electrophysiological evidence that intrastriatally administered N-methyl-D-aspartate augments striatal dopamine tone in the rat. J Neural Transm Park Dis Dement Sect 4:1–14.

Overton P., Clark D (1997) Burst firing in midbrain dopaminergic neurons. Brain Res Rev 25:312–334.

Park A, Stacy M (2009) Non-motor symptoms in Parkinson's disease. J Neurol 256 Suppl :293–298.

Pennartz CMA, Ito R, Verschure PFMJ, Battaglia FP, Robbins TW (2011) The hippocampal-striatal axis in learning, prediction and goal-directed behavior. Trends Neurosci 34:548–559.

Pentney RJW, Gratton A (1991) Effects of local delta and mu opioid receptor activation on basal and stimulated dopamine release in striatum and nucleus accumbens of rat: An in vivo electrochemical study. Neuroscience 45:95–102.

Pert CB, Kuhar MJ, Snyder SH (1976) Opiate receptor: autoradiographic localization in rat brain. Proc Natl Acad Sci U S A 73:3729–3733.

Petit F, Glowinski J (1986) Stimulatory effect of substance P on the spontaneous release of newly synthesized [3H]dopamine from rat striatal slices: A tetrodotoxin-sensitive process. Neuropharmacology 25:1015–1021.

Pfeiffer M, Kirscht S, Stumm R, Koch T, Wu D, Laugsch M, Schröder H, Höllt V, Schulz S (2003) Heterodimerization of substance P and mu-opioid receptors regulates receptor trafficking and resensitization. J Biol Chem 278:51630–51637.

Phillips P, Stamford JA (2000a) Differential recruitment of N-, P- and Q-type voltage-operated calcium channels in striatal dopamine release evoked by “regular” and “burst” firing. Brain Res 884:139–146.

Phillips PE, Stamford JA (2000b) Differential recruitment of N-, P- and Q-type voltage-operated calcium channels in striatal dopamine release evoked by “regular” and “burst” firing. Brain Res 884:139–146.

Pickel VM, Nirenberg MJ, Milner TA (1996) Ultrastructural view of central catecholaminergic transmission: immunocytochemical localization of synthesizing enzymes, transporters and receptors. J Neurocytol 25:843–856.

Pickrell AM, Pinto M, Hida A, Moraes CT (2011) Striatal dysfunctions associated with mitochondrial DNA damage in dopaminergic neurons in a mouse model of Parkinson’s disease. J Neurosci 31:17649–17658.

Pisani A, Bonsi P, Centonze D, Calabresi P, Bernardi G (2000) Activation of D2-like dopamine receptors reduces synaptic inputs to striatal cholinergic interneurons. J Neurosci 20:RC69.

Planert H, Berger TK, Silberberg G (2013) Membrane properties of striatal direct and indirect pathway neurons in mouse and rat slices and their modulation by dopamine. Brown JT, ed. PLoS One 8:e57054.

Priebe NJ, Ferster D (2008) Inhibition, spike threshold, and stimulus selectivity in primary visual cortex. Neuron 57:482–497.

Puopolo M, Raviola E, Bean BP (2007) Roles of subthreshold calcium current and sodium current in spontaneous firing of mouse midbrain dopamine neurons. J Neurosci 27:645–656.

Putzier I, Kullmann PHM, Horn JP, Levitan ES (2009) Cav1.3 channel voltage dependence, not Ca2+ selectivity, drives pacemaker activity and amplifies bursts in nigral dopamine neurons. J Neurosci 29:15414–15419.

Quartara L, Maggi CA (1997) The tachykinin NK1 receptor. Part I: ligands and mechanisms of cellular activation. Neuropeptides 31:537–563.

Ramakrishnan NA, Drescher MJ, Drescher DG (2009) Direct interaction of otoferlin with syntaxin 1A, SNAP-25, and the L-type voltage-gated calcium channel Cav1.3. J Biol Chem 284:1364–1372.

Ramírez OA, Couve A (2011) The endoplasmic reticulum and protein trafficking in dendrites and axons. Trends Cell Biol 21:219–227.

Redgrave P, Gurney K, Reynolds J (2008) What is reinforced by phasic dopamine signals? Brain Res Rev 58:322–339.

Rees K, Stowe R, Patel S, Ives N, Breen K, Ben-Shlomo Y, Clarke CE (2011) Anti-hypertensive drugs as disease-modifying agents for Parkinson's disease: evidence from observational studies and clinical trials. Cochrane Database Syst Rev:CD008535.

Reid M, Herrera-Marschitz M, Hökfelt T, Terenius L, Ungerstedt U (1988) Differential modulation of striatal dopamine release by intranigral injection of γ-aminobutyric acid (GABA), dynorphin A and substance P. Eur J Pharmacol 147:411–420.

Rettig J, Sheng ZH, Kim DK, Hodson CD, Snutch TP, Catterall WA (1996) Isoform-specific interaction of the alpha1A subunits of brain Ca2+ channels with the presynaptic proteins syntaxin and SNAP-25. Proc Natl Acad Sci U S A 93:7363–7368.

Reuter H (1995) Measurements of exocytosis from single presynaptic nerve terminals reveal heterogeneous inhibition by Ca(2+)-channel blockers. Neuron 14:773–779.

Rice ME, Cragg SJ (2004) Nicotine amplifies reward-related dopamine signals in striatum. Nat Neurosci 7:583–584.

Rice ME, Patel JC, Cragg SJ (2011) Dopamine release in the basal ganglia. Neuroscience 198:112–137.

Richfield EK, Penney JB, Young AB (1989) Anatomical and affinity state comparisons between dopamine D1 and D2 receptors in the rat central nervous system. Neuroscience 30:767–777.

Ritchie AK (1979) Catecholamine secretion in a rat pheochromocytoma cell line: two pathways for calcium entry. J Physiol 286:541–561.

Rivera A, Alberti I, Martin AB, Narvaez JA, de la Calle A, Moratalla R (2002) Molecular phenotype of rat striatal neurons expressing the dopamine D5 receptor subtype. Eur J Neurosci 16:2049–2058.

Robinson DL, Wightman. RM (2007) Rapid Dopamine Release in Freely Moving Rats. CRC Press.

Roeper J (2013) Dissecting the diversity of midbrain dopamine neurons. Trends Neurosci 36:336–342.

Roffler-Tarlov S, Graybiel AM (1987) The postnatal development of the dopamine-containing innervation of dorsal and ventral striatum: effects of the weaver gene. J Neurosci 7:2364–2372.

Romo R, Schultz W (1990) Dopamine neurons of the monkey midbrain: contingencies of responses to active touch during self-initiated arm movements. J Neurophysiol 63:592–606.

Rusakov DA (2006) Ca2+-dependent mechanisms of presynaptic control at central synapses. Neuroscientist 12:317–326.

Rymar V V, Sasseville R, Luk KC, Sadikot AF (2004) Neurogenesis and stereological morphometry of calretinin-immunoreactive GABAergic interneurons of the neostriatum. J Comp Neurol 469:325–339.

Saheki Y, Bargmann CI (2009) Presynaptic CaV2 calcium channel traffic requires CALF-1 and the alpha(2)delta subunit UNC-36. Nat Neurosci 12:1257–1265.

Sakaba T, Neher E (2001) Quantitative Relationship between Transmitter Release and Calcium Current at the Calyx of Held Synapse. J Neurosci 21:462–476.

Sakamoto S, Goto S, Ito H, Hirano A (1992) Striosomal organization of substance P-like immunoreactivity in parkinsonian patients. Neurology 42:1071–1075.

Salamone JD (1996) The behavioral neurochemistry of motivation: methodological and conceptual issues in studies of the dynamic activity of nucleus accumbens dopamine. J Neurosci Methods 64:137–149.

Salthun-Lassalle B, Traver S, Hirsch EC, Michel PP (2005) Substance P, neurokinins A and B, and synthetic tachykinin peptides protect mesencephalic dopaminergic neurons in culture via an activity-dependent mechanism. Mol Pharmacol 68:1214–1224.

Samii A, Nutt JG, Ransom BR (2004) Parkinson's disease. Lancet 363:1783–1793.

Schlick B, Flucher BE, Obermair GJ (2010) Voltage-activated calcium channel expression profiles in mouse brain and cultured hippocampal neurons. Neuroscience 167:786–798.

Schmidt F, Levin J, Kamp F, Kretzschmar H, Giese A, Bötzel K (2012) Single-channel electrophysiology reveals a distinct and uniform pore complex formed by α-synuclein oligomers in lipid membranes. PLoS One 7:e42545.

Schultz W (2007a) Multiple dopamine functions at different time courses. Annu Rev Neurosci 30:259–288.

Schultz W (2007b) Behavioral dopamine signals. Trends Neurosci.

Schultz W, Dayan P, Montague PR (1997) A neural substrate of prediction and reward. Science 275:1593–1599.

Senior SL, Ninkina N, Deacon R, Bannerman D, Buchman VL, Cragg SJ, Wade-Martins R (2008) Increased striatal dopamine release and hyperdopaminergic-like behaviour in mice lacking both alpha-synuclein and gamma-synuclein. Eur J Neurosci 27:947–957.

Sheng ZH, Rettig J, Takahashi M, Catterall WA (1994) Identification of a syntaxin-binding site on N-type calcium channels. Neuron 13:1303–1313.

Shepard PD, Stump D (1999) Nifedipine blocks apamin-induced bursting activity in nigral dopamine-containing neurons. Brain Res 817:104–109.

Sidach SS, Mintz IM (2000) Low-Affinity Blockade of Neuronal N-Type Ca Channels by the Spider Toxin omega -Agatoxin-IVA. J Neurosci 20:7174–7182.

Sidhu A, Niznik HB (2000) Coupling of dopamine receptor subtypes to multiple and diverse G proteins. Int J Dev Neurosci 18:669–677.

Sidló Z, Reggio PH, Rice ME (2008) Inhibition of striatal dopamine release by CB1 receptor activation requires nonsynaptic communication involving GABA, H2O2, and KATP channels. Neurochem Int 52:80–88.

Simón-Sánchez J et al. (2009) Genome-wide association study reveals genetic risk underlying Parkinson's disease. Nat Genet 41:1308–1312.

Simuni T, Borushko E, Avram MJ, Miskevics S, Martel A, Zadikoff C, Videnovic A, Weaver FM, Williams K, Surmeier DJ (2010) Tolerability of isradipine in early Parkinson's disease: a pilot dose escalation study. Mov Disord 25:2863–2866.

Singleton AB et al. (2003) alpha-Synuclein locus triplication causes Parkinson's disease. Science 302:841.

Sivam SP, Cox J (2006) Postnatal administration of D1 dopamine agonist reverses neonatal dopaminergic lesion-induced changes in striatal enkephalin and substance P systems. Brain Res 1073-1074:159–163.

Skinbjerg M, Sibley DR, Javitch JA, Abi-Dargham A (2012) Imaging the high-affinity state of the dopamine D2 receptor in vivo: fact or fiction? Biochem Pharmacol 83:193–198.

Smith Y, Bennett BD, Bolam JP, Parent A, Sadikot AF (1994) Synaptic relationships between dopaminergic afferents and cortical or thalamic input in the sensorimotor territory of the striatum in monkey. J Comp Neurol 344:1–19.

Smith Y, Kieval JZ (2000) Anatomy of the dopamine system in the basal ganglia. Trends Neurosci 23:S28–S33.

Smith, David A, Bolam, Paul J (1990) The neural network of the basal ganglia as revealed by the study of synaptic connections of identified neurones. Trends Neurosci 13:259–265.

Snutch T, Zamponi G, Dolphin AC (2013) The α2δ subunits of voltage-gated calcium channels. Biochim Biophys Acta - Biomembr 1828:1541–1549.

Snutch TP, Peloquin J, Eleanor M, McRory JE (2005) Molecular Properties of Voltage-Gated Calcium Channels - Madame Curie Bioscience Database - NCBI Bookshelf.

Somogyi P, Bolam JP, Totterdell S, Smith AD (1981) Monosynaptic input from the nucleus accumbens--ventral striatum region to retrogradely labelled nigrostriatal neurones. Brain Res 217:245–263.

Specht CG, Schoepfer R (2001) Deletion of the alpha-synuclein locus in a subpopulation of C57BL/6J inbred mice. BMC Neurosci 2:11.

Stanley EF, Atrakchi AH (1990) Calcium currents recorded from a vertebrate presynaptic nerve terminal are resistant to the dihydropyridine nifedipine. Proc Natl Acad Sci U S A 87:9683–9687.

Starr M (1982) Influence of peptides on 3H-dopamine release from superfused rat striatal slices. Neurochem Int 4:233–240.

Subramanian J, Morozov A (2011) Erk1/2 inhibit synaptic vesicle exocytosis through L-type calcium channels. J Neurosci 31:4755–4764.

Südhof TC, Rizo J (2011) Synaptic vesicle exocytosis. Cold Spring Harb Perspect Biol 3:a005637–.

Südhof TC, Rothman JE (2009) Membrane fusion: grappling with SNARE and SM proteins. Science 323:474–477.

Sulzer D (2007) Multiple hit hypotheses for dopamine neuron loss in Parkinson's disease. Trends Neurosci 30:244–250.

Sulzer D, Pothos EN (2000) Regulation of quantal size by presynaptic mechanisms. Rev Neurosci 11:159–212.

Sunstro¨m E, Stro¨mberg I, Tsutsumi T, Olson L, Jonsson G (1987) Studies on the effect of 1-methyl-4-phenyl-1,2,3,6-tetrahydropyridine (MPTP) on central catecholamine neurons in C57 BL/6 mice. Comparison with three other strains of mice. Brain Res 405:26–38.

Surmeier DJ (2007) Calcium, ageing, and neuronal vulnerability in Parkinson's disease. Lancet Neurol 6:933–938.

Surmeier DJ, Carrillo-Reid L, Bargas J (2011a) Dopaminergic modulation of striatal neurons, circuits, and assemblies. Neuroscience.

Surmeier DJ, Ding J, Day M, Wang Z, Shen W (2007) D1 and D2 dopamine-receptor modulation of striatal glutamatergic signaling in striatal medium spiny neurons. Trends Neurosci 30:228–235.

Surmeier DJ, Guzman JN, Sanchez-Padilla J, Schumacker PT (2011b) The role of calcium and mitochondrial oxidant stress in the loss of substantia nigra pars compacta dopaminergic neurons in Parkinson's disease. Neuroscience 198:221–231.

Surmeier DJ, Sulzer D (2013) The pathology roadmap in Parkinson disease. Prion 7:85–91.

Tai C, Yang YC, Pan MK, Huang CS, Kuo CC (2011) Modulation of subthalamic T-type Ca 2 channels remedies locomotor deficits in a rat model of Parkinson disease. J Clin Invest 121:3289–3305.

Tajima K, Fukuda T (2013) Region-specific diversity of striosomes in the mouse striatum revealed by the differential immunoreactivities for mu-opioid receptor, substance P, and enkephalin. Neuroscience 241:215–228.

Tang A-H, Karson MA, Nagode DA, McIntosh JM, Uebele VN, Renger JJ, Klugmann M, Milner TA, Alger BE (2011) Nerve terminal nicotinic acetylcholine receptors initiate quantal GABA release from perisomatic interneurons by activating axonal T-type (Cav3) Ca^{2+} channels and Ca^{2+} release from stores. J Neurosci 31:13546–13561.

Tanner CM, Goldman SM (1996) Epidemiology of Parkinson's disease. Neurol Clin 14:317–335.

Tate CG, Grisshammer R (1996) Heterologous expression of G-protein-coupled receptors. Trends Biotechnol 14:426–430.

Tautenhahn M, Leichsenring A, Servettini I, Pesic M, Sperlagh B, Nörenberg W, Illes P (2012) Purinergic modulation of the excitatory synaptic input onto rat striatal neurons. Neuropharmacology 62:1756–1766.

Taylor RC, Cullen SP, Martin SJ (2008) Apoptosis: controlled demolition at the cellular level. Nat Rev Mol Cell Biol 9:231–241.

Tempel A, Zukin RS (1987) Neuroanatomical patterns of the mu, delta, and kappa opioid receptors of rat brain as determined by quantitative in vitro autoradiography. Proc Natl Acad Sci U S A 84:4308–4312.

Tepper JM, Abercrombie ED, Bolam JP, Tepper JM, Abercrombie ED, Bolam JP (2007) Basal ganglia macrocircuits. Prog Brain Res 160:3–7.

Thornton E, Tran TTB, Vink R (2010) A substance P mediated pathway contributes to 6-hydroxydopamine induced cell death. Neurosci Lett 481:64–67.

Thornton E, Vink R (2012) Treatment with a substance p receptor antagonist is neuroprotective in the intrastriatal 6-hydroxydopamine model of early Parkinson's disease. PLoS One 7:e34138.

Threlfell S, Clements MA, Khodai T, Pienaar IS, Exley R, Wess J, Cragg SJ (2010) Striatal muscarinic receptors promote activity dependence of dopamine transmission via distinct receptor subtypes on cholinergic interneurons in ventral versus dorsal striatum. J Neurosci 30:3398–3408.

Threlfell S, Cragg SJ (2011) Dopamine signaling in dorsal versus ventral striatum: the dynamic role of cholinergic interneurons. Front Syst Neurosci 5:11.

Threlfell S, Lalic T, Platt NJ, Jennings KA, Deisseroth K, Cragg SJ (2012) Striatal dopamine release is triggered by synchronized activity in cholinergic interneurons. Neuron 75:58–64.

Tippens AL, Pare J-F, Langwieser N, Moosmang S, Milner TA, Smith Y, Lee A (2008) Ultrastructural evidence for pre- and postsynaptic localization of Cav1.2 L-type Ca2+ channels in the rat hippocampus. J Comp Neurol 506:569–583.

Tremblay L, Kemel ML, Desban M, Gauchy C, Glowinski J (1992) Distinct presynaptic control of dopamine release in striosomal- and matrix-enriched areas of the rat striatum by selective agonists of NK1, NK2, and NK3 tachykinin receptors. Proc Natl Acad Sci U S A 89:11214–11218.

Trendelenburg A., Bültmann R (2000) P2 receptor-mediated inhibition of dopamine release in rat neostriatum. Neuroscience 96:249–252.

Trueta C, De-Miguel FF (2012) Extrasynaptic exocytosis and its mechanisms: a source of molecules mediating volume transmission in the nervous system. Front Physiol 3:319.

Tsai H-C, Zhang F, Adamantidis A, Stuber GD, Bonci A, De Lecea L, Deisseroth K (2009) Phasic firing in dopaminergic neurons is sufficient for behavioral conditioning. Science (80-) 324:1080–1084.

Tsuchida K, Shigemoto R, Yokota Y, Nakanishi S (1990) Tissue distribution and quantitation of the mRNAs for three rat tachykinin receptors. Eur J Biochem 193:751–757.

Turner TJ, Adams ME, Dunlap K (1992) Calcium channels coupled to glutamate release identified by omega-Aga-IVA. Science 258:310–313.

Ungless MA, Magill PJ, Bolam JP (2004) Uniform inhibition of dopamine neurons in the ventral tegmental area by aversive stimuli. Science 303:2040–2042.

Unwin N (2003) Structure and action of the nicotinic acetylcholine receptor explored by electron microscopy. FEBS Lett 555:91–95.

Vacher H, Mohapatra DP, Trimmer JS (2008) Localization and targeting of voltage-dependent ion channels in mammalian central neurons. Physiol Rev 88:1407–1447.

Valjent E, Bertran-Gonzalez J, Hervé D, Fisone G, Girault J-A (2009) Looking BAC at striatal signaling: cell-specific analysis in new transgenic mice. Trends Neurosci 32:538–547.

Van Dongen YC, Mailly P, Thierry A-M, Groenewegen HJ, Deniau J-M (2008) Three-dimensional organization of dendrites and local axon collaterals of shell and core medium-sized spiny projection neurons of the rat nucleus accumbens. Brain Struct Funct 213:129–147.

Velimirovic BM, Koyano K, Nakajima S, Nakajima Y (1995) Opposing mechanisms of regulation of a G-protein-coupled inward rectifier K+ channel in rat brain neurons. Proc Natl Acad Sci 92:1590–1594.

Venton BJ, Seipel AT, Phillips PEM, Wetsel WC, Gitler D, Greengard P, Augustine GJ, Wightman RM (2006) Cocaine increases dopamine release by mobilization of a synapsin-dependent reserve pool. J Neurosci 26:3206–3209.

Venton BJ, Zhang H, Garris PA, Phillips PEM, Sulzer D, Wightman RM (2003) Real-time decoding of dopamine concentration changes in the caudate-putamen during tonic and phasic firing. J Neurochem 87:1284–1295.

Vergara R, Rick C, Hernández-López S, Laville JA, Guzman JN, Galarraga E, Surmeier DJ, Bargas J (2003) Spontaneous voltage oscillations in striatal projection neurons in a rat corticostriatal slice. J Physiol 553:169–182.

Verkhratsky A (2005) Physiology and pathophysiology of the calcium store in the endoplasmic reticulum of neurons. Physiol Rev 85:201–279.

Vilchis C, Bargas J, Ayala GX, Galván E, Galarraga E (1999) Ca2+ channels that activate Ca2+-dependent K+ currents in neostriatal neurons. Neuroscience 95:745–752.

Voorn P, Vanderschuren LJMJ, Groenewegen HJ, Robbins TW, Pennartz CMA (2004) Putting a spin on the dorsal-ventral divide of the striatum. Trends Neurosci 27:468–474.

Wang H, Pickel VM (2002) Dopamine D2 receptors are present in prefrontal cortical afferents and their targets in patches of the rat caudate-putamen nucleus. J Comp Neurol 442:392–404.

Wang J, Angulo JA (2011) Synergism between methamphetamine and the neuropeptide substance P on the production of nitric oxide in the striatum of mice. Brain Res 1369:131–139.

Wang L-Y, Fedchyshyn MJ, Yang Y-M (2009) Action potential evoked transmitter release in central synapses: insights from the developing calyx of Held. Mol Brain 2:36.

Watabe-Uchida M, Zhu L, Ogawa SK, Vamanrao A, Uchida N (2012) Whole-Brain Mapping of Direct Inputs to Midbrain Dopamine Neurons. Neuron 74:858–873.

Watanabe H, Yamashita T, Saitoh N, Kiyonaka S, Iwamatsu A, Campbell KP, Mori Y, Takahashi T (2010) Involvement of Ca2+ channel synprint site in synaptic vesicle endocytosis. J Neurosci 30:655–660.

Weber AM, Wong FK, Tufford AR, Schlichter LC, Matveev V, Stanley EF (2010) N-type Ca2+ channels carry the largest current: implications for nanodomains and transmitter release. Nat Neurosci 13:1348–1350.

Weiss N, Hameed S, Fernandez-Fernandez JM, Fablet K, Karmazinova M, Poillot C, Proft J, Chen L, Bidaud I, Monteil A, Huc-Brandt S, Lacinova L, Lory P, Zamponi GW, De Waard M (2012) A Cav3.2/syntaxin-1A signaling complex controls T-type channel activity and low-threshold exocytosis. J Biol Chem 287:2810–2818.

Whitty CJ, Paul MA, Bannon MJ (1997) Neurokinin receptor mRNA localization in human midbrain dopamine neurons. J Comp Neurol 382:394–400.

Wiecki T V, Frank MJ (2010) Neurocomputational models of motor and cognitive deficits in Parkinson's disease. Prog Brain Res 183:275–297.

Wikström MA, El Manira A (1998) Calcium influx through N- and P/Q-type channels activate apamin-sensitive calcium-dependent potassium channels generating the late afterhyperpolarization in lamprey spinal neurons. Eur J Neurosci 10:1528–1532.

Wilson CJ, Chang HT, Kitai ST (1990) Firing patterns and synaptic potentials of identified giant aspiny interneurons in the rat neostriatum. J Neurosci 10:508–519.

Wiser O, Trus M, Hernandez A, Renstrom E, Barg S, Rorsman P, Atlas D (1999) The voltage sensitive Lc-type Ca2+ channel is functionally coupled to the exocytotic machinery. Proc Natl Acad Sci 96:248–253.

Witkovsky P, Patel JC, Lee CR, Rice ME (2009) Immunocytochemical identification of proteins involved in dopamine release from the somatodendritic compartment of nigral dopaminergic neurons. Neuroscience 164:488–496.

Wolfart J, Roeper J (2002) Selective Coupling of T-Type Calcium Channels to SK Potassium Channels Prevents Intrinsic Bursting in Dopaminergic Midbrain Neurons. J Neurosci 22:3404–3413.

Wu D-Y, Pollock JD, Shurtleff D, Yost J, Mansvelder HD, Mertz M, Role LW (2009) Nicotinic modulation of synaptic transmission and plasticity in cortico-limbic circuits. Semin Cell Dev Biol 20:432–440.

Wu L, Saggau P (1994) Presynaptic calcium is increased during normal synaptic transmission and paired-pulse facilitation, but not in long-term potentiation in area CA1 of hippocampus. J Neurosci 14:645–654.

Wu LG, Borst JG, Sakmann B (1998) R-type Ca2+ currents evoke transmitter release at a rat central synapse. Proc Natl Acad Sci U S A 95:4720–4725.

Yamada T, McGeer PL, Baimbridge KG, McGeer EG (1990) Relative sparing in Parkinson's disease of substantia nigra dopamine neurons containing calbindin-D28K. Brain Res 526:303–307.

Yan Z, Song WJ, Surmeier J (1997) D2 dopamine receptors reduce N-type Ca2+ currents in rat neostriatal cholinergic interneurons through a membrane-delimited, protein-kinase-C-insensitive pathway. J Neurophysiol 77:1003–1015.

Yan Z, Surmeier DJ (1996) Muscarinic (m2/m4) receptors reduce N- and P-type Ca2+ currents in rat neostriatal cholinergic interneurons through a fast, membrane-delimited, G-protein pathway. J Neurosci 16:2592–2604.

Young WS, Bonner TI, Brann MR (1986) Mesencephalic dopamine neurons regulate the expression of neuropeptide mRNAs in the rat forebrain. Proc Natl Acad Sci U S A 83:9827–9831.

Yu S, Li X, Liu G, Han J, Zhang C, Li Y, Xu S, Liu C, Gao Y, Yang H, Uéda K, Chan P (2007) Extensive nuclear localization of alpha-synuclein in normal rat brain neurons revealed by a novel monoclonal antibody. Neuroscience 145:539–555.

Yu YJ, Arttamangkul S, Evans CJ, Williams JT, von Zastrow M (2009) Neurokinin 1 receptors regulate morphine-induced endocytosis and desensitization of mu-opioid receptors in CNS neurons. J Neurosci 29:222–233.

Yuan H-H, Chen R-J, Zhu Y-H, Peng C-L, Zhu X-R (2013) The neuroprotective effect of overexpression of calbindin-D(28k) in an animal model of Parkinson's disease. Mol Neurobiol 47:117–122.

Yung KKL, Bolam JP, Smith AD, Hersch SM, Ciliax BJ, Levey AI (1995) Immunocytochemical localization of D1 and D2 dopamine receptors in the basal ganglia of the rat: Light and electron microscopy. Neuroscience 65:709–730.

Yung KKL, Smith AD, Levey AI, Bolam JP (1996) Synaptic Connections Between Spiny Neurons of the Direct and Indirect Pathways in the Neostriatum of the Rat: Evidence from Dopamine Receptor and Neuropeptide Immunostaining. Eur J Neurosci 8:861–869.

Zampini V, Johnson SL, Franz C, Lawrence ND, Münkner S, Engel J, Knipper M, Magistretti J, Masetto S, Marcotti W (2010) Elementary properties of CaV1.3 Ca(2+) channels expressed in mouse cochlear inner hair cells. J Physiol 588:187–199.

Zamponi GW, Bourinet E, Snutch TP (1996) Nickel block of a family of neuronal calcium channels: subtype- and subunit-dependent action at multiple sites. J Membr Biol 151:77–90.

Zanazzi G, Matthews G (2009) The molecular architecture of ribbon presynaptic terminals. Mol Neurobiol 39:130–148.

Zhang H, Sulzer D (2004) Frequency-dependent modulation of dopamine release by nicotine. Nat Neurosci 7:581–582.

Zhao C, Dreosti E, Lagnado L (2011) Homeostatic synaptic plasticity through changes in presynaptic calcium influx. J Neurosci 31:7492–7496.

Zhou FM, Liang Y, Dani JA (2001) Endogenous nicotinic cholinergic activity regulates dopamine release in the striatum. Nat Neurosci 4:1224–1229.

Zubrzycka M, Janecka A (2000) Substance P: transmitter of nociception (Minireview). Endocr Regul 34:195–201.